NSIRC RESEARCH & INNOVATION CONFERENCE 2022

INDUSTRY-LED POSTGRADUATE RESEARCH

21-22 JULY 2022

nsirc | 10th ANNIVERSARY

00.10.09.21.00

a.r.u. | Anglia Ruskin University

Develop your business

Every partnership starts with a conversation

Start the conversation with us today

business@aru.ac.uk

aru.ac.uk/business-employers

WELCOME - NSIRC RESEARCH & INNOVATION CONFERENCE 2022

A warm welcome to this year's two-day NSIRC Research and Innovation Conference which, once again, we are delighted to bring you as an in-person experience! As well as including TWI's Core Research Programme in the conference programme again, we are also holding the TWI Innovation Network Convention 2022 concurrently with the conference at TWI Cambridge, on Friday 22 July. In doing so, we hope that delegates for both events will benefit from the cross-fertilisation of research and development (R&D) activities, and industry-academia networking.

2022 to date has marked two momentous achievements in the NSIRC story, both of which we are proud to share with you. This year sees NSIRC celebrate its **10th anniversary**, since being established by founding partners Lloyd's Register Foundation, bp and TWI. During this time, NSIRC students, supported by their supervisors, have worked tirelessly and diligently to advance fundamental research into real world applications for a safer world, enabled through undertaking industry-based PhDs and MScs.

Key NSIRC achievements include:

- 208 Doctoral and 160 Masters students undertaking postgraduate research in an industrial setting to advance their knowledge and make scientific breakthroughs
- 100% employment rate for PhD students within one year of graduating
- Females represent 32% of NSIRC PhD students, compared to a UK engineering workforce female representation of 16.5%
- A network of more than 45 university partners, via signed agreements, in the UK and overseas
- £150m invested in facilities, equipment and studentships
- 800+ publications
- 13 standards updates contributed to by NSIRC research

Our second cause for celebration is the launch of **NSIRC International**, the objective of which is to extend NSIRC's pioneering industry-academia model out to university partners internationally, supporting the career development of future engineers, and contributing to the economic and societal infrastructure, in overseas regions. Memorandums of Understanding have now been signed between TWI and King Mongkut's University of Technology North Bangkok (KMUTNB) to establish NSIRC Thailand, and with Parahyangan Catholic University (UNPAR) to create NSIRC Indonesia. NSIRC International, funded by Lloyd's Register Foundation, will offer qualifications based on NSIRC's Technology Strategy and Roadmap themes of digitalisation, smart manufacturing, new materials and circular economy, and net zero.

TWI's Core Research Programme (CRP) is designed to meet the needs of our Industrial Member companies, via projects that address the most significant challenges facing both them and TWI, in relation to technology areas and/or industry sectors that have been identified as being of critical interest to future operations. Projects, a selection of which will be presented during the conference, focus on either engineering, materials or manufacturing technologies, as well as provide opportunities for NSIRC students to work on some of them. Visit the new CRP website on twi-global.com for an in-depth look at this flagship TWI programme.

The **TWI Innovation Network (TWIIN) Convention** is an annual platform bringing together partners from the UK, Europe and internationally to share the latest thinking in technology R&D, project collaboration and public funding. As well as supporting companies and organisations of all sizes with technology acceleration through different centres and programmes, TWIIN also offers Innovation Consultancy Services alongside training courses introduced this year, designed to upskill participants in concept development and proposal writing for public funding bids, as well as navigate publicly funded project audits. This year's convention programme includes stimulating speakers, and our popular partner matching and brokerage sessions.

Lastly, I hope you enjoy this year's in-person events, and will join me in congratulating the NSIRC students on their outstanding work which they look forward to sharing with you during the conference.

Tat-Hean

Professor Tat-Hean Gan
NSIRC Director
TWI Director, Innovation & Skills

nquiringminds

AI - CYBER - IOT

SECURE INDUSTRIAL EDGE & CLOUD

INDUSTRIAL CONNECTIVITY

NquiringMinds TDX cloud and edge platfrom, connects easily and securely to industrial equipment and processes. TDX provides out of the box API and analytical capabilities.

INDUSTRIAL APPLICATIONS

The systems has been proven in field with applicatoins as diverse as predictive maintainance, yield optimisation, advanced control systems and human in loop workflows

CYBER SECURITY

Providing a ZeroTrust development framework, the TDX can create dynamic inventroy of connected devices and use advanced AI techniques to detect and protect against cyber attack

Available for Collaborative Projects and Operational Deployments
info@nqminds.com

info@nqminds.com
www.nqminds.com
@nqminds

CYBER ESSENTIALS
CERTIFIED PLUS

Most Innovative Cyber SME 2022 Finalist

Department for Digital, Culture, Media & Sport

THANK YOU TO OUR FOUNDING PARTNERS

We would like to sincerely thank our founding partners, Lloyd's Register Foundation, TWI Ltd and bp, as well as our lead academic partner Brunel University London, for their continued support of our students.

Brunel University London

bp

Lloyd's Register Foundation

TWI

nsirc 10th ANNIVERSARY

33

Number of countries NSIRC students come from

£150m

Invested in PhD research facilities, equipment and studentships

NSIRC - ABOUT US

NSIRC (National Structural Integrity Research Centre) is a state-of-the-art postgraduate engineering facility, established and managed by structural integrity specialist TWI Ltd, and founded in October 2021, with the aim of becoming the world centre for structural integrity research.

The centre works closely with industrial partners Lloyd's Register Foundation, TWI and bp, as well as lead academic partner Brunel University London.

Since 2012, NSIRC has collaborated with over 40 world-leading universities, including the University of Cambridge, University of Oxford and the National University of Singapore, to meet industrial challenges. The collaborating partners provide academic excellence to address the need for fundamental research, as well as high-quality, industry-relevant training, for the next generation of structural integrity engineers.

NSIRC advances fundamental research to:

- Support the safe operation of products and structures
- Develop innovative, fit-for-purpose technologies and design rules
- Demonstrate solutions for long-term asset management

This includes risk-based management, engineering critical assessment, non-destructive testing, structural health and condition monitoring, and health management for use in real world settings.

96

PhDs successfully completed

AFFILIATED UNIVERSITIES

At NSIRC we combine academia with industry, working closely alongside lead academic partner Brunel University London, as well as more than 40 other affiliated universities...

KEYNOTE SPEAKERS

Dr Jan Przydatek
Director of Technologies, Lloyd's Register Foundation

In this role, Jan has led activities that have taken a safety perspective of current and future engineering and supply chain activities and created programmes focused on enhancing safety.

He chairs the Structural Integrity Research Foundation, is on the boards of Lloyd's Register Decarbonisation Hub, HSE's Discovering Safety programme, Assuring Autonomy International programme and International Consortium of Nanotechnology (ICoN). He is also on Innovate UK's Trustworthy Autonomous Systems Strategic Advisory Board.

In addition, Jan represents the Foundation in the Safetytech Accelerator Ltd. Prior to joining the Foundation, he had 20 years' experience in the engineering industry following his degree in Materials Science and Engineering and PhD at Imperial College, London.

Dr John Morlidge
Deputy Director Aerospace, Innovate UK

Working with industry and government to maintain and grow the UK's competitive position in civil aerospace design and manufacture, supporting investments in next generation flight that aim to revolutionise the way people, goods and services move.

Prior to joining Innovate UK, John spent over 15 years in the private sector working in research and technology transfer.

His technical expertise is in materials science and instrumentation, specialising in structural heath monitoring and the prevention of corrosion and degradation of materials in demanding environments.

He is a Chartered Engineer and a Fellow of the Institute of Materials, Minerals and Mining.

Over 800 collective years of postgraduate academic research that was called for by global industry

nsirc | 10th ANNIVERSARY

AGENDA - DAY 1

Time	Lecture Room 1	Lecture Room 2
09:00	Arrival and Refreshments	
09:30	Introduction and Welcome to Annual NSIRC Research and Innovation Conference 2022 Prof Tat-Hean Gan, NSIRC Director	
09:50	Celebrating 10 years of Engineering a Safer World Jan Przydatek, Director of Technologies, Lloyd's Register Foundation	
10:20	Move to Designated Presentation Rooms	
	Lecture Room 1	**Lecture Room 2**
	Coatings Technologies	**Additive Manufacturing**
10:30	**Aamna Asad** Novel Characterisation of Additives for Advanced Materials	**Saad Ahmed** Correlating Defects to Fatigue Performance in Selective Laser Melted Al-Si10-Mg Alloys
10:55	**Adriana Castro Vargas** Simulation of the Damage Tolerance of TSA-Coated Steel in Artificial Seawater	**Siddharth Patil** Bead Geometry and Thermal Analysis of the Low Carbon Steel Manufactured by Directed Energy Deposition (DED) Arc Process
11:20	Break	
11:40	**Ana Carolina Araujo Lascano** Performance of Painted TSA in Simulated Marine Environment	**Francesco Careri** Optimisation of L-PBF Parameters for a Novel A20X® Alloy Thin-walled Heat Exchanger
12:05	**Nigar Malik** Development of Novel Coatings for the Protection of High Strength Steels	**Ahamed Ameen** Effect of Heat Input on Microstructure of C-Mn Steel Walls Fabricated by Wire-and-Arc Additive Manufacturing
12:30	Lunch, Networking and Exhibition	

Read the Conference Abstracts here - **www.nsirc.co.uk/conference2022**

13:30	**Muhammad Haris** Developing Novel Coatings for Improved Performance of Fasteners for Dissimilar Material Joining Applications	**Ali Alperen Bakir** Structural Integrity Assessment of Cold Spray Repaired of High-Strength Aluminium Alloy 7075 Specimens
13:55	Core Research Programme Showcase Presentation: **Kranthi Maniam** REACH Compliant Aluminium Pretreatments (Cr(VI) Replacement (33541)	Core Research Programme Showcase Presentation: **Cui Er Seow** Investigation of Integrated Additive Manufacturing from Feedstock to Part Quality (33631)
	Joining Technologies	**Inspection and Monitoring**
14:20	**Man Chi Cheung** Design of a Novel Hybrid Composite-to-Metal Joint for the Application in Naval Vessels	**Dandan Liu** Hydrogen Induced Cracks Monitored with Acoustic Emission Under the Laboratory Condition
14:45	**Break**	
15:05	**Kartikey Mathur** Real Time Evaluation of Weld Quality for Friction Stir Welding (FSW)	Core Research Programme Showcase Presentation: **Kyriakos Flentzeris** Characterisation of Discontinuities with Advanced UT (33578)
15:30	Core Research Programme Showcase Presentation: **Abbasi Gandhi** Addressing the Challenges Of Electrification and Recycling (33559)	Core Research Programme Showcase Presentation: **Miles Weston** Development of Novel Ultrasonic Inspection Capability for Sizing of Rough Cracks (33596)
15:55	**Haolin Fei** Digital Process Iteration Human-Robot for Improved Brazing Safety and Productivity	
16:20	**Amarachi Frances Onwuegbuchulem** Influence of Laser Surface Modification on the Adhesion Properties of PEEK	
16:45	**Closing Words**	
17:00	**End of Day 1**	

AGENDA - DAY 2

Time	Lecture Room 1	Lecture Room 2
09:00	Arrival and Refreshments	
09:30	Welcome Tat-Hean Gan, NSIRC Director	
09:45	Innovate UK's Landscape on R&D John Morlidge, Deputy Director Aerospace, Innovate UK	
10:15	Move to Designated Presentation Rooms	
	Lecture Room 1	**Lecture Room 2**
	Structural Integrity	**Composites and Polymers**
10:25	**Anurag Niranjan** Crack Behaviour in the Residual Stress Field at Fillet Welds in Ship Structures	**Burak Sakarya** Development of a Quantitative Leak-before-break Design Concept for Composite Pressure Vessels
10:50	**Hanwei Zhou** Fatigue Propagation from Short Cracks in Thick Welded Steels	**Magali Rego** Developing a Closed-Loop Recycling of Epoxy Thermoset Resins Through a Chemical Design Approach
11:15	Break	
11:35	**Funke Dacosta-Salu** Thermal Fatigue at Mixing Points in Industrial Pipework	**Hamad Raheem** Resonant Coupling of Piezoelectric Micromachined Ultrasound Transducers with Polymer Specimens in Different Media

Time		
12:00	**Adam Fisher** Using Kinetic Activation-Relaxation Technique to Investigate Crystal Growth in NiAl Superalloys	**Maciej Gierulski** Electrofusion Welding of Thermoplastic Composite Pipes
12:25	Lunch, Networking and Exhibition	
13:30	Core Research Programme Showcase Presentation: **Emre Akgun** Investigation of Corrosion fatigue of offshore wind substructures (33593)	Core Research Programme Showcase Presentation: **Mike Troughton** Effect of Insufficient Homogenisation of Pigmented Resin During the Extrusion of Polyethylene Pipes on the Mechanical Performance of Butt Fusion Joints (30554)
13:55	**Zeng Chen** A Novel Unified Parameter for Characterising Constraint Level of Multi-Axial Bend Specimen	**Mohammad Alghfeli** An Approach to Enhanced HDPE Nanocomposites
14:20	**Paul Sukpe** Crack Tip Constraint in Typical High Strength Steel Components in Arctic Conditions	**Thamasha Samarasinghe** Design and Development of Composite Panels with Variable Thermal Conductivity for Li-ion Battery Module
14:45	Break	
15:05	Core Research Programme Showcase Presentation: **Yin Jin Janin** Integrating Diverse Approaches to Reliability of Engineering Structures (32878)	
15:30	Awards and Closing Words	
16:00	Award Winner Photos and Close	

Aamna Asad

Aamna graduated with a first class BEng(Hons) from Lancaster University in 2017. She later pursued an MSc in Advanced Chemical Engineering from The University of Manchester where her research focused on the determination of self-diffusivities of gases in petroleum using Molecular Modelling techniques. In October 2018, Aamna started an industrial CASE PhD with the University of Cambridge and TWI Ltd. Her work focuses on establishing a methodology to characterise, design and optimise the functionalisation process of silica nano-particles, particularly Stober and fumed silica nano-particles.

Novel Characterisation of Additives for Advanced Materials

Alan Taylor[1], Mick Mantle[2]
[1]TWI, [2]University of Cambridge
4th Year of PhD

Keywords: Silica, NMR, nano-particles, hydrophobic, functionalisation.

I. INTRODUCTION

Silica nano-particles (SNP) have various applications in many industries such as microelectronics, food, sorption, catalysis, coatings and healthcare [1], [2]. In most of these applications the advantages of silica arise from its structure and chemical nature of its surface, and hence most of its performance is controlled by these properties. The process of functionalising nanoparticles has been known for many years and is used to alter the properties of a surface. The surface of silica nano-particles can be made hydrophobic by functionalising or grafting with certain silanes (coupling agents), such as hexamethyldisilazane (HMDZ), in order to form trimethylsilyl (TMS) groups (- Si(CH3)3). Grafting can also be achieved by using other modifying agents, such as alkoxy-, and chlorosilanes [3]. Surface functionalisation has different applications in a variety of applications including catalysis, biochemical sensing, biolabeling, coatings and photonics. Hydrophobised silica nanoparticles in general, are of interest from a practical point of view because these materials are well-suited for many applications including the enhancement of coatings, adhesives and polymers.

This research focuses on developing an innovative method to establish improved characterisation methods to quantify the surface of silica additives. Enhanced characterisation methods will allow more surface chemistry specific correlation of the additives with the behaviour, such as thickening effects, free flow aids, filler loadings, rheology control etc. This will enable differentiation between the growing range of commercial additives and allows these differences to be qualified and quantified. Current work also includes building a dynamic model to be able to replicate high-quality nuclear magnetic resonance (NMR) qualititative spectral data using knowledge of cross polarisation (CP) NMR dynamics. This technique is a useful tool that can be used to save valuable experimental time.

II. METHODOLOGY

As part of this research, a number of commercially available (functionalised and unfunctionalised) pyrogenic silicas were reacted via vapour deposition techniques with hexamethyldisilazane to facilitate and attain maximum functionalisation. Table 1 summarises physical properties of the respected silicas. Samples were dried at 200ºC for 24 hours in order to remove any residual HMDZ and physically adsorbed water. Solid-state ^{1}H, ^{13}C and ^{29}Si nuclear magnetic resonance (NMR) techniques were used to study the extent of additional functionalisation on the silica particles.

Sample	A200	R 812S	R 8200	R 9200
Average Surface Area (BET) m^2/g	200 ± 25	260 ± 30	160± 25	170± 20
Average Primary Particle size (nm)	12	7	-	-
Loss on drying 2hrs @105 C (%)	≤ 1.5	≤ 0.5	≤ 0.5	≤ 1.5
C content (wt. %)	-	2.0 – 3.0	2.0 – 4.0	0.7 – 1.3
Functionalising agent	-	HMDZ	HMDZ	Dichlorodimethyl-silane

Table 1: Pyrogenic silicas - basic properties

III. RESULTS AND DISCUSSION

The chemistry of silica has been studied through history by various authors, using ^{1}H and ^{29}Si NMR methods. The various species that can be identified in the following spectra are summarised in Figure 1. Each species can be identified with a certain chemical shift on the NMR spectrum.

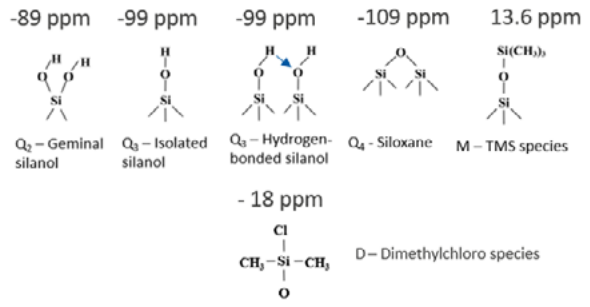

Figure 1: Species present on the silica surface

Figure 2 displays the collective ^{1}H MAS NMR spectra of all pre-functionalised and all post-functionalised silicas. The peak at approximately 1 ppm corresponds to the functionalisation peak. On functionalisation, the intensity of this peak increases. However, the resolution of ^{1}H MAS NMR is unable to depict with certainty whether this peak is due to a M or D group.

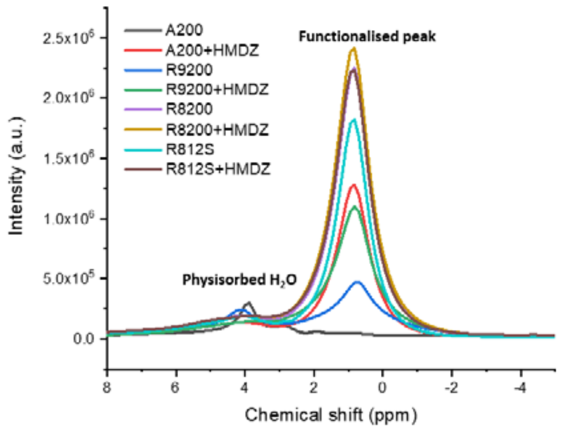

Figure 2: ^{1}H MAS spectra of as-received and additionally functionalised aerosils

Figure 3 shows the ^{13}C Cross Polarisation (CP)-collective MAS spectra of all functionalised silica samples which signifies the carbon content in these materials. It is evident that all the fumed silicas, except R9200, show an M region at 0 ppm indicating that they are all TMS functionalised. The R9200 exhibits a D region (3 ppm) which indicates that it is functionalised with a dimethyl silane species. On further functionalisation with HMDZ, R9200 exhibits a broad region that extends to 0 ppm. The presentation will discuss the characteristics of the further functionalised fumed silicas (R series) in greater detail.

The equivalent ^{29}Si Cross Polarisation (CP)-MAS spectra is displayed in Figure 4 for A200, R9200 along with their functionalised counterparts. The M peak, for additionally functionalised samples is almost the intensity of the Q3 peak (-99 ppm). This is due to high abundancy of hydrogen atoms on the TMS groups which provides greater cross polarisation energy transfer and results in a better signal. The Q3:Q4 ratio decreases on functionalisation which indicates that the Q3 species are the active sites taking part in the functionalisation reaction. However, in order to quantify and qualify the data and obtain more structural information it is essential to gather a better understanding of the CP kinetics and dynamics.

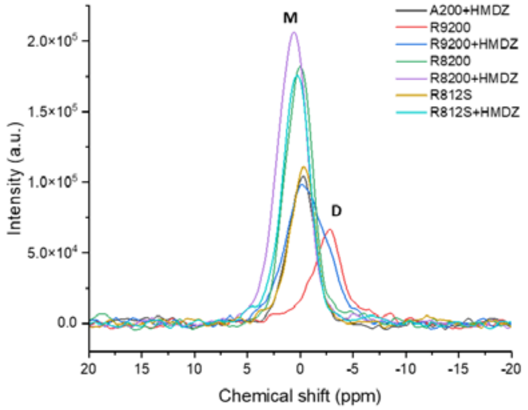

Figure 3: ^{13}C CP-MAS spectra of as-received and additionally functionalised silicas

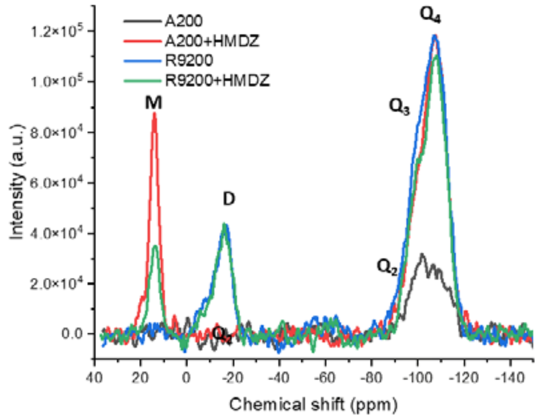

Figure 4: ^{29}Si CP-MAS spectra of as-received and additionally functionalised silicas

IV. FUTURE PLAN

In the current state, this research is focused on understanding the chemistry of the pyrogenic silica surface and the changes made following additional functionalisation. It has been determined that it is possible to further functionalise i.e. reach potential maximum functionalisation on the commercial R-series silicas. Future work consists of trying to understand the kinetics and dynamics of the CP NMR measurements to form a model. This model will help optimise the experiments in hand and quantify the data and gather further structural information of the samples.

REFERENCES

[1] C. C. Liu et. al, J. Am. Chem. Soc., vol. 118, no. 21, pp. 5103–5119, Jan. 1996.

[2] T. I. Suratwala et. al, Journal of non-crystalline solids 316.2-3 (2003): 349-363.

[3] I. S. Protsak et. al, , Nanoscale Res. Lett., vol. 14, no. 1, p. 160, Dec. 2019.

Adriana Castro-Vargas

Adriana joined NSIRC in January 2021 as a PhD scholar on ProCoat project at the University of Leicester sponsored by Lloyd's Register Foundation. The project is looking at the protection of offshore wind turbines using low-cost, damage tolerant, sacrificial coatings. Her work is focused on developing new corrosion models to predict coatings performance and validating the models using innovative evaluation techniques. Adriana has a background in Metallurgy and Materials Science, furthermore has done research and teaching in Materials Engineering. She is a member of the American Society of Mechanical Engineers (ASME), Colombian Association of Corrosion and Protection (ASCOR) and the Association for Materials Protection and Performance (AMPP).

Simulation of the Damage Tolerance of TSA-Coated Steel in Artificial Seawater

Shiladitya Paul[1], Simon Gill[2]
[1]TWI, [2]University of Leicester
2nd Year of PhD

Keywords: sacrificial protection; thermal spray aluminium; damage tolerance; corrosion modelling.

I. INTRODUCTION

Thermal Spray Aluminium (TSA) coating is primarily used to protect offshore structures, including atmospheric, splash and submerged areas [1]. TSA acts as a barrier and offers cathodic protection even if some damage occurs during the operational life or installation, such as floating debris or accidental impact. Nevertheless, damage to the TSA, i.e., in the presence of exposed steel, reduces service life due to the anodic nature of the coating.

The protection mechanism offered by TSA coating with an exposed steel surface in artificial seawater involves multiple and simultaneous reactions; it can be summarised as follows, (see Figure 1): (i) When aluminium and steel are in electrical contact, a galvanic couple is established between these metals (TSA as anode and exposed steel as cathode) hence, TSA provides cathodic protection by acting as a sacrificial anode; (ii) on the cathodic surface, the oxygen reduction and/or hydrogen evolution take place; consequently, the local pH increases due to the production of OH- ions promoting the co-precipitation of insoluble compounds rich in magnesium and calcium; (iii) the formation of deposits on steel reduces the cathodic area, and the diffusion of dissolved oxygen is hindered; (iv) aluminium corrosion products precipitate on the surface as well as inside the pores of the coating, providing the plugging effect which reduces the self-corrosion of aluminium [1].

The damage tolerance can be defined as the ability of TSA coating to polarise exposed steel to protective potentials (according to DNV-RP-B401) without excessive consumption of the coating. However, the quantification of the damage level that TSA can tolerate is not fully explored. While lab tests conclude that TSA provides protection when the defect surface is around 5% [1], there are limited data on damage tolerance in the presence of a large cathode.

This work seeks to address the above gaps through numerical simulations considering the combined effect of deposits and corrosion products using data from the previous studies of cathodic reactions by Electrochemical Impedance Spectroscopy (EIS) [2].

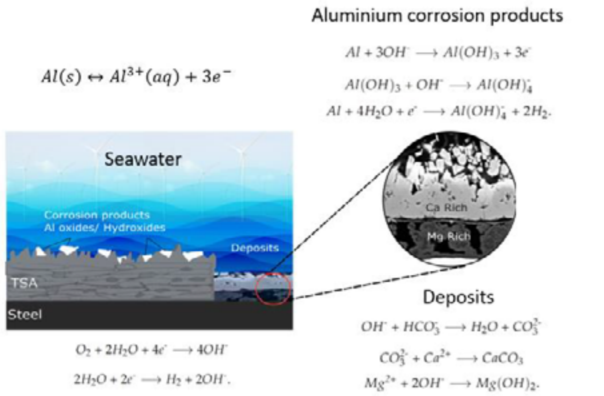

Figure 1. Schematic representation of TSA coating with damage.

II. APPROACH

Exposed steel surfaces of 5%, 50%, and 90% were recreated in a 2D axi-symmetric dimension component by varying the defect radius with 5.0 mm, 16.0 mm, and 21.4 mm respectively. A film resistance was assumed as a boundary condition on each electrode surface to evaluate the combined effect of corrosion products and deposits on the TSA damage tolerance and will be named as follows: E0: No corrosion products or deposits; E1: Corrosion products and deposits formed in 10 d; E2: Corrosion products and deposits formed in 20 d.

III. FINDINGS

Potentials are against Ag/AgCl (Sat. KCl) reference electrode (Eref= +0.199 V vs. SHE). Figure 2 shows a comparison between the simulated potential for TSA-coated steel with 5% and 50% of exposed steel, and the effect of the deposits/corrosion products formed after 20 days. In the case of 90% of exposed steel, potentials of -0.73 V and -0.796 V were calculated with the effect E0 and E2, respectively.

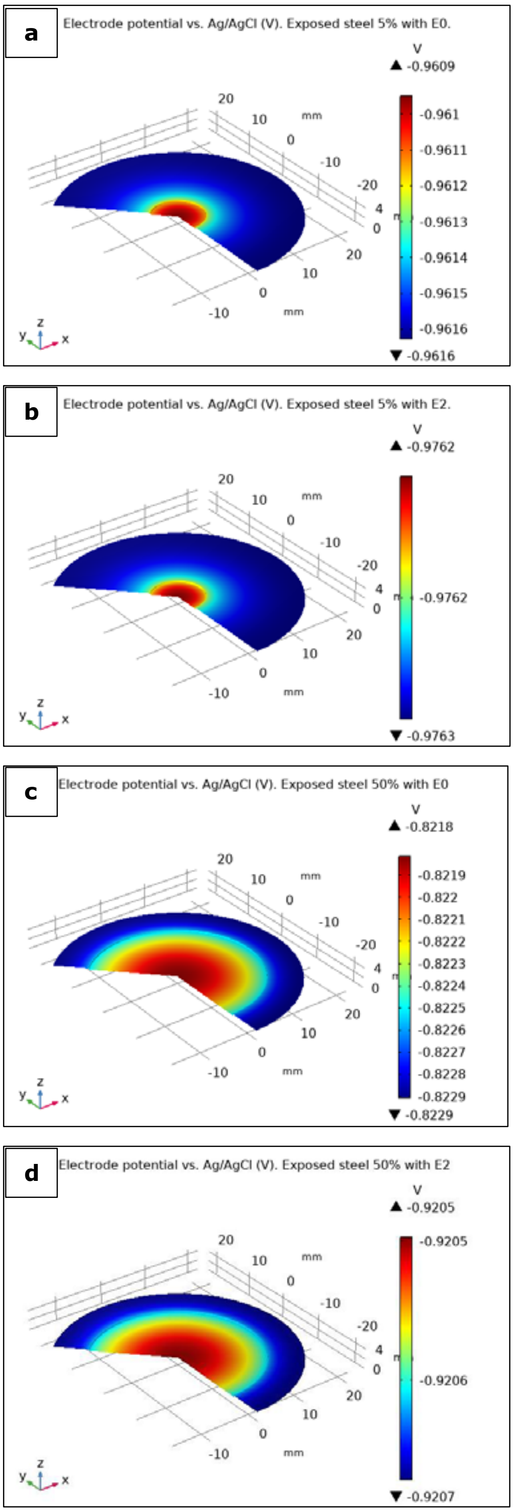

Figure 2. Simulated potential. (a). 5% and E0, (b). 5% and E2, (c). 50% and E0, (d). 50% and E2

The corrosion rate of TSA was calculated from anodic current density using Faraday's law. The results shown in Figure 3 corroborate the findings of several previously reported works in the estimation of corrosion rates by Linear Polarisation Resistance (LPR) and dissolved ions [1,2].

At the beginning of the immersion, rapid corrosion of the aluminium occurs, which tends to protect the exposed steel due to its anodic nature. Over time, the corrosion rate decreases due to the accumulation of deposits/corrosion products on the exposed steel and coating surface.

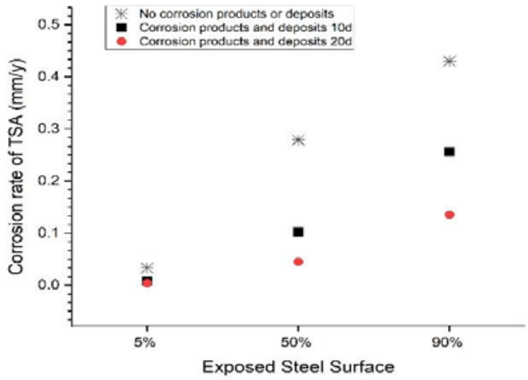

Figure 3. Simulated corrosion rate of TSA

IV. CONCLUSIONS

- Corrosion rate of TSA increases with an increase in the area of exposed steel.
- The instantaneous corrosion rate of TSA decreases with exposure time.
- Corrosion products and deposits (Ca- and Mg-compounds) reduce the corrosion rate of TSA even in the presence of defects.

V. FUTURE PLAN

In situ optical monitoring as a complementary technique will allow a better understanding of the mechanism of protection offered by TSA in presence of damages in a simulated marine environment.

VI. ACKNOWLEDGEMENTS

This publication was made possible by the sponsorship and support of Lloyd's Register Foundation (LRF) and University of Leicester. The work was enabled through, and undertaken at, the National Structural Integrity Research Centre (NSIRC), a postgraduate engineering facility for industry-led research into structural integrity established and managed by TWI through a network of both national and international Universities.

REFERENCES

[1] R. Grinon-Echaniz et al., Prediction of Thermal Spray Coatings Performance in Marine Environments by Combination of Laboratory and Field Tests. Coatings 11, 1-15 (2021).

[2] R. Grinon-Echaniz et al., Study of Cathodic Reactions in Defects of Thermal Spray Aluminium Coatings on Steel in Artificial Seawater. Corrosion Science 187, 109514 (2021).

Ana Carolina Araujo-Lascano

Ana received her education in Chemical Engineering from the University San Francisco of Quito in Ecuador (BSc). To pursue her aspirations, she gained a partial scholarship to study Structural Integrity with Brunel University London (MSc), where she graduated with distinction. She carried out her second master program in Corrosion Control Engineering from The University of Manchester (MSc), where she also gained a distinction. Ana is currently a NSIRC PhD student of Coventry University funded by Lloyd's Register Foundation and Coventry University. Her research study is focused on the "Performance of Painted Thermally Sprayed Aluminium (TSA) in Simulated Marine Environment".

Performance of Painted TSA in Simulated Marine Environment

Shiladitya Paul[1], David Parfitt[2]
[1]TWI, [2]Coventry University
3rd Year of PhD

Keywords: duplex coatings, thermally sprayed aluminium, TSA, organic coatings

I. INTRODUCTION

One common approach to mitigate corrosion in offshore applications requires the use of cathodic protection often in conjunction with dielectric coatings. Nevertheless, once the protective organic coating is damaged they offer little or no protection to the asset. An alternative mitigation method is the use of duplex coating systems that includes a sacrificial layer of thermal spray coatings (either Al or Zn-Al) top-coated with paint.

An overall service life of 50 years was expected to achieve from these systems. Thermally sprayed aluminium (TSA) has been widely used on large scale projects in marine environments with great success. Difficulties, arise, however, when a thick organic coating is applied on TSA. Degradation of TSA with the formation of blisters has been reported in as little as ten years of operation [1]. It has been assumed that the presence of blistering is primarily due to corrosion products under the organic coating [1].

The mechanism of this blistering, however, has not been fully explored. The aim of this project is to address this knowledge gap by exploring the corrosion mechanism of damaged duplex TSA coatings. To study this degradation process, damaged duplex coating (TSA top coated with epoxy and polyurethane 'PU') on S355 steel were exposed to synthetic seawater. The open circuit potential was monitored. Lastly, microstructural characterisation of the samples is being performed to understand the blistering mechanism.

II. METHODOLOGY

A. Sample Preparation

Duplicate samples with dimensions of 76x50x6 mm were prepared with S355 steel as substrate material and TSA, epoxy and PU as coatings.

S355 steel samples, supplied by Parker steel, were ultrasonic cleaned in acetone to remove the impurities, adhered grease and residual surface debris. To produce suitable roughness profile, the specimens were blasting with chilled iron grit media (G12) at 40 psi set pressure. The samples were then sprayed with 1050 aluminium wire, supplied by Metallisation Ltd., to achieve a TSA thickness of ~200 µm using twin-wire arc spray. After TSA application, these samples were coated (brush applied) with AkzoNobel's epoxy (intergard 410) and polyurethane (interthane 990). The wet layer was evened using a bar coater to attain a uniform dry film thickness of ~150 µm of each layer. The nominal dry film thickness was measured with PosiTest gauge at three locations.

Additionally, a circular holiday (artificial defect) was introduced at the center of the samples using a flat drill with a diameter of 16 mm and 0.9 mm depth corresponding to 5% of sample surface area to exposed steel and imitate damage during service. After the introduction of the holiday, electrical connections between the samples and the potentiostat were created by a threaded rod (insulated with heat-shrink tubing and lacquer). All faces of the samples, except the side with the coatings, were also isolated with lacquer.

B. Immersion Experiments

A conventional three electrode cell consisting of a working electrode (sample), Pt/Ti counter electrode and a reference electrode of Ag/AgCl (saturated with KCl) was used to conduct long-term tests in synthetic seawater ASTM D1141. The potential was monitored using a Biologic VMP-300 potentiostat. The samples were under immersion for over 18 months.

C. Microstructural Characterization

Material characterization is performed with optical microscope, Scanning Electron Microscope (SEM) with Energy Dispersive X-Ray Analysis (EDX) and Raman Spectroscopy.

III. FINDINGS/RESULTS

Figure 1 shows the corrosion potential of painted TSA coating on steel (with 5% defect) in synthetic seawater measured against Ag/AgCl reference. DNVGL-RP-B401 suggests a protective potential of steel structures from -0.75 to -1.10 V vs Ag/AgCl (saturated KCl) [2]. The inset in Figure 1 shows that the sample was under-protected during the first 2-days of immersion. After this period, the steel specimen was polarized towards the protective potential range till the end of the test.

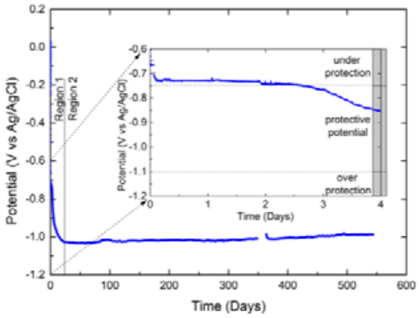

Figure 1: Potential of the sample over 1-year and 6-months in synthetic seawater

The evolution of potential (Figure 1) shows a sharp drop of potential within the initial days of immersion (region 1), followed by a plateau with small variation of potential with time (region 2).

Region 1: The potential falls to -0.73 V in 2.5 hours of immersion. This then decreased gradually to around -0.75 V within 3 days. A marked decline is subsequently observed to values below to -1 V in 20 days. Two factors are possible to explain the reduction of potential. Firstly, the initiation of the corrosion process in the specimen leads to the formation of deposit films on steel (cathode). As the exposed surface area of steel is decreased, the potential is also reduced. Secondly, the air-formed oxide film of TSA is dissolved due to the interaction with seawater. Hence, more active surface area of aluminium (anode) becomes available to, subsequently, corrode and provide sacrificial protection to steel. What can be clearly seen at this stage is that the values of potential at the start of exposure represent the mixed potential between aluminium and steel in seawater.

Region 2: After the reduction of potential, a plateau is reached at ~-1.02 V. The potential then increases only slightly with time to above -0.99 V. The stabilization of potential at -1.0 V is influenced by the protective nature of the oxide (on aluminium) and the morphology of the deposits (on steel). The ratio of the cathode surface area with respect to the anode also plays an important role on the corrosion process. When a larger cathode is joined to a smaller anode, a higher current density of the anode is released to balance the cathodic reaction, thus increasing the corrosion rate of the anode and affecting the potential values. The exposed surface area of steel and aluminium is 190 and 9.8 mm^2, respectively. Since steel surface area is over nineteen times more than TSA, a higher dissolution of Al is expected. This faster consumption of aluminium tends to slightly raise the potential towards that of steel with time, as observed from day 20 to the end of the test.

Figure 2 shows the images of the sample before and after 18 months of immersion in synthetic seawater. It can be noticed that white corrosion products are developed below the organic coating located near to the defect region, promoting the appearance of blisters. The EDX spectra (Figure 3A) shows Al and O as main constituents, alluding the presence of Al oxides and hydrated oxides.

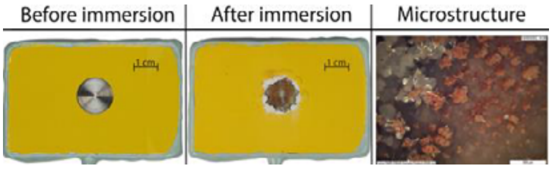

Figure 2: Images of the sample before and after immersion in synthetic seawater

Figure 2 also shows white and brown deposits developed on top of steel, most likely associated with the formation of calcareous deposits and rust, respectively. The EDX spectra (Figure 3B) also confirms the presence of Ca, Mg and Fe elements.

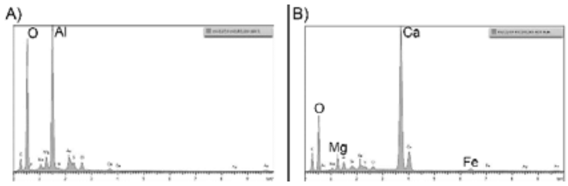

Figure 3: EDX pattern A) at the edge of the holiday, B) at the centre of the holiday

IV. DISCUSSION/CONCLUSIONS

- When duplex coating is damaged, degradation of TSA occurs to cathodically protect steel, leading to the formation of aluminium corrosion products on TSA and calcareous deposits on steel.
- Painted TSA coatings forms blisters when exposed to seawater.

V. FUTURE PLAN/DIRECTION

- To identify the corrosion deposits by using Raman Spectroscopy.

REFERENCES

[1] Knudsen O. O, Rogne T, Rossland T. Rapid degradation of painted TSA. Corrosion 2004.
[2] Det Norske Veritas. Recommended Practice DNV-RP-B401: CATHODIC PROTECTION DESIGN. 2011.

ACKNOWLEDGEMENTS

This publication was made possible by the sponsorship and support of Lloyd's Register Foundation (LRF) and Coventry University. The work was enabled through, and undertaken at, the National Structural Integrity Research Centre (NSIRC), a postgraduate engineering facility for industry-led research into structural integrity established and managed by TWI through a network of both national and international Universities.

Nigar Malik

Nigar graduated with Materials engineering degree (2009) from University of Engineering and technology, Pakistan (BSc). Her master degree is in Mechanical engineering (2016) from Queen Mary university of London. She is currently an NSIRC PhD student at University of Leicester. Her PhD involves development of novel coatings for corrosion protection of high strength steel.

Development of novel coatings for the protection of high strength steels

Shiladitya Paul[1], Ben Robinson[1], Karl Ryder[2]
[1]TWI, [2]University of Leicester
3rd Year of PhD

Keywords: Cadmium, REACH, zinc-nickel coatings, electrodeposition.

I. INTRODUCTION

Cadmium (Cd) coatings are commonly used for enhanced corrosion protection of various materials in numerous industrial sectors such as aerospace, defence, automotive, electronics, etc. These coatings, when employed on steel, act as sacrificial coatings owing to their corrosion potential being more negative than that of steel. Thus, in case of corrosion these coatings deteriorate preferentially thereby protecting steel [1]. Cadmium demonstrates admirable engineering properties namely exceptional corrosion protection, good electrical conductivity, high lubricity and solderability [2]. However, it is toxic in nature and in addition to being a carcinogen, it also contributes to respiratory illnesses and kidney failure. Moreover, cadmium sublimes in hard vacuum environments and these sublimation products can redeposit on different equipment which could lead to malfunction of that equipment. This is particularly dangerous in aerospace industry [26]. Thus, it is a substance of high solicitude and its usage is restricted in various industrial sectors.

There is ongoing research for cadmium's replacement and the objective of this research is to develop coatings that can be used as cadmium's alternative. Acquired coatings should be REACH* complaint. Some of the potential candidates that are under consideration include electrodeposited zinc (Zn) [4], zinc alloys [5] and aluminium (Al) [6]. Zinc-nickel coatings have been of particular interest due to their superior corrosion resistance compared to pure zinc or zinc alloy coatings [2]. Studies reveal that nickel content of 10-15 wt % in electrodeposited Zn-Ni alloy coatings result in optimum corrosion protection of steel substrate [6]. At this composition range, corrosion resistance provided by these alloy coatings is 5 – 6 times better than that for pure zinc coatings of equal thickness [4].

In this work, zinc-nickel (Zn-Ni) alloy coatings are electrodeposited using an alkaline bath as coatings deposited using acid baths are susceptible to hydrogen embrittlement. These coatings are electrodeposited keeping in consideration the complexity of shapes that will be coated, thickness of coatings and cost of production.

II. METHODOLOGY

Zn-Ni alloy coatings were electrodeposited on mild steel hull cell panels (100 x 75mm) using an alkaline bath having a pH of 13.4. This bath contained 0.02M nickel (II) sulphate hexahydrate (NiSO4.6H2O), 0.16M zinc oxide (ZnO), 3.75M sodium hydroxide (NaOH) and 0.03M diethylenetriamine ([NH(CH2CH2-NH2)2]). A nickel sheet (66 x 75mm) was used as anode. Electrodeposition was carried out in a hull cell for 10 minutes at room temperature and the coated samples were air dried.

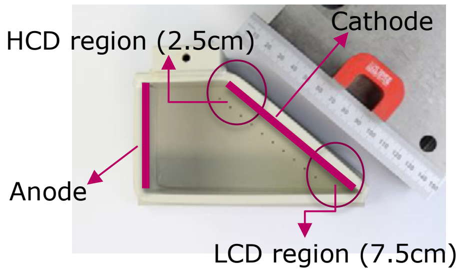

Pre-treatment of samples was done by acid pickling (utilising 10% HCl) of panels for approx. 30 seconds. This was done to strip them of the galvanised zinc coating. Panels were then rinsed in distilled water and immersed in the electrolyte.

III. RESULTS

SEM analysis revealed that when a total current of 0.5A was applied, globular clusters were observed at a distance of 2.5cm and 5cm from the high current density (HCD) region of the panel whereas a dendritic structure was observed at a distance of 7.5cm from HCD area. When the average current was increased to 1 and 1.5A, arrangement of globular clusters in a certain criss-cross structure was perceived. At higher current of 2, 2.5 and 3Amps, change in the shape of crystals was noticed however alignment of these crystals remained unchanged. EDX analysis of all samples confirmed the presence of both zinc and nickel with more amount of zinc then nickel present in coatings.

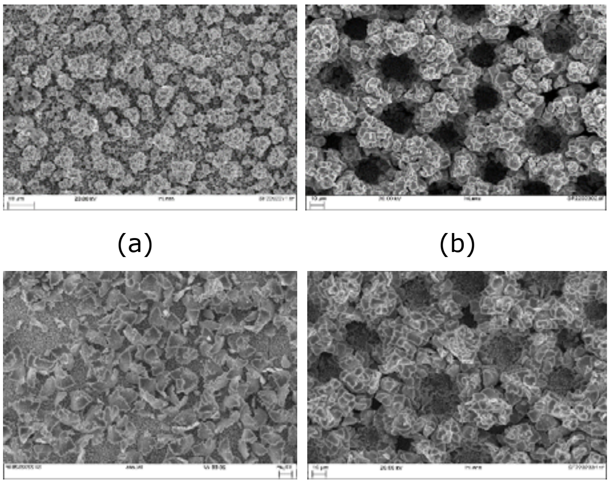

(a) (b)

(c) (d)

Figure 1- SEM images of ZnNi coatings on mild steel hull cell panels at 0.5A (fig 'a' and 'b') and 2.5A (fig 'c' and 'd').

At an average current of 0.5A , XRD analysis revealed different peaks of Zn and a zinc nickel gamma phase, γ-NiZn3, was noticed at low and medium current density region (2.5 and 5cm, respectively). When the current was increased to 1A and above (up to 3A), in addition to zinc and ϒ-Ni Zn3 peaks, zinc nickel delta, δ-Ni3Zn22 , and another zinc nickel gamma phase, ϒ- Ni5 Zn21 was observed.

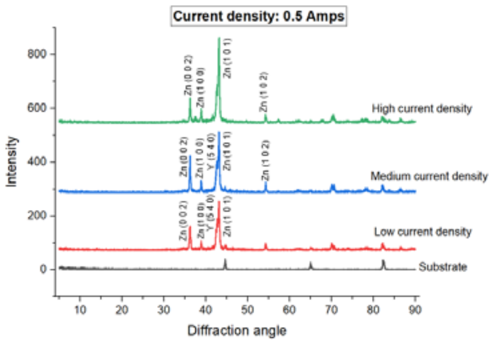

(a)

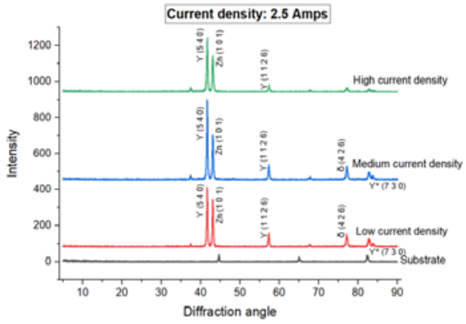

(b)

Figure 2- XRD analysis of zinc nickel coatings produced at 0.5 (a) and 2.5Amps (b).

IV. DISCUSSION/CONCLUSIONS

i) Pits observed in the microstructure of these coatings are attributed to bubble formation in the electrolyte while electrodeposition was being carried out.

ii) Coatings produced were porous particularly in high current density areas.

V. FUTURE PLAN/DIRECTION

Next steps will include electrochemical analysis of these samples, development and analysis of coatings using an acetate bath. This will be followed by replicating the work on high strength steel substrate.

REFERENCES

[1] Lee EU, Hilgeman A, Beck E, Brown S, Matzdorf C. Cadmium Alternative Coating Corrosion Performance on 4340 Steel.:1–18.

[2] Division SE, Nal C. Zn - Ni alloy – A probable replacement to Cadmium coating R Mani Sravani, Meenu Srivastava 3.1 Electrolyte composition and deposition conditions adopted: 1–5.

[3] Twite RL, Bierwagen GP. Review of alternatives to chromate for corrosion protection of aluminium aerospace alloys. 1998.

[4] a l f a n t a z i am, erb u. pulse plating of zn-ni alloy coatings. vol. 26, journal of applied electrochemistry. 1996.

[5] Wilcox GD, Gabe DR. Electrodeposited zinc alloy coatings. Corros Sci. 1993;35(5–8):1251–8.

[6] Benballa M, Nils L, Sarret M, Mü C. Zinc-nickel codeposition in ammonium baths [Internet]. Vol. 123, Surface and Coatings Technology. 2000. Available from: www.elsevier.nl/locate/surfcoat.

*REACH is European Union regulation concerning the Registration, Evaluation, Authorisation and restriction of Chemicals. It came into force on 1st June 2007 and replaced a number of European directives and regulations with a single system.

Muhammad Haris

I am a doctoral researcher in Mechanical and Aerospace engineering at Brunel University London. I have previously worked on areas related to nanocontainer-based anticorrosive coating in oil and gas industry at the Centre of Corrosion Research, University Technology PETRONAS, and Malaysia where I worked on development of anti-corrosive coatings using halloysite nanotubes (HNT's). I hold a Bachelors' degree in Metallurgical Engineering from NED University of engineering & technology, Pakistan. I am also member of the Energy Institute, BWSCC and AMPP (formerly NACE).

Developing Novel Coatings for Improved Performance of Fasteners for Dissimilar Material Joining Applications

Sullivan Smith[1], Lorna Anguilano[2], Ben Robinson[1], Timothy Mitton[2]
[1]TWI Ltd, [2]Brunel University London
2nd Year of PhD

Keywords: galvanic corrosion, dissimilar materials, coatings, fasteners

I. INTRODUCTION

The requirement for high strength light weight structures is growing, especially in the transportation industry. This has become an important challenge with the increase in demand due to requirement of high strength and lightweight materials. These light weight structures are beneficial for both environmental challenges and requires less fuel consumption resulting in lower CO2 emission. These structural components reduce the weight of cars, trucks, aircraft, or aerospace vehicle which in turn decreases the fuel consumption of the vehicle resulting in saving money and environment due to less operational costs. The demand of light weight structures is expected to continue as more stringent regulations are expected to reduce the CO2 emission for example, UK has set a net-zero target of at least 100% (previously 80%) emission reduction by 2050 [1] which means the progress needs to be accelerated in coming years and lightweight structures will be an integral part for the structural integrity and transportation industry. The use of lightweight materials such as composites and plastics is growing, especially in automotive industry. To be able to use lightweight materials in combination with more traditional materials such as aluminium, steel or alloys etc. current joining techniques must be adapted to be able to join these dissimilar materials. Industries that need to join dissimilar materials are looking for simple and fasters techniques of joining them. These dissimilar joining techniques offer unique challenges one of which is the formation of galvanic coupling between two dissimilar materials joints causing corrosion and degradation of the structure overall.

In many industrial applications, metal and composites are joined together to achieve desired properties for example by using fasteners like rivets, adhesives, or bolts. However, it is known that when joining two dissimilar materials it creates a galvanic coupling between two conducting materials in presence of corrosive environment. This occurrence can also be observed when CFRP and other metals or alloys are joined together or simply in contact for a specific time. In general Carbon fibre composites are a very efficient cathode and almost behave as a noble metal, as considered in galvanic coupling [9, 11, 12].

The research objectives are as follows:

- To examine the galvanic coupling behaviour between the dissimilar materials by using electrochemical techniques.
- To experimentally determine corrosion performance of
- suitable commercially available coatings in fastener applications.
- To experimentally determine mechanical performance of coated rivet joints by using single lap-shear test.

II. DESIGN/METHODOLOGY

A. Joint Preparation:

Dissimilar materials joints were made by joining Aluminium alloy 6061 with Carbon fibre reinforced polymer (CFRP) composites by using Self-Piercing rivet (SPR) joining process. Al alloy sheets were cut using a hydraulic metal shear machine while CFRP sheets were cut by using water jet. A stack thickness of 3.5 mm was achieved by joining two sheets of CFRP and aluminium having thickness of 1.5mm and 2mm respectively. The SPR joint was made by using rivets having shank diameter of

5mm and effective length of 5.5mm A flat die was used that had a flat bottom surface, a diameter of 10 mm, and a cavity depth of 1.2 mm. The specimens were prepared using a force-driven electro-hydraulic riveting system. A combination of rivet-die-setting force was used initially and after a series of trials to achieve an optimized joint quality.

Figure 1. SPR machine (left) Joint made using SPR technique (right).

B. Electrochemical test:

Potentiodynamic polarization test was used to investigate the corrosion mechanisms. A single lap joint (CFRP, Al, Rivet) configuration was used to study corrosion mechanism. Before the start of the test, an open circuit potential was measured for 6 hours to allow the corrosion cell to reach a steady state. The corrosion cell comprises of 3-electrode cell and ACM Ins Potentiostat. The specimen that was studied was made to be the working electrode, a saturated KCL Ag/AgCl electrode was used as a reference electrode, while counter electrode was stainless steel. The samples were washed with distilled water and acetone, dried to remove any impurities on the surface. All the tests were conducted at ambient temperatures of 25°C in 3.5wt. % NaCl. All the chemical used are of reagent grade. The electrochemical scan was performed in the potential range of -2.0 V to 2.0V. The rivet head in the joint has an exposed area of 0.230 cm2.

III. FINDINGS

The test will be conducted to investigate the coating performance of Al-Zn coated rivet when used to join CFRP-Al. The test would exhibit the corrosion performance of rivet when coupled with dissimilar materials. These results will enable us to identify the noble material characteristic in dissimilar materials joints. The obtained trend would identify the dissolution of the coating material from the rivet head, giving current densities values that will be studied to find the characteristics of dissolution of coatings and its effect of rivet base material.

IV. CONCLUSIONS

In current state this research is focused in investigating the different coating of rivets when joined with dissimilar materials. It will interesting to know how different coatings can be functionalised to help mitigate galvanic corrosion of dissimilar material joint.

V. FUTURE PLAN/DIRECTION

The future plan is to study coatings that can be used and protective of rivets while they are used in dissimilar material joints. These coatings will be applied by using available techniques and will be investigated electrochemically. Mechanical tests for joint strength will be performed as well.

VI. ACKNOWLEDGEMENTS

This publication was made possible by the sponsorship and support of TWI and Brunel University London. This work was enabled through, and undertaken at, the National Structural Integrity Research Centre (NSIRC), a postgraduate engineering facility for industry-led research into structural integrity established and managed by TWI through a network of both national and international universities.

REFERENCES

[1] C. C. Committee. (2021). Progress Report to Parliament. Available: https://www.theccc.org.uk/uk-action-on-climate-change/reaching-net-zero-in-the-uk/.

[2] X. Wu, J. Sun, J. Wang, Y. Jiang, and J. Li, "Investigation on galvanic corrosion behaviours of CFRPs and aluminium alloys systems for automotive applications," Materials and Corrosion, vol. 70, no. 6, pp. 1036-1043, 2019.

[3] M. Shan, K. Guo, G. Gou, Z. Fu, B. Yang, and W. Lu, "Effect of anodizing on galvanic corrosion behaviour of T300 CFRP/5083P-O Al bolted joints," Materials and Corrosion, vol. 71, no. 3, pp. 409-418, 2020.

[4] M. Ostapiuk, M. G. Taryba, L. M. Calado, J. Bieniaś, and M. F. Montemor, "A study on the galvanic corrosion of a sol-gel coated PEO Mg-CFRP couple," Corrosion Science, vol. 186, p. 109470, 2021/07/01/ 2021.

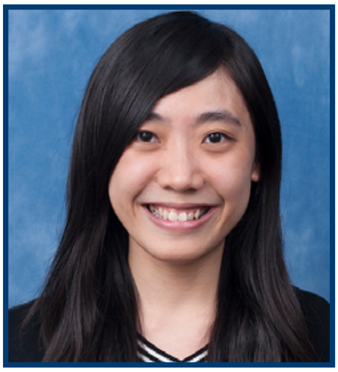

Man Chi Cheung

Pursued an MSc in Oil and Gas Engineering at Brunel University London with a research focusing on the integrity of composite structures in oil and gas industry using extended finite element method (XFEM), Man Chi continues her study with Brunel University London on designing a novel hybrid metal-to-composite joint for the application in naval vessels by adopting an existing stud forming technology in TWI. The specified objectives of her PhD project are primarily driven by an extensive simulation programme, and verified and validated against experimental results.

Design of a Novel Hybrid Composite-to-Metal Joint for the Application in Naval Vessels

Dr Chris Worrall[1], Dr Nenad Djordjevic[2], Dr Mihalis Kazilas[2]
[1]TWI, [2]Brunel University London
2nd Year of PhD

Keywords: hybrid joints; woven glass fabric; resin infusion; finite element modelling

I. INTRODUCTION

It has long been a goal of hybrid joining to produce a composite naval superstructure containing a metallic edge that can be easily welded to the metal deck of a vessel using conventional shipyard welding techniques, such as arc welding. Adhesive bonding and mechanical fastening are the two major methods for joining composite material to metal to achieve the above mentioned goal. However, adhesive bonding has poor resistance to peel or cleavage loads. Besides, it is sensitive to surface preparation and susceptible to environmental degradation. To join dissimilar materials by mechanical fastening, holes have to be drilled for fastener installation, which cuts the fibres in the composite and thus reduces its strength. As well as this, fasteners add weight to the structures.

This project develops a hybrid composite-to-metal joint shown in Figure 1, where a stud which has been machined out of the metal adherent is assembled with the composite adherent, by piercing the composite in through thickness direction. This design does not require additional material to form the through-the-thickness studs, it provides smooth surfaces without screw heads or nuts, yet potentially improves the reliability of conventional bolted or bonded joints. The adherends used in this project are 5000 serious aluminium alloy and plain woven glass fabric reinforced epoxy. The joint will be tested following single-lap shear test standard ASTM D1002-10 [1].

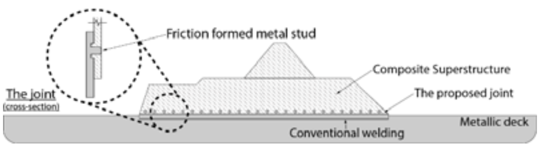

Figure 1: Design concept of the metal stud joint

The results will be compared to conventional adhesive bonded joints to evaluate the joint performance. The load-displacement curves and failure mechanisms will be analysed in detail. The above objectives will be primarily driven by an extensive simulation programme, which will be verified and validated against the experimental results.

II. METHODOLOGY

The joint to be developed in this project consists of the metal and composite adherends and an array of metal studs which are formed on the surface of the metal adherend and run through the thickness of the composite adherend as shown in Figure 2. The arrangements of the metal studs will be investigated based on numerical simulations using finite element analysis.

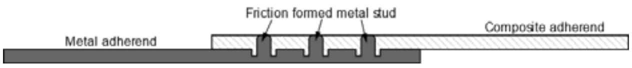

Figure 2: Design concept of the metal stud joint

Figure 3 shows the metal stud manufacturing technique adopted for this project [2]. To form a metal stud, the sleeve plunges into the plate with high speed rotation. The contact between the metal plate and the sleeve produces frictional heat, which softens and restructures the metal plate to form metal studs.

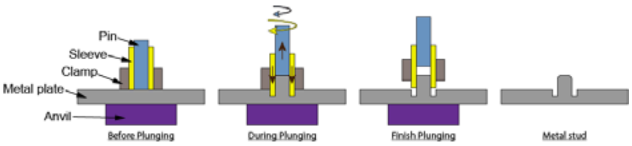

Figure 3: Metal stud manufacturing process [2]

Figure 4 shows the joint specimen manufacturing process using resin infusion. The dry woven fabric is first placed onto the metal adherend, where the metal stud pushes the fibre tows staying around during the assembly without damaging them. After all the materials are put in place, resin is infused into the dry fabric to form the composite adherend.

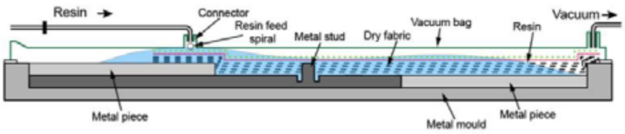

Figure 4: The resin infusion set-up arrangement

III. NUMERICAL RESULTS

The project objectives are driven by numerical simulations, which has two stages:

- Stage I: To study the behaviour of the fibre tows when the woven fabric is assembled with the studs.
- Stage II: To investigate the joint performance by simulating the assembly in a single-lap test setting and incorporating the deformed woven fabric from Stage I.

For Stage I simulation, a quasi-static finite element analysis model is developed as shown in Figure 5. The woven fabric is modelled in meso-scale, which consists of homogeneous anisotropic fibre tows. The metal stud is assumed to be a rigid body. All the elements are modelled using 8-node linear brick solid elements with reduced integration.

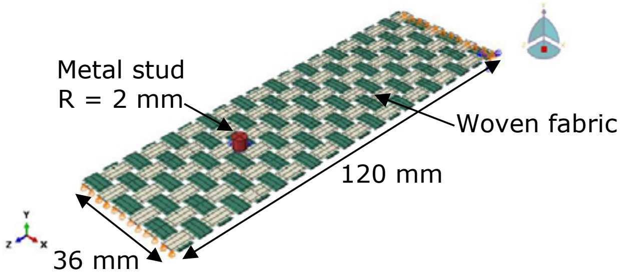

Figure 5: Simulation model for studying tows deformation under metal stud perforation

The metal stud moves towards the woven fabric at the rate of 4 mm/s. The woven fabric is simply supported with two short edges of the woven fabric fixed in perforation direction. Figure 6 shows the von Mises stress of the fabric during assembly.

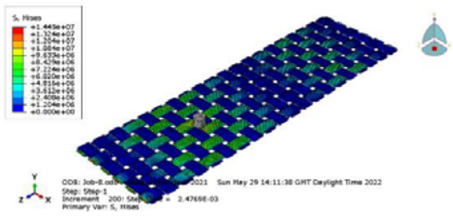

Figure 6: Von Mises stress after the metal stud perforates the woven fabric

IV. DISCUSSION

The dominant deformation mode of the woven fabric during the assembling is bending. The top side of the fibre tow is in compression, while the bottom side is in tension as shown in Figure 7. During the perforation, the fibre tows slip away from each other in longitudinal Z-direction and are pushed away from the metal stud as shown in Figure 8 and Figure 9. This is concluded that no tow failure is found around the metal stud.

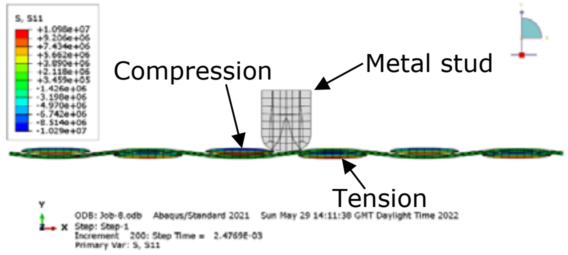

Figure 7: Cross-section of a fibre tow under the metal stud

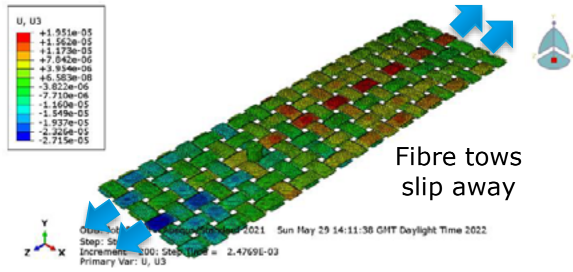

Figure 8: Fibre tows displacement in Z-direction

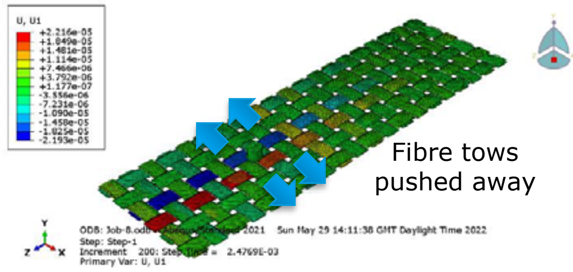

Figure 9: Fibre tows displacement in X-direction

V. FUTURE PLAN

Stage II simulation will be to incorporate the deformed woven fabric from Stage I to form a joint specimen with a single metal stud, as shown in Figure 10, for investigating the joint failure mechanism and performance. Experiments will also be carried out for verifying and validating the simulation results.

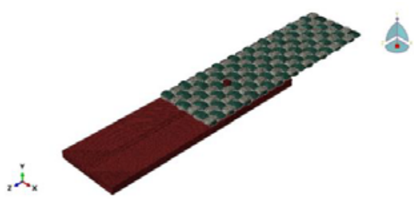

Figure 10: Single-lap test model with single stud

REFERENCES

[1] ASTM International, "Standard Test Method for Apparent Shear Strength of Single-Lap-Joint Adhesively Bonded Metal Specimens by Tension Loading (Metal-to-Metal)," ASTM D1002-10, 2019.

[2] TWI Ltd, "Refill Friction Stir Spot Welding," 27 June 2018. [Online]. Available: https://www.twi-global.com/technical-knowledge/job-knowledge/refill-friction-stir-spot-welding-150.

Kartikey Mathur

Funded by Lloyds Register Foundation (LRF), I started my PhD at NSIRC in January 2021. With bachelor's in Mechantronics engineering and master's in Naval Architecture & Ocean Engineering, I have a diverse experience in the field of automation. For my PhD I would be focusing on monitoring of Friction Stir Welding and the project aims to induce more confidence in the process adressing major knowledge gaps in the domain.

Real Time Evaluation of Weld Quality for Friction Stir Welding (FSW)

Stephen Cater[1], Andrew Kennedy[2] ,Yingtao Tian[2]
[1]TWI, [2]Lancaster University
2nd Year of PhD

Keywords: Friction Stir Welding, FSW, Acoustic Emission,AE, CNN

I. INTRODUCTION

The Friction Stir Welding (FSW) process has been adopted by manufacturers due to its stability against external factors and ability to weld dissimilar metals. (FSW) has seen a vast expansion in the past decade. Past research has proven that online control of welding parameters has the potential to improve weld quality[1][2]. The present sensing and control methodology is subjective to the type of defects shown in Fig.1(i.e- Lack of fill, internal voids). A multi-sensory approach has been discussed to address the limitation of the current monitoring methods and have more confidence in the process. The project aims to use Artificial Intelligence for the development of classification and control methods. At the current stage in the project timeline, forces in the axial direction and lateral direction along with acoustic emission of the process are used for the development of a weld classification system.

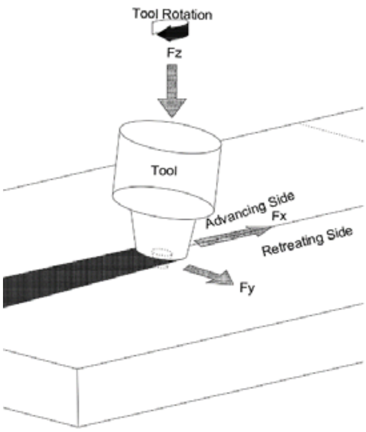

Figure 1- Forces involved in Friction

Figure 2. Forces involved in Friction Stir welding illustrating weld defects

The completion of the project would yield a deep learning-based weld quality prediction and control system.

II. DESIGN/METHODOLOGY/APPROACH

T To achieve the aim of the project, the methodology can be explained in two parts. The first part would be based on training the neural network using the data obtained from a sound weld. A trained network can then be employed in a weld in real-time ,along with real-time monitoring of process parameters (i.e. RPM, axial force, torque and acoustic emission (AE)). Obtaining the optimised weld parameters from the controller assesses the deviation between the real-time and predicted weld parameters.

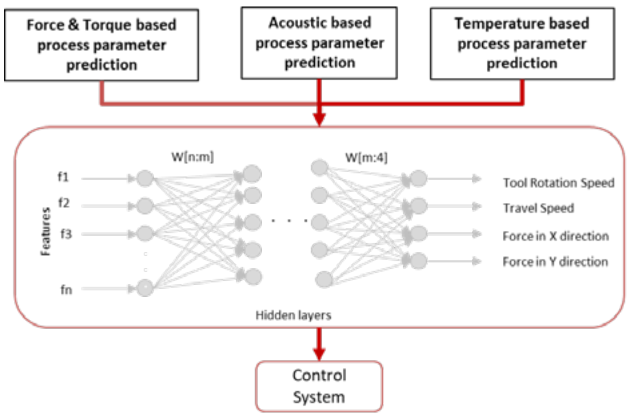

Figure 2. Data flow for the predictive control system

FINDINGS/RESULTS

To address the knowledge gap present in the domain of AE-based monitoring, initial trials were focused on correlating force data with a variation in AE during the welding. A good co-relation between both parameters was observed as shown in Fig 3. To determine the ability to detect material disruption with AE signals, material disruption is caused by introducing holes during the welding. It was also observed that the position of the sensor also affected the measurement and when the sensors are placed on the support, the measurement was influenced by the RPM of the tool. From the trials, it could be concluded that an AE based weld monitoring system would result in higher confidence in the process.

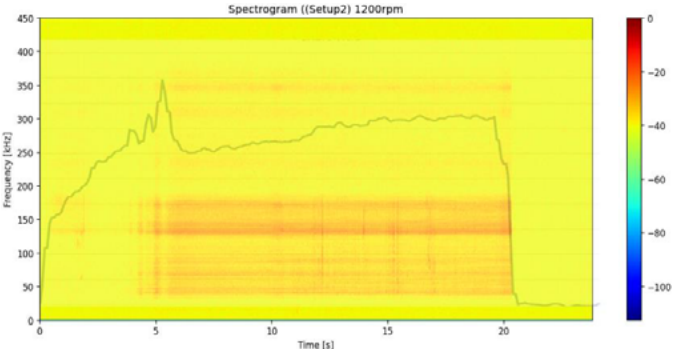

Figure 3. Spectrogram of the AE data with axial force plotted in the background

III. DISCUSSION/CONCLUSIONS

From the experiments it could be concluded that AE signals are sensitive to material disruption that could not be detected by force measurement. Training and testing of a Convolutional Neural Network(CNN) with Mel-Spectrogram yielded 97% accuracy for a VGG16 inspired network.

IV. FUTURE PLAN/DIRECTION

Considering the results from the experiments, further research is needed to understand the affect of damping of elastic waves with increase in the size of nugget zone. Additionally, a weld scoring system based on the AE signals and force signal for better weld classification needs to be developed.

REFERENCES

[1] A. Baraka, G. Panoutsos, and S. Cater, "A real-time quality monitoring framework for steel friction stir welding using computational intelligence," J. Manuf. Process.

[2] D. Ambrosio et al., "On the potential applications of acoustic emission in friction stir welding," J. Manuf. Process.

Haolin Fei

Haolin Fei joined TWI and became a PhD candidate at Lancaster University in October, 2020. Haolin Fei received a BEng in Electronic Information Engineering from the University of Electronic Science and Technology of China and a BEng with Honours of the first class in Electronics and Electrical Engineering from the University of Glasgow in 2020. The main theme of his research is the application of robotics and artificial intelligence (AI) in the brazing process. His research is funded by Lloyd's Register Foundation.

Digital Process Iteration Human-Robot for Improved Brazing Safety and Productivity

Dr Nick Ludford[1], Dr Stefano Tedeschi[1], Prof. Andrew Kennedy, Dr Yingtao Tian [2], Dr Darren Williams [1, 2]
[1]TWI, [2]Lancaster University
2nd Year of PhD

Keywords: Brazing, robotics, reinforcement, leaning, imitation learning, visual serving

I. INTRODUCTION

Brazing is a well-established manufacturing process for a range of different safety-critical components. It provides unique features over other joining methods, including the ability to join dissimilar materials, and providing ductile and strong joints with low costs [1]. However, a number of steps still require the use of a skilled operator such as applying the consumables for each joint, which is a repetitive and time-consuming task. Driven by the desire for automation and smart manufacturing into the fourth industrial revolution (also referred to as Industry 4.0), robots capable of safe, collaborative working with operators are promising to perform tasks with higher accuracy and efficiency. While the brazing filler metal (BFM) deposition process (pre-placement) is one of the most significant variables in producing qualified joints [2], very little research has been carried out to establish the link between the deposition process parameters and the quality of joints. Consequentially, this process is difficult to model and requires re-programming when dealing with different geometries, which greatly hinders the automation and digitisation of the process. Nowadays for industries, it is hard to guarantee total accuracy and efficiency by a human operator, who applies BFM manually using brushes or gun applicators [3].

Therefore, an automated human-robot collaborative framework for BFM deposition is a promising method to improve the accuracy and efficiency of the brazing process. However, there still exist many problems in human-robot interaction, such as the variation in human performance, noise and generalisation problems [4].

Figure 1. The proposed framework.

To overcome these issues, some methods collect multiple human demonstrations and use data-driven method to circumvent the variation in human performance, trying to understand the implicit task goal through iterations [5]. In addition, robot application scenarios are diverse, and it is hard to transfer the learned skill from one task to another. Therefore, it is desirable to develop a framework that is able to learn multiple tasks with only one human demonstration, without expert knowledge or any prior information of the system.

Modelling imitation learning analytically, as a state estimation problem, is a promising solution which allows the robot to learn from a single human demonstration. The imitation learning process is divided into two stages: interaction with the task object, and approaching the start position of the interaction, which is known as the bottleneck position [3]. However, this method poses a challenge for the approaching phase, which relies heavily on the accuracy of achievement. Towards this problem, this research proposed a new visual servo framework, based on a sample-efficient reinforcement learning algorithm for the accurate achievement of task objects.

In summary, the main contribution of our research is a new, efficient framework for samples, to allow robots to learn from a demonstration that allows achievement the precise goal from a single human demonstration.

II. DESIGN/METHODOLOGY/APPROACH

The framework proposed for this research is divided into two parts as shown in Fig. 1: the "eye" of the algorithm, which estimates the difference between the current state, as shown in the left side of the figure below, and the "brain" part, which controls the arm with information provided by the "eye".

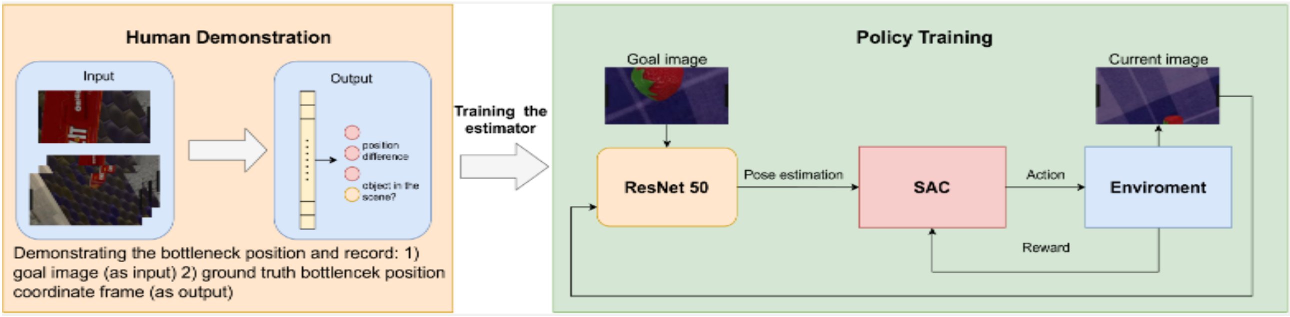

More specifically, an object position estimator was trained to estimate the position difference between the bottleneck position's image (goal) and the current images, which are observed by the "eye-in-hand" camera. This information is then taken by a deep reinforcement learning (DRL) based policy network that automatically determines the desired actions to move the end-effector of a robotic arm. This reduces the estimation error with an additional policy network which takes the estimation results as input, while at the same time greatly reducing the observation space, which allows the network to converge more easily and accelerates the training process.

III. FINDINGS/RESULTS

Given a single human demonstration in a simulated environment for different task objects and environment backgrounds, without any other prior knowledge, the proposed approach is able to recognise the bottleneck position and reach the demonstrated position, with the object placed at another location within the robot's field of view.

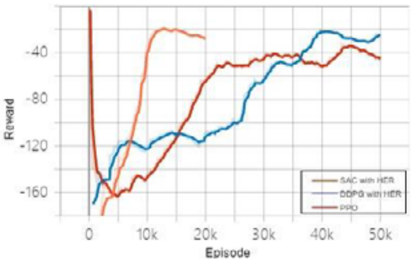

The figure demonstrates the convergence of the algorithm which proves the feasibility of the method. It can be observed from the figure that the SAC with HER replay buffer has a faster convergence rate compared with the other two algorithms.

IV. DISCUSSION/CONCLUSIONS

In this research, we exploit the full-state observation capability of the simulator and train a position difference estimator to estimate the state of the robot that takes the goal image at the bottleneck position and the current state image as the input. As the estimator cannot always predict the true state of the environment, we use a reinforcement learning controller to drive the robot to the bottleneck position with information provided by the estimator. Since the adapted estimator provides lower dimensional state information, compared with methods that feed images, so that it learns the policy much faster and is easier to converge. Implementation of the framework will result in a more intelligent and flexible method of teaching a robot to swiftly switch from one production line to another, without any expert knowledge or complicated engineering.

V. FUTURE PLAN/DIRECTION

In the future, we will continue to work on combining the algorithm into the whole workflow of human demonstration in the brazing process. Although the method proposed in our paper provides a promising way towards reaching an object without any prior knowledge, with a bottleneck position image as a goal image, there is still room for future improvement. First of all, the network architecture of the estimator module can be further improved to increase the location estimation accuracy. Secondly, as the action of the robot is continuous, the implicit, temporal relation between states can provide information for the action, which might lead to further improvement on the performance. Thirdly, the algorithm can be more practical by further extending the success criteria to the success rate of the whole, learning from the demonstration process instead of using a threshold value to judge whether the robot is close enough in location to the object. This can be done by setting the reward to the success of the whole task, but addressing the new challenge of how to train the algorithm.

REFERENCES

[1] Way, Matthew, Jack Willingham, and Russell Goodall. "Brazing filler metals." International Materials Reviews 65.5 (2020): 257-285.

[2] Roberts, Philip. Industrial brazing practice. Crc Press, 2003.

[3] Johns, Edward. "Coarse-to-fine imitation learning: Robot manipulation from a single demonstration." 2021 IEEE International Conference on Robotics and Automation (ICRA). IEEE, 2021.

[4] Ravichandar, Harish, et al. "Recent advances in robot learning from demonstration." Annual review of control, robotics, and autonomous systems 3.ARTICLE (2020): 297-330.

[5] El Zaatari, Shirine, et al. "iTP-LfD: Improved task parametrised learning from demonstration for adaptive path generation of cobot." Robotics and Computer-Integrated Manufacturing 69 (2021): 102109.

Amarachi F. Obilor

Amarachi F. Obilor received her education in Materials and Metallurgical Engineering (M.Sc.) from the University of Lagos, Nigeria where she gained a distinction in 2017. Her dissertation was on the synthesis and characterization of hybrid polypropylene matrix composite reinforced with carbonized Terminalia catappa shell particles (an agro waste). Amarachi has always had interest in the enhancement of polymer properties, which was shaped during her industrial work experience. Sponsored by TWI and Loughborough University, Amarachi's PhD study focuses on laser surface functionalization of polymers for biomedical applications. She is effectively sharing her research findings through conference participations and paper publications. She is currently in the third year of her study.

Influence of laser surface modification on the adhesion properties of PEEK

Dr. Andy Wilson[1], Dr. Manuela Pacella[2] Prof. Vadim Siberschmidt[2]
[1]TWI, [2]Loughborough University
3rd Year of PhD

Keywords: PEEK, biomedical, wettability, surface topography, bond strength, adhesion.

I. INTRODUCTION

The performance of biopolymers in a biological environment depends largely on surface properties as well as physical and mechanical properties. The favourable mechanical properties of thermoplastic materials such as PEEK makes it a popular choice for permanent bioimplants [1].

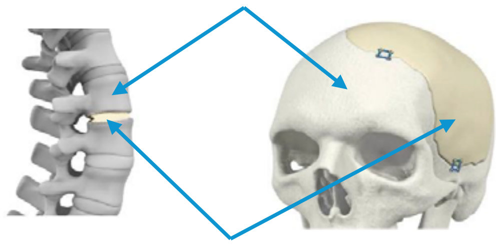

Fig 1. Some biomedical implant applications of PEEK [2]**.**

Unfortunately, PEEK's bioinert surface poses a challenge for bonding and rapid integration with healthy body tissue. From past studies, effective enhancement of surface free energy and wettability have been shown to improve the adhesive response of PEEK surface. To this effect, several methods have been developed to modify polymer surfaces for improved adhesive performance. These can be classified into (i) mechanical treatments which mainly affects surface topography such as sand blasting, (ii) chemical treatments involving the use of chemical substances (e.g. solvent cleaning and ultrasonic bath) and (iii) energetic treatments such as corona discharge, plasma and laser treatments. Although the main objective of energetic treatments is to remove organic contaminants, activate oxidation and increase polarity along with wettability of polymer surfaces, surface topography changes may occur due to the removal of weak cohesive layers [3]. Therefore, it is advantageous to apply energetic treatments on polymer surfaces to enhance adhesive performance. The use of lasers to provide energetic treatments offers more flexibility compared to alternative techniques because lasers can be targeted to specific areas and positions of a substrate with greater precision.[3].

Although several studies have investigated the influence of laser treatment on PEEK, there is limited information on the influence of ultra-short, pulsed laser on adhesive bond strength of PEEK. The main objective of this work is to investigate the influence of ultrashort laser treatment on the adhesive bond strength of a PEEK surface.

II. METHODOLOGY

A. Material

Victrex PEEK 450G rectangular coupons measuring 50 mm x 25 mm x 4 mm were used. Prior to laser treatment, samples were cleaned with isopropanol to remove debris and other surface contaminants.

B. Experimental design

Laser processing was done using a Fianium Hylase 25 W Nd:YAG laser. Following preliminary trials, three factors (fluence, pitch and scan speed) were selected to be varied at different levels (Table 1). A design of experiment was done using IBM SPSS software. Additional parameter settings were included to generate a robust design of experiment. A total of forty two parameter settings were generated.

Table 1. Range of processing parameters varied for laser processing of PEEK surface.

Factors	Minimum value	Maximum value
Fluence (J/cm^2)	0.79	3.11
Scan speed (mm/s)	100	1000
Pitch (mm)	0.02	0.2

C. Characterization

Treated PEEK surfaces were characterized using Alicona 3D profilometer and single lap shear tests (ASTM D3163). Lap shear tests were performed on bonded PEEK-to-PEEK joints. Bonded joints were produced using Henkel Loctite 4061 adhesive, which is ISO 10993 biological tested for use in medical devices and designed for bonding plastics where fast fixturing is required.

III. FINDINGS

1. Bond strength

Results of single lap shear tests conducted on all treated samples showed improved adhesive bond performance compared to untreated PEEK. Bond strength increased up to six times (Fig 2).

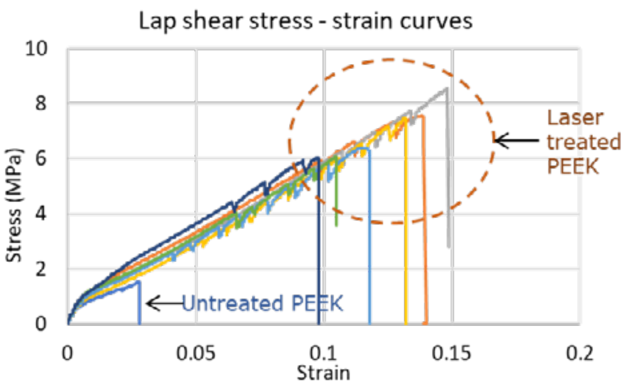

Fig 2. Increased shear strength achieved with energy fluence of 2.28 J.cm^2 and 3.11 J.cm^2 at scan speeds of 100 mm/s and 200 mm/s.

2. Failure modes

A variety of failure modes were observed on treated and untreated PEEK following shear tests. (A) Adhesion failure of adhesive and adherend occurred in untreated PEEK-to-PEEK joints where a layer of adhesive remained in adherend surfaces. This failure mode is indicative of poor bond strength.

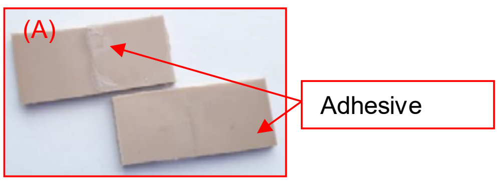

Fig 3. Adhesive failure in untreated PEEK indicating weak bond strength.

(B) Adherend failure: This is failure of the parent material, which indicates strong bond strength given that failure occurs away from the bonded area which is laser treated surface.

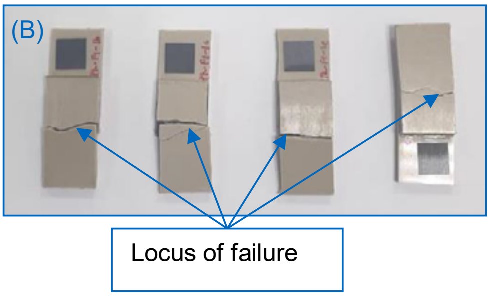

Fig 4. Adherend failure in laser treated PEEK indicating strong bond strength.

IV. CONCLUSIONS

Picosecond laser surface treatment can be used to improve adhesive bond strength in PEEK-to-PEEK joints. Fluence of 2.28 J/cm^2 is effective in improving adhesion function in PEEK. While a fluence of 3.11 J/cm^2 effectively increases the hydrophobicity of PEEK. Also, the presence of microvoids within grooves serve as pockets to trap liquid for enhanced bonding.

V. FUTURE PLAN

With increased bond strength achieved on laser textured PEEK, it is worth analysing the effect of this treatment on other mechanical properties such as hardness. This is essential given the loading mechanisms that biomedical implants are subjected to while in service.

From previous studies, laser surface texturing results in surface chemistry modifications in addition to surface topography changes. Since topography changes have been studied, surface chemistry modifications resulting from laser treatment will be investigated using Fourier transform infrared spectroscopy.

REFERENCES

[1] P. Ferreira, P. Alves, P. Coimbra, and M. H. Gil, "Improving polymeric surfaces for biomedical applications: a review," J. Coatings Technol. Res., 1998, doi: 10.1007/s11998-015-9658-3.

[2] Benjamin Chun-Kit Tong, "乳鼠心肌提取 HHS Public Access," Physiol. Behav., vol. 176, no. 5, pp. 139–148, 2017, doi: 10.1227/NEU.0000000000000899.The.

[3] A. F. Obilor, M. Pacella, A. Wilson, and V. V. Silberschmidt, "Micro-texturing of polymer surfaces using lasers: a review," Int. J. Adv. Manuf. Technol., 2022, doi: 10.1007/s00170-022-08731-1.

ACKNOWLEDGEMENT

This work was made possible by the sponsorship of TWI and Loughborough University through the National Structural Integrity Research Centre (NSIRC).

Saad Syed Iqbal Ahmed

Saad graduated with a first class BEng (Hons) in Mechanical Engineering from Heriot-Watt University in 2017. He later pursued an MSc in Advanced Materials Engineering from The University of Manchester where his research focussed on developing a comparative study of different data analysis methods to study the residual stresses profiles of aero-engine components by X-ray diffraction. In July 2019, Saad started an Lloyds Register Foundation sponsored PhD with The University of Manchester and TWI Ltd. His work focuses on developing appropriate procedures towards standardizing fatigue design guidance for Selective Laser Melted (SLM) components. This work would try to correlate defects to fatigue performance in SLMed Al-Si10-Mg alloys using X-ray Computed Tomography and microstructure characterisation techniques.

Correlating Defects to Fatigue Performance in Selective Laser Melted Al-Si10-Mg Alloys

Saad Ahmed[2], Prof. Matthew Dore[1], Dr. Yanhui Zhang[1], Dr. Matthew Roy[2] & Professor Philip Withers[2]
[1]TWI, [2]University of Manchester
3rd Year of PhD

Keywords: Additive Manufacturing, Selective Laser Melting, Fatigue Performance, AlSi10Mg Alloys, X-ray Computed Tomography

I. INTRODUCTION

Selective Laser Melting (SLM) is a revolutionary technology pertinent to many high-value applications in the biomedical, automotive, and aerospace industries. It has the potential to produce topographically optimized parts comprising of complex geometries previously not possible by traditional subtractive manufacturing methods [1]. SLM technologies have majorly appealed to low volume production of custom parts for specialist applications like medical implants and fine meshed internal structures. It has also enabled on-demand remote manufacturing and repair of functionally-graded parts like turbine blades [2].

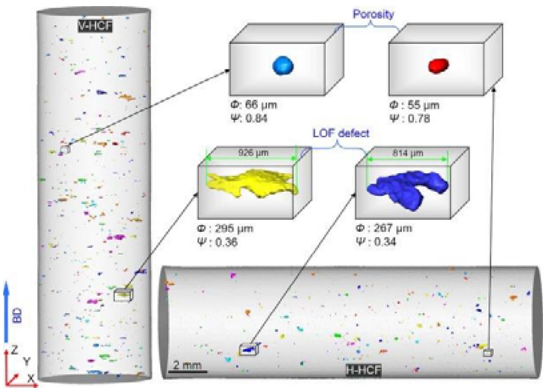

Figure 1 Defect distribution in horizontlly and vertically oriented AlSi10Mg alloy samples using X-Ray Computed Tomography (CT) [6]

SLM alloys also have potentially extensive application in mechanical structures [3]. This is a result of SLM components experiencing unique thermal histories specific to their build, significantly affecting the resulting microstructure and the associated mechanical properties [4], resulting in demonstrable tensile behaviour compared to wrought materials. However their implementation is still restricted to non-critical applications due to lower fatigue strength and a larger scatter in fatigue life. To enable their implementation in safety critical applications, it is critical to develop an adept understanding of their fatigue behaviour [5].

Till date, defects have been an unavoidable part of the manufacturing process of SLM components. This is due to the lack of fusion (LOF) and gas porosity defects that originate during fabrication of these components. These defects act as crack initiation sites and have largely been associated with short crack initiation and propagation [6]. Certain thermo-mechanical treatments like HIPing and T6 Heat Treatment are known to improve ductility and reduce porosity within these components but have led to an overall reduction in the fatigue strength of the material [3]. These treatments provide a potential solution to obtaining consistent fatigue properties with less scatter in the data. However, even in components that have undergone a post-processing treatment like HIPing, these pores have not been completely eliminated. Thus, it is essential to develop an understanding of the process-microstructure-fatigue relationship of this technique [1].

II. METHODOLOGY

Defects such as gas pores or lack of fusion pores as shown in Fig 1 are formed between two continuous layers and are aligned parallel to them, reducing the effective load-bearing area. When these defects exceed a certain size threshold, they detrimentally impact fatigue properties [2]. These defects also create a large scatter in fatigue lifetimes due to their randomness. This is more critical for situations where there is a higher probability of encountering large irregular pores closer to the surface as this can have more detrimental impact on the fatigue life [5

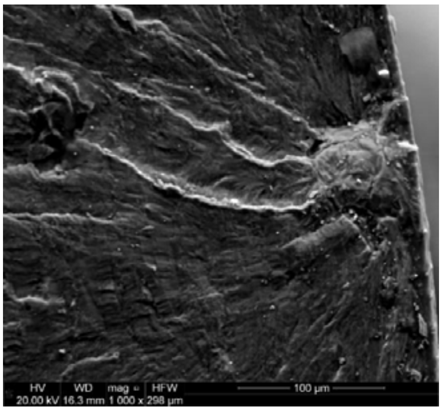

Figure 2 Fatigue Crack Initiation Defect

This project aims to correlate a critical defect from the fracture surface that has caused fatigue crack initiation to its pre fatigue state examined using X-ray CT, to develop quantitative methods of fatigue life prediction using various fatigue models. Additionally, the aim is to develop a probabilistic prediction of fatigue life for a given distribution of pores along with a comparison of multiple heat treatment methods. Also, the effect of crack initiation and propagation on the microstructure is being studied. This entails that for a given distribution of pores in a sample, it can be predicted what the probable likelihood of failure is. Finally, to predict a probabilistic distribution of pores from a set of distributions available for both horizontally and vertically oriented samples, extending it to predict the fatigue life. This enables us to quantify the fatigue performance of SLM AlSi10Mg alloys in multiple orientations. This can also be used to develop a model to predict the fatigue crack initiation site within AlSi10Mg alloys based on a certain porosity distribution using existing fatigue crack initiation and fatigue crack growth models.

III. RESULTS & DISCUSSION

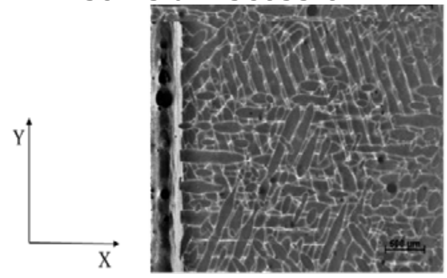

Figure 3 Cross-section view of the Melt pool using Optical Microscopy

Initial Results indicate that the most detrimental pores lie on the surface or sub-surface as indicated in Fig 2. The fatigue lives of samples in both orientations is fairly consistent with previous studies. EBSD mapping as shown in Fig 4, of the microstructure was carried out to identify any texture within the material as well as to eliminate the role of microstructure in the fatigue crack initiation within the material. The melt pool cross-section microstructure of the material shown in Fig 3 depicts the laser scan tracks over multiple layers of deposition. The dark phase represents Aluminium while the bright phase represents silicon particles which are scattered indifferently across the surface. The melt pool grain structure can also be identified from the EBSD map wherein there are longitudinal grain across the centre of the melt-pool and small equiaxed grains towards the edges

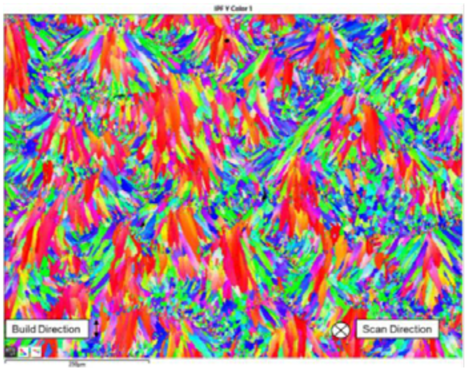

Figure 4 EBSD Map along the Build Direction

IV. FUTURE PLAN

The future plan has been shwon in Fig. 5 below.

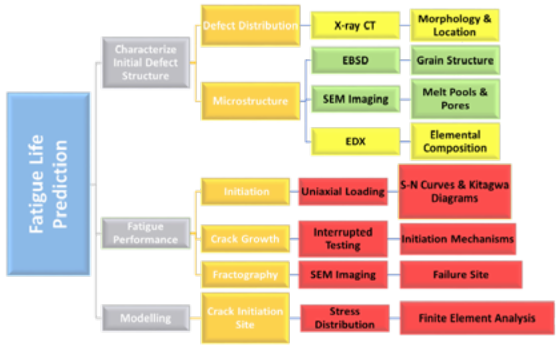

Figure 5 Color coded Future Testing Plan

This publication was made possible by the sponsorship and support of Lloyds Register Foundation & The University of Manchester. The work was enabled through, and undertaken at, The University of Manchester, and supervised by academic experts from TWI.

REFERENCES

[1] B. Maschinen, A. Investition, G. Beschaffungen, B. Ersatzbeschaffungen, and S. Mittelherkunft.
[2] A. Yadollahi and N. Shamsaei, Int. J. Fatigue, 2017, doi: 10.1016/j.ijfatigue.2017.01.001.
[3] A. Jaafar, A. Rahmat, I. Zainol, and Z. Hussain, J. Appl. Sci., vol. 12, no. 8, pp. 775–780, Aug. 2012, doi: 10.3923/jas.2012.775.780
[4] D. L. McDowell, S. Yip, Ed. Dordrecht: Springer Netherlands, 2005, pp. 1193–1214
[5] Y. N. Hu et al., Int. J. Fatigue, vol. 136, p. 105584, Jul. 2020, doi: 10.1016/j.ijfatigue.2020.105584
[6] Y. N. Hu et al., Mater. Des., vol. 192, 2020, doi: 10.1016/j.matdes.2020.108708.

Siddharth Patil

Post graduate researcher from NSIRC and Coventry University. Siddharth completed his MSc in Welding Engineering from Cranfield University in 2018. He also has 9+ years of industry experience as a 'Welding and quality engineer' in various sectors. Siddharth's research topic is 'Development of directed energy deposition (DED) arc process to achieve consistent bead geometry and microstructure with optimised feedstock chemistry'. The main aim of his research is process optimisation and consistent bead geometry through control methods in low carbon steels. This publication was made possible by the sponsorship and support of Lloyd's Register Foundation. Lloyd's Register Foundation helps to protect life and property by supporting engineering-related education, public engagement and the application of research.

Bead Geometry and Thermal Analysis of the Low Carbon Steel Manufactured by Directed Energy Deposition (DED) Arc Process

Cui Er Seow[1], Xiang Zhang[2]
[1]TWI, [2]Coventry University
2nd Year of PhD

Keywords: DED-arc process, low carbon steel, arc energy, bead geometry

I. INTRODUCTION

Arc-based directed energy deposition (DED-Arc) is gaining more interest in industry as an alternative to conventional manufacturing. In DED-Arc, the layer-by-layer addition of arc energy results in complex thermal cycling of the part, and geometrical variations (e.g. intersections) can lead to varying heat dissipation profiles, resulting in inconsistencies in deposited bead geometries. DED-Arc deposition parameters are generally controlled using a "constant-input" approach, which can lead to dimensional irregularities particularly at geometrical intersections.

One way to counteract the heat sink effects caused by the adjacent intersecting material is to account for differences in heat dissipation and adjust the input deposition parameters at such geometrical intersections. The aim of this paper is to develop a control method to achieve consistent bead geometry in low carbon steels.

A systematic identification of the key factors affecting bead geometry at intersections and development of parameters as one of the control methods has been carried out.

II. DESIGN/METHODOLOGY/APPROACH

Six axis welding robot, Fronius arc welding power source, wire feeder and welding torch [FIGURE 1] were used for deposition trials. Experiments were carried out with shielding gas, which is a mixture of argon and carbon dioxide. M24 gas was used and a flow rate of 18 l/min was kept constant throughout the experiments. Experiments have been conducted with the readily available feedstock wire ER70S-6. Wire diameter of 1.2 mm was used for all experiments. A readily available rolled plate of EN 10025 S275JR was selected as substrate for all experiments.

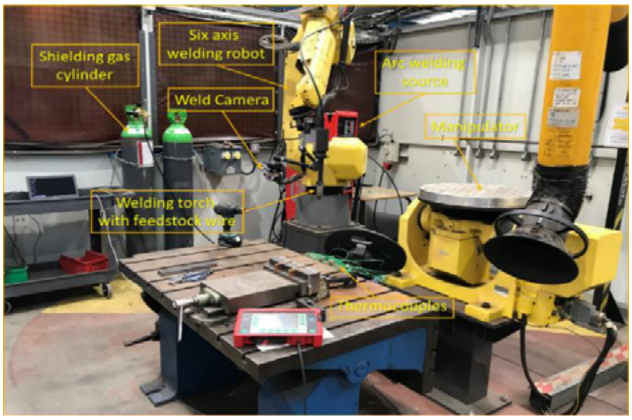

FIGURE 1: DED-Arc process setup comprises of six axis welding robot, fronius welding power source

III. FINDINGS/RESULTS

The aim of these trials is to find out the effect of deposited heat sink on experimental bead. Experiments were conducted with heat sink that was deposited near to experimental bead. FIGURE 2, exhibits deposited heat sink and experimental bead. In these trials, parameters for experimental bead were kept constant with arc energy of 0.36 kJ/mm, however offset and heat sink layers were varied. For comparison purposes, specimens were divided into 2 groups, with 3 speciments in each group. Offset is the distance between two bead centrelines.

In group 1, offset distance was constantly 4mm and heat sink layers varied from 1 to 3 layers. On the other hand, in group 2 there were constantly 2 heat sink layers and offset distance changed from 4 to 6mm. Group 1 and 2 further subdivided into group 1HS and 2HS.

	Offset (mm) (distance between bead centrelines)	No. of heat sink layers
Group 1 (3 Samples)	4	1, 2 ,3
Group 2 (3 Samples)	4, 5, 6	2

Table 1: Samples grouped depending on offset distance and no. of heat sink layers.

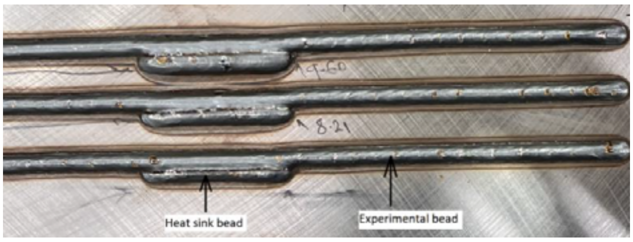

FIGURE 2: Bead deposition with deposited heat sink and experimental bead

IV. DISCUSSION/CONCLUSIONS

Same arc energy, which is 0.36 KJ/mm, was directed towards the substrate. It can be observed from the graph [FIGURE 5] that for group 1 bead width in the range of 7.1 to 7.2mm has a bead height of 3.8mm. For group 1HS bead width is similar, ranging from 6.6 to 6.7mm and bead width varying from 3.5 to 4.6mm. When it comes to group 2, bead width is between 7 to 7.2mm and bead height 3.7 to 4mm. Bead width for group 2HS varies from 6.7 to 7.4mm and bead height is between 3.5 to 3.7mm. It can be said that the number of heat sink layers has limited effect on the deposited bead as bead beometry did not change in group 1. Offset distance plays an important role when it comes to group 2, as the offset distance increases there is reduction in bead width and height. There is significant change in bead width and minute change in bead height when group 1 and 2 compared against group 1HS and 2HS.

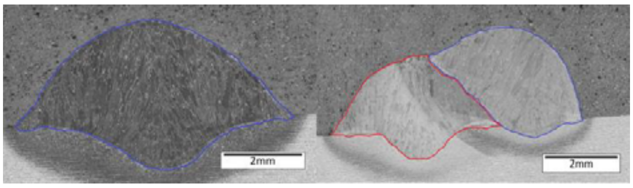

FIGURE 3: Macrographs of experimental bead of sample from group 1 (left) and experimental bead with blue outline and sink bead marked with red outline for sample group 1HS (right).

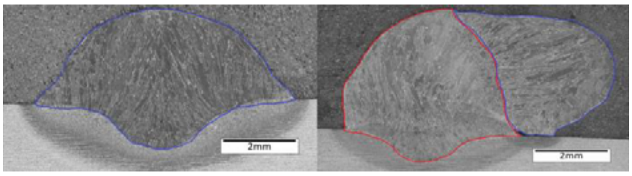

FIGURE 4: Macrographs of experimental bead of sample group 1 (left) and experimental bead with blue outline and sink bead marked with red outline for sample group 1HS (right) where it shows lack of fusion.

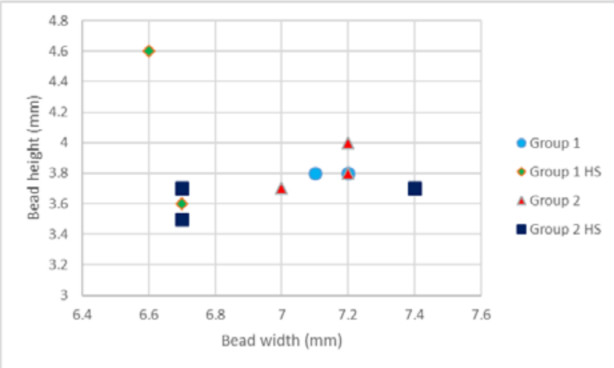

FIGURE 5: Bead height and width for various process conditions for bead deposition with deposited heat sink (HS = heat sink).

The findings of the bead geometry with deposited heat sink trials shows that as the offset distance increases, there is a reduction in bead width and height. However, the number of heat sink layers have minimal effect on bead geometry of deposited heat sink.

V. FUTURE PLAN/DIRECTION

Use of more control methods to achieve consistent bead geometry with optimised feedstock and compare the results between optimised and standard feedstock.

REFERENCES

[1]Jafari, D., Vaneker, T. H. J., & Gibson, I. (2021). Wire and arc additive manufacturing: Opportunities and challenges to control the quality and accuracy of manufactured parts

[2]Long, P., Wen, D., Min, J., Zheng, Z., Li, J., & Liu, Y. (2021). Microstructure Evolution and Mechanical Properties of a Wire-Arc Additive Manufactured Austenitic Stainless Steel

[3]Williams, S. W., Martina, F., Addison, A. C., Ding, J., Pardal, G., & Colegrove, P. (2016). Wire + Arc additive manufacturing. Materials Science and Technology (United Kingdom), 32(7), 641–647

[4]Xu, X., Ding, J., Ganguly, S., Diao, C., & Williams, S. (2018). Oxide accumulation effects on wire + arc layer-by-layer additive manufacture process. Journal of Materials Processing Technology, 252(October 2017), 739–750.

Francesco Careri

Francesco is a PhD student at the University of Birmingham and TWI Ltd through the EPSRC CDT in Topological Design and the National Structural Integrity Research Centre (NSIRC). His project, funded by the European Union's Horizon 2020 research and innovation programme, is focused on the development of additive layer manufacturing technology as a potential means to produce thin features and more efficient Al-alloys heat exchangers for aerospace applications. Francesco obtained his MSc degree in Mechanical Engineering at the University of Calabria in Italy. During his final year project, he collaborated as a visiting student at the AMPlab, University of Birmingham, where he carried out experimental and numerical analyses of different post-processing strategies for Ni-superalloys structures, fabricated using direct energy deposition.

Optimisation of L-PBF Parameters for a Novel A20X® Alloy Thin-walled Heat Exchanger

Raja Khan[1], Catherine Todd[2], Moataz Attallah[3]
[1]TWI, [2]Meggitt, [3]University of Birmingham
2nd Year of PhD

Keywords: Additive manufacturing; Heat exchangers; Al Alloy; Process optimisation; Lattice structures.

I. INTRODUCTION

Compact heat exchangers (HXs) have found wide use in various industrial sectors, especially aerospace, thanks to the combination of relatively small volumes, and consequently low weight and high thermal efficiency [1]. In particular, compact HXs are essential to ensure the control of lubricating oil temperatures in ultra-high bypass ratio (UHBR) engines, where they will be core-mounted with limited installation space and higher ambient temperatures, compared with fancase mounting on current aero-engines. They are inserted in the front part of the aero-engine and must necessarily operate at high temperatures and in harsh operating conditions, mostly on aircraft with longer standstill times and long periods of operation, in areas with ocean atmosphere and dynamic vibrations [2]. Currently, scientific research is investigating the use of hollow structures which, combined with the design of a lattice structure, could significantly increase the heat exchanger (HX) efficiency. In particular, the combination of high thermal conduction and convection, and low flow resistance in hollow areas of the lattice structure, results in highly efficient heat exchange [3]. These new hollow-lattice HXs, fabricated through additive manufacturing (AM), have great potential for industrial development. However, the feasibility of leak-tight lattice structures' thin walls, and the prevention of high surface roughness or shape deviation, remain challenges the scientific community is still trying to face.

The aim of this work is to develop a process strategy for laser powder bed fusion (L-PBF) in order to fabricate defect-free, novel design HXs using a new composite A20X® aluminium alloy. The influence of L-PBF process parameters on the quality of the produced samples was investigated and the optimal parameters were implemented to manufacture complex shaped HX segments. Finally, the manufacturability was assessed by analysing the HX segments in terms of surface quality and accuracy.

II. DESIGN/METHODOLOGY/APPROACH

A20X® (AlCu-TiB2) alloy in powder form, with an average particle size of 40μm, was filled in by Concept Laser M2 CUSing L-PBF machine, with a 400W laser for the fabrication of samples that needed to be analysed during this work.

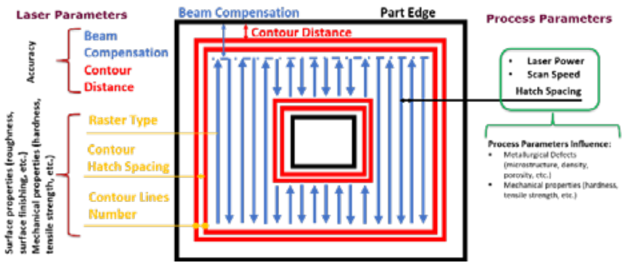

Fig. 1. Schematisation of process and laser parameters for L-PBF and their influence on material and surface properties.

The optimisation and analysis of the process parameters (laser power, scanning speed, hatch spacing, as shown in Fig. 1) were carried out in several stages with a 30 μm fixed layer thickness. The influence of process parameters on single laser tracks and their correlation was established. In particular, scanning electron microscopy (SEM) was employed to assess the quality of deposit of the laser tracks. Bulk samples were used to determine the porosity and surface roughness using optical microscopy and profilometer respectively, whereas mechanical properties were assessed in terms of microhardness tests. Furthermore, the influence of the laser parameters related to the accuracy, beam compensation (BC) and contour distance (CD), for the production of features characterised by thin thicknesses were evaluated. This influence was analysed using both optical and SEM images of segments, consisting of walls and holes with 2 and 0.2 mm dimensional features. Finally, two HX segments were designed using a BCC lattice structure with 350 µm and 500 µm wall thicknesses.

III. FINDINGS/RESULTS

The laser track analysis led to the construction of a contour map correlating the quality of track to different process parameters, in particular, laser power and scan speed. This contour map, represented in Fig. 2, is a useful tool during the design phase of the manufacturing strategy as it can reduce the range of process parameters ideal for production, and also provides useful information on the morphology of the laser track and consequently the correct formation of each layer.

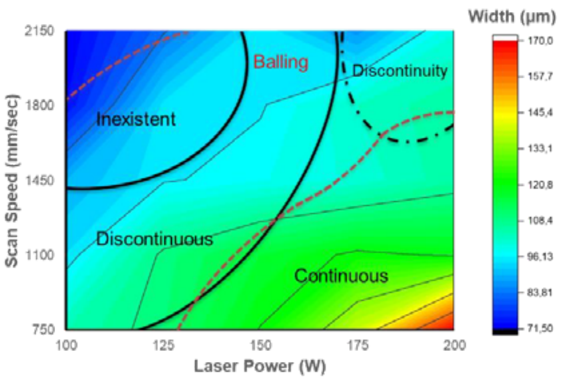

Fig. 2. Contour map showing morphology and width value of single laser track, varying laser power and scan speed.

In particular, the interaction of each laser track during the formation of each layer, and with the previous layer, can create metallurgical defects within the component. Generally, defects such as high porosity and surface roughness are due to the use of incorrect process parameters. Consequently, these defects can be correlated to energy density, and an optimal range is sought. The best energy density range to ensure a defect-free AlCu-TiB2 material with a density comparable to the bulk material obtained by traditional manufacturing methods was found to be between 60 and 80 J/mm3. Finally, the optimal process parameters for L-PBF were defined through further microhardness and surface roughness analyses. It was even necessary to evaluate the correlation of the laser parameters of beam compensation (BC) and contour distance (CD) for accuracy in the production of such thin features. The analyses carried out on the segment samples were undertaken using image processing software, evaluating the difference between the nominal and real dimensions of the characteristics. An optimal combination of BC and CD, at 25 and 50 µm respectively, was found to be suitable for the production of sub-millimetre thin features.

Fig. 3. HX segments with thin-walled features built using optimised L-PBF process parameters.

Finally, the HX segments (Fig. 3) with thin-walled lattice features were successfully built using optimal an L-PBF process and laser parameters, highlighting the feasibility of manufacturing complex-shaped industrial parts. Although the up-skin roughness was consistent with the value obtained during the process optimisation, the down-skin surface roughness was found to be quite high; an indication that the design and process parameters influencing the surface roughness still need to be optimised. The accuracy analysis showed good consistency in wall thickness values for thin lattice features with negligible porosity defects.

IV. DISCUSSION/CONCLUSIONS

The results indicate that the L-PBF process and laser parameters used lead to good material properties, and the thin-walled features are in good agreement with the CAD design. The analysis helped in the optimisation of the process parameters for the correct fabrication of thin-walled lattice HXs with two different wall thicknesses, i.e., 350 µm and 500 µm.

V. FUTURE PLAN/DIRECTION

The relatively large L-PBF SLM500 quad-laser machine will be used to manufacture HXs segments in order to prove a faster build rate, which will be quite beneficial during building the full-size industrial HXs. Moreover, the effect of L-PBF process parameters on thin-walled lattice feature quality will be assessed.

ACKNOWLEDGEMENT

This work is part of C-ALM AOHE project funded by the European Union's Horizon 2020 research and innovation programme under grant agreement No 831880.

REFERENCES

[1] C. Balaji, B. Srinivasan, S. Gedupudi, Chapter 7 - Heat exchangers, in: Heat Transfer Engineering, Academic Press, 2021, pp. 199-231.

[2] B. Sundén, J. Fu, Chapter 6 - Aerospace Heat Exchangers, Heat Transfer in Aerospace Applications, Academic Press, 2017, pp. 89-115.

[3] H.N.G. Wadley, D.T. Queheillalt, Thermal Applications of Cellular Lattice Structures, Materials Science Forum, 539-543 (2007) 242-247.

Ahamed Ameen
A doctoral student with NSIRC, TWI and Coventry University, Ahamed is working on the microstructural optimisation of wire-fed direct energy eeposition (DED) of low alloy steels. The work is funded by Lloyd's register Foundation. Ahamed has completed a Masters in materials science from the Royal institute of Technology, Stockholm and a Bachelors in metallurgical engineering.

Effect of Heat Input on Microstructure of C-Mn Steel Walls Fabricated by Wire-and-Arc Additive Manufacturing

Joanna Nicholas[1], Vit Janik[2]
[1]TWI, [2]Coventry University
2nd Year of PhD

Keywords: wire arc additive manufacturing, low alloyed steels

I. INTRODUCTION

Additive manufacturing (AM) paves the way for technological advancement in the manufacturing industry by enabling efficient use of resources. The ability to manufacture complex geometry and accelerate material development concurrently has attracted lots of research focused on AM. The method can can be classified as powder- or wire-based, depending on the kind of feedstock used during deposition. Based on the energy input, it can be classified into laser, electron or arc-based manufacturing. Powder-based processes can deposit on structures with complex geometries but are limited by the maximum size that can be deposited. Wire based direct energy deposition (DED) methods offer the advantage of depositing on larger structures with comparatively less geometrical accuracy.

Given its unique advantages over conventional processing methods, some discrepancies need to be addressed for wire-based DED. Introducing a fresh layer of molten metal over an existing layer leads to changes in the material, particularly creating inhomogeneity in mechanical properties and microstructure. Achieving a uniform microstructure will influence its mechanical properties such as strength and toughness. Deposition trials with different heat inputs were made with low alloyed steels (C/Mn) to observe the effect on microstructure while measuring the thermal history of a particular layer (layer 5). Continuous cooling transformation curves were plotted with Thermo-Calc for the feedstock (ER70S-6) composition. A correlation between process parameters and theoretical simulations will be established which will be useful in optimising feedstock composition for future works.

II. EXPERIMENTAL DESIGN

In this study, five wall depositions with differing heat inputs were made on individual steel substrate blocks (50mm x 250mm x 12mm). A six-axis welding robot, with a Fronius arc welding power source, wire feeder and welding torch was used with the heat input values, as given in Table 1, for conducting the experiments. Temperature measurements were made using K-type thermocouples (0.8mm diameter calibrated at TWI), inserted into the molten pool and recorded with the picologger.

Table 1: Heat input values for WireDED depositions

Trial number	I301	I302	I303	I304	I305
Heat input (KJ/mm)	0.594	0.550	0.513	0.527	0.504

The composition for thermodynamic simulations was obtained by spectroscopic analysis performed on the as-built material of trial I301 (given in Table 2)

Table 2: Composition of deposited walls

Element	C	Mn	Si	Cr	S	P	Ni,Co,Zr
Weight %	0.08	1.18	0.7	0.01	0.02	0.01	<0.05%

Specimens for examination were extracted perpendicular to the building direction from the as-built condition. These were mounted and prepared by the standard metallographic procedure for microstructural examination. Optical microscopy and scanning electron nicroscopy were used to capture micrographs at different locations across the built wall. Electron Backscatter Diffraction (EBSD) analysis of the samples was made to identify and verify any preferred orientation during deposition, and grain data such as grain size distribution and average grain size across different layers.

III. RESULTS

1. Thermo-couple measurements

The initial deposition of up to four layers was made on the substrate using the arc deposition process. After the fourth pass, an interval of 100s is allowed to place the thermo-couple over the wall, and further deposition is continued over the thermocouple. A total of 14 layers was deposited to construct a 27mm high wall on the substrate. A graph of temperature measured against the time during deposition is shown in Figure 1

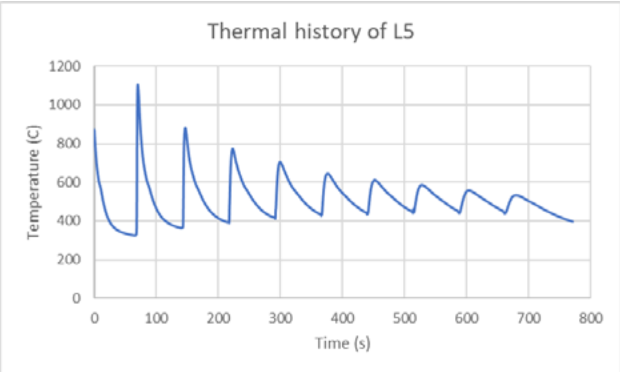

Figure 1: Temperature measured by placing thermocouple over 4th layer

2.Thermodynamic simulations

Thermodynamic simulations using Thermo-Calc 2021B version (product of Thermo-Calc AB) were made using the TCFE11 database. Equilibrium calculation was made with the help of Thermo-Calc to estimate the transformation temperatures (Ae1 and Ae3) with TC Poly3 function. The Ae1 temperature and Ae3 temperatures at equilibrium were around 690°C and 890°C respectively.

The continuous cooling transformation (CCT) curve for the base composition was calculated (with different reference cooling rates) using Thermo-calc graphical mode and shown in Figure 2.

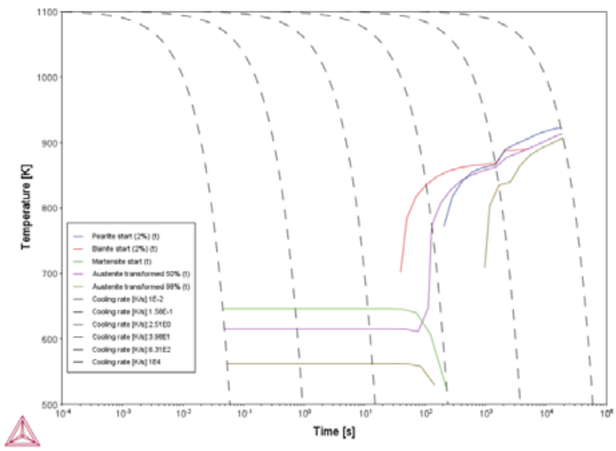

Figure 2: CCT diagram calculated for base composition with Thermo-calc

3. Microstructural examination

The EBSD microstructure of the as-built sample from different layers is shown in Figure 3. A clear distinction in the grain size can be observed from the different micrographs.

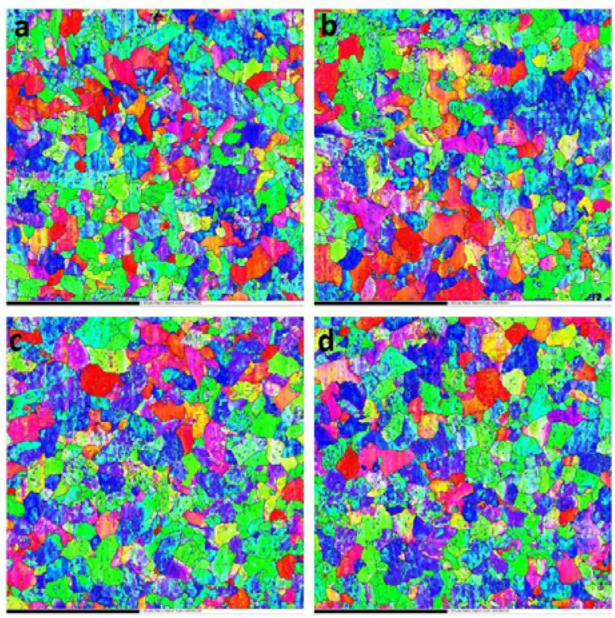

Figure 3: Inverse pole figure maps taken at different layers of the I301 specimen. a) layer 5 b) layer 6 c) layer 7 d) layer 8.

IV. DISCUSSION/CONCLUSIONS

From the inverse pole figures shown in Figure 3, the lack of preferential orientation in the grains can be observed, which is commonly reported in AM builds. Also, consistent refinement of grain size is evident as subsequent depositions are made over a layer. This denotes the grain refinement effect of the heating cycle and requires an understanding of the thermal history recorded, with observed microstructure and theoretical simulations.

V. FUTURE PLAN/DIRECTION

The microstructure and thermal history of different builds from I301 to I306 should be compared with each other, by measuring their average grain size, diameter and hardness map across the build direction. This will provide more details in correlating the practical measurements and theoretical predictions from Thermo-Calc.

REFERENCES

[1] Hashmi, M. (2014). Comprehensive materials processing : 13 volume set.

[2] Greer, C., Nycz, A., Noakes, M., Richardson, B., Post, B., Kurfess, T., & Love, L. (2019). Introduction to the design rules for Metal Big Area Additive Manufacturing. Additive Manufacturing, 27(C), 159-166.

Ali Alperen Bakir

Ali is a second year PhD student at Coventry University and NSIRC by the sponsorship and support of Lloyd's Register Foundation. He completed his BSc in mechanical engineering at Middle East Technical University, and worked there for two years as a volunteer research student in the Nanomechanics Laboratory. He then gained his MSc from Nottingham University, where he worked on the creep behaviour of additively manufactured Inconel 718. This project is funded by Lloyd's Register Foundation that helps to protect life and property by supporting engineering-related education, public engagement and the application of research.

Structural Integrity Assessment of Cold Spray Repaired of High-Strength Aluminium Alloy 7075 Specimens

Matthew Dore [1,2], Xiang Zhang[2], Kashif Khan[2]
[1]TWI, [2]Coventry University
2nd Year of PhD

Keywords: Cold spray, repair, aluminium alloy 7075, structural integrity

I. INTRODUCTION

Aluminium alloy (AA) 7075 is widely used in the aerospace industry due to their high strength to weight ratio and long term durability. However, these components have in-service damages, such as wear, corrosion pits, and cracks; caused by corrosion, fatigue loads and much more. Therefore, it is important to repair these components to minimise the cost, maintenance time and environmental impact.

For the last two decades, cold spray (CS) has seen an emerging role in repair applications, especially for temperature and oxidation-sensitive materials such as aluminium alloys.

CS is a solid-state material deposition method during which the temperature stays below the melting point of the deposited alloy, thus eliminating the negative effects associated with high-temperature processes. As shown in Figure 1, powder particles are accelerated with a hot gas and sprayed onto the substrate via a De Laval Nozzle.

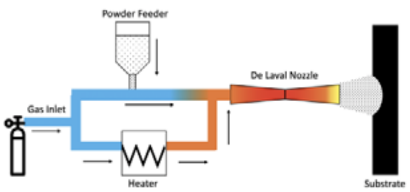

Figure 1. The Impact Innovation 5/11 high-pressure CS system at TWI Ltd, Cambridge, UK

Due to the continuous particle impact during the CS process, residual stress (RS) builds up. RS profile depends on powder properties and process parameters. Peng et al. [1] demonstrated that heat-treated samples had lower fatigue life, which they hypothesised was due to the beneficial residual stress relaxation during heat treatment.

Due to our lack of understanding of the effects of heat treatment of powder and CS repaired parts on residual stress, the mechanical performance of such parts under static and cyclic loading have yet to be fully understood. In this project, the structural integrity of cold spray repaired AA7075 specimens will be investigated.

II. DESIGN/METHODOLOGY/APPROACH

In this study, gas-atomised AA7075 powders and AA7075-T651 plates are used.

An initial study was performed to select the process parameters since they considerably affect the mechanical performance of CS repaired samples. This parameter selection was based on the adhesion strength between the CS deposition and substrate, and the porosity defect in the deposited materials. Three different gas temperatures (300°C, 400°C and 500°C) and pressures (3MPa, 4MPa and 5MPa) were compared. The selected parameters are provided in the results section.

In order to assess the structural integrity of the repaired specimens, a microstructure analysis, pull-off adhesion test (ASTM C633), Vicker's hardness test (ASTM E384), tensile test (ASTM E8) and fatigue test (ASTM E466) were performed. Preparation of repaired specimens and specimen dimensions are schematically shown in Figure 2.

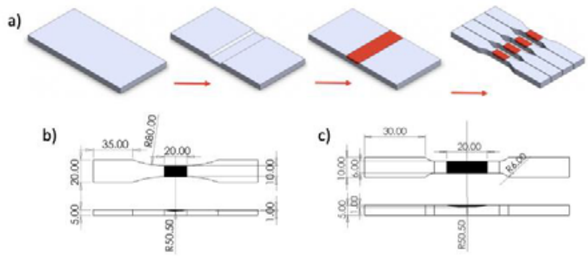

Figure 2. a) Sample preparation process for the cold spray repaired specimens, b) fatigue c) tensile specimen dimensions

III. FINDINGS/RESULTS

Initial results show that repaired samples can be produced with low volume density of porosity (<1%) and high adhesion strength (>65MPa) using the selected process conditions (6MPa, 500°C). Figure 3 shows an optical micrograph of the coating and substrate with the selected parameters. However, with these conditions, the deposition efficiency was low, at around 7%.

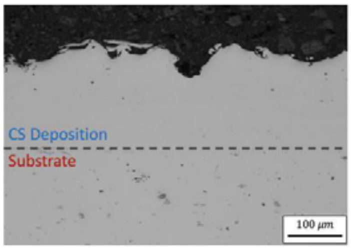

Figure 3. Microstructure of a cold spray deposition with the selected process parameters.

Vicker's hardness test revealed that the cold spray deposition hardness (146.9±5.9HV) is 20% lower than the substrate material (183.6±3.0). Figure 4 shows the hardness variation through the sample. Through the deposition, no considerable difference is observed.

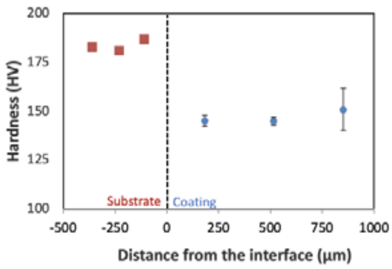

Figure 4. Vicker's hardness variation through the cold spray deposition and substrate

Wrought specimens showed 576.3MPa ultimate tensile strength (UTS) and 17.4% ductility, whereas the CS deposition in repaired specimens failed at 460MPa UTS and around 0.7% strain. However, after the repair failure, the test continued, and the stress-strain diagram in Figure 5 was obtained. As seen from the diagram, the substrate failed at around 8% strain. Figure 6 shows the specimen after the fracture. Delamination was observed between the repair and the substrate. Also, the fracture planes of the CS repair and the substrate are different.

Nevertheless, the CS repaired samples showed similar fatigue lives with the wrought samples, at the high cycle regium, exceeding 1 million cycles under a cyclic stress (σ_{max} =200MPa, R=0.1). More tests are underway for higher stress.

IV. DISCUSSION/CONCLUSIONS

Initial experimental results showed that CS is a promising repairing method for AA7075. Adhesion strength and porosity can be improved at the cost of reducing the deposition efficiency.

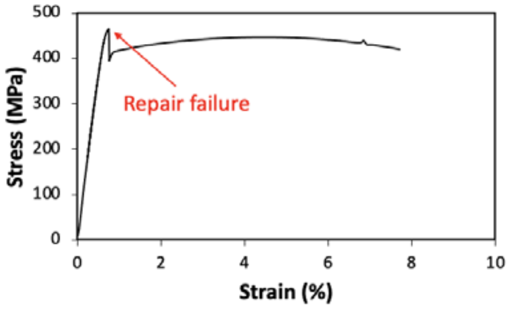

Figure 5. Stress-strain diagram of a representative CS repaired AA 7075 specimen.

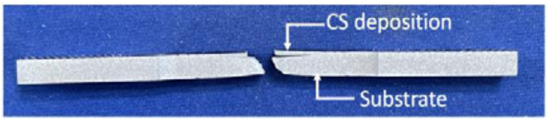

Figure 6. CS repaired tensile specimen image after the fracture.

Similar to other studies, poor tensile performance was observed for the coating, which might be improved with post-deposition heat treatment. On the other hand, initial fatigue tests reveal that CS repaired samples have high fatigue performance at high cycle (low stress) regium.

V. FUTURE PLAN/DIRECTION

To improve the deposition efficiency, tensile and fatigue performances, the AA7075 powder will be solution heat treated and quenched (SHT+Q) prior to deposition.

The mechanical performance of the CS repaired specimens produced with different powder conditions (as-received or SHT+Q), will be investigated and compared with the wrought material performance.

To understand the effect of pre and post deposition heat treatments on the residual stress profile, the contour method will be used. Measured residual stress will be correlated with the fatigue performance since compressive residual stress affects fatigue performance, it is essential to identify the residual stress after deposition.

REFERENCES

[1] D. Peng, R. Jones, N. Matthews, and C. CaTang, 'On the role of the interface on the damage tolerance and durability of cold spray repairs to AA7075-T7351 aluminium alloy wing skins', *Appl. Surf. Sci. Adv.*, vol. 3, p. 100044, Mar. 2021, doi: 10.1016/j.apsadv.2020.100044.

[2] H. Zhou *et al.*, 'Pores Structure Change Induced by Heat Treatment in Cold-Sprayed Ti6Al4V Coating', *J. Therm. Spray Technol.*, vol. 28, no. 6, pp. 1199–1211, Aug. 2019, doi: 10.1007/s11666-019-00882-0.

[3] A. Sabard, 'Solution heat treatment of gas-atomised aluminium alloy powder for cold spray', Dec. 31, 2020. http://eprints.nottingham.ac.uk/63696/ (accessed Dec. 16, 2021).

Dandan Liu

Dandan graduated from the Xi'an University of Science and Technology, China in Mechanical Manufacturing and Automation in 2019 (MSc). She joined the NSIRC PhD programme in January 2020 with Brunel University London and is sponsored by Lloyd's Register Foundation. Dandan is currently pursuing a PhD on "Hydrogen Induced Cracking in Oil and Gas Pipelines and Its Monitoring" and is in the 3rd year of her study.

Hydrogen Induced Cracks Monitored with Acoustic Emission Under the Laboratory Condition

Dr. Stephen Grigg[1], Dr. Bin Wang[2]
[1]TWI, [2]Brunel university
3rd Year of PhD

Keywords: acoustic emission, hydrogen induced cracking, feature extraction, clustering

I. INTRODUCTION

Hydrogen induced cracking (HIC)/Hydrogen blistering (HB) are phenomenons in which the material's mechanical properties are severely degraded due to hydrogen absorption or hydrogen penetration, resulting in brittle fracture. HIC cannot be eliminated once it initiates within a material, thus the state and development of the crack is required to be monitored. Acoustic Emission (AE) monitoring can detect the transient elastic wave generated when the material or structure degrades. It has been shown that monitoring and analysing the electrical signals which are generated from these waves over time with AE equipment will give an indication of the health of the structure.

In this study, an electrochemical hydrogen charging method is used to generate HIC/HB under laboratory conditions. To better analyse the state of the material under HIC conditions from the information carried by the signals, the first step is to extract the AE signals related to HIC accurately. This research work focuses on distinguishing three kinds of AE sources: H_2 bubbles, corrosion and HIC. This is done by manual methods step by step with a series of test procedures. However, the results of manual classification of the signals are reliable for several main features, such as duration, energy and frequency, but only for experiments with the same parameters. An unsupervised learning algorithm [1], which can eliminate human intervention, was applied to directly cluster all the AE signals and possibility to become a potential universal classification method.

II. DESIGN/METHODOLOGY/APPROACH

HIC-sensitive steels were considered to ensure that HIC can be obtained. In the light of a report by Kane et al. [2], it is indicated that HIC susceptibility is high for a carbon steel with high sulphur content (>0.002%) in the as-rolled condition. Rolled ASTM A516 Grade 65 carbon steel plate with banded ferrite-pearlite microstructure was chosen for this study whose dimentions are 200 x 50 x 5mm while the platinum was used as Anode. The setup of this study is shown in Figure 1. The electrolyte of 0.5 mol/L H_2SO_4 and 0.5g/L $NaAsO_2$ was dissolved in deionised water. The acidic solution was used to provide more H^+ while $NaAsO_2$ was used to inhibit the recombination of hydrogen atoms. The area exposed to the electrolyte was reduced to a $1cm^2$ square area by covering it with Belzona 4311 coating to reduce background noise from hydrogen activities. Four Nano-30 piezoelection sensors were placed on four corners (as shown in Figure 1) to collect the signals. After adding current, H_2 bubbles are generated and the corrosion by H2SO4 is suppressed. Theoretically, there are 3 kinds of signal sources in this test which come from bubbles, corrosion and HIC [3]. To distinguish and analyse the signals from HIC, three different tests were designed and the information is summarised in Table 1.

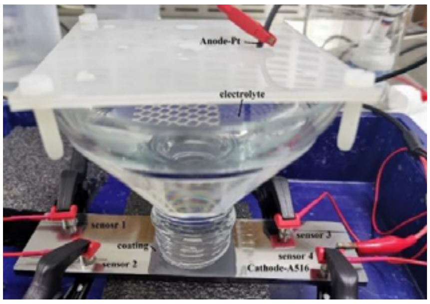

Figure 1. Setup of electrochemical H-charging test

Tests	Solution	I	D	AE sources
1	H_2SO_4	x	1	Bubble+corrosion
2	H_2SO_4	5	1	Bubble+corrosion (suppressed)
3	H_2SO_4 $NaAsO_2$	5	20	Bubbles+corrosion +HIC

*I: Current (mA/cm2); D: Duration (h)

Table 1. Information of three tests

III. FINDINGS/RESULS

The morphology of the surface and cross-section were observed after all three tests. HIC/HB were only observed in the specimen of Test 3 as shown in Figure 2. No evidence of HIC/HB was observed in Tests 1 and 2.

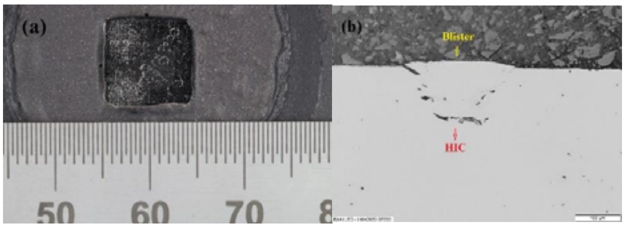

Figure 2. (a) surface morphology of hydrogen blisters (b) OM observation of HIC on the cross-sections, in Test 3

It was concluded from the work of Smanio that AE signals from H_2 bubbles have the characteristics of low frequency, low duration and low energy [4]. After analysing the results of Tests 1 and 2, the signals from bubbles and corrosion were distinguished by frequency, energy and duration whose characteristics can be summarised:

Signals from H_2 activities: 50KHz < Peak Frequency & Frequency Gravity < 200KHz; Energy < 1000eu; Duration < 1000us.

Signals from corrosion: Peak Frequency > 300KHz or Frequency Gravity > 200KHz with wide spectrum.

Compared with the signals of Tests 1 and 2, a new AE group of signals appeared with low frequency but high energy and high duration. Considering that this type of signal is only detected in Test 3, they are likely associated with HIC/HB. Therefore, the signals with peak frequency < 250KHz and duration > 1000us are artificially clustered as a group related to HIC and an Energy-Duration plot of the clusters is shown in Figure 3 (a). The unsupervised Learning method, Principle Component Analysis (PCA) and K-means, was carried out with seven signal parameters, including peak frequency and amplitude. The cluster result is shown in Figure 3 (b). It can be seen that the results of the unsupervised learning method are comparable to those of manual classification. Figure 4 illustrates the cumulate energy of signals of 3 clusters with time. It shows that a large amount of HIC behaviors will be generated after approximately 7 hours of experimental work.

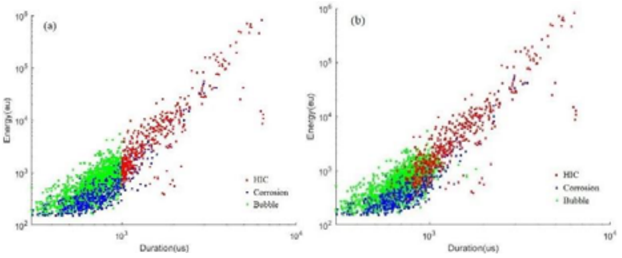

Figure 3. Representation of signals in Test 3 about the Energy-Duration graph clustered by (a) manual operation (b) unsupervised learning

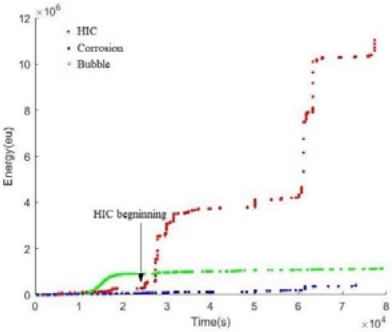

Figure 4. The cumulate energy of signals of 3 clusters with time

IV. DISCUSSION/CONCLUSIONS

Under laborate conditions, the electrochemical hydrogen charging method was more suitable to generate HIC/HB due to the short test duration and lower toxicity. An experimental procedure was applied to differentiate the different AE sources and demonstrate the characteristics of signals related to HIC/HB are high duration, high energy and low frequency. The unsupervised learning method was also used in this work, PCA + K-means, completely eliminate human intervention and created a comparable result which indicated that it is a potential tool to cluster signals from tests with different parameters as an universal method.

V. FUTURE PLAN/DIRECTION

The next step of this work is to do more testing with different external parameters to verify the universal applicability of this unsupervised learning cluster method. In addition, the localisation of HIC events will also be investigated in the future work and focus on improving accuracy.

REFERENCES

[1] Shiyuan Ju, Dongsheng Li, Jinqing Jia. Machine - learning - based methods for crack classification using acoustic emission technique[J]. Mechanical Systems and Signal Processing, 2022, 178, 109253.

[2] R. D. Kane, M. S. Cayard. Roles of H2S in the behaviour of engineering alloys: a review of literature and experience[C]. Corrosion98. 1998.

[3] Jin Sung Park, Jin Woo Lee, Joong Ki Hwang, et al. Effects of Alloying Elements (C, Mo) on Hydrogen Assisted Cracking Behaviors of A516-65 Steels in Sour Environments[J]. Materials, 2020, 13, 4188.

[4] Ve´ronique Smanio, Marion Fregonese, Jean Kittel, et al. Wet hydrogen sulfide cracking of steel monitoring by acoustic emission: discrimination of AE sources[J]. J Mater Sci, 2010, 45:5534–5542.

Anurag Niranjan

Anurag is a third year PhD student at Coventry University and NSIRC, with sponsorship and support from the Lloyd's Register Foundation. He completed his M.Tech in Metallurgical Engineering and Material Science from the Indian Institute of Technology Bombay. Before pursuing a PhD he has worked as a Failure Analysis Engineer for almost five years at Element, Abu Dhabi. His PhD (started in September 2020) focuses on studying a surface-breaking flaw at the weld toe region in a fillet weld under cyclic load using both numerical modelling and residual stress measurement at pre-defined crack depths. The outcome of this project will inform integrity assessment with respect to the treatment of residual stress in fillet welds and will be greatly beneficial for flaw tolerance assessments (BS 7910, API 591).

Crack Behaviour in the Residual Stress Field at Fillet Welds in Ship Structures

Yin Jin Janin[1], Jazeel Chukkan[1], Michael Fitzpatrick[2], Niall Smyth[2]
[1]TWI, [2]Coventry University
3rd Year of PhD

Keywords: Weld residual stress, residual stress redistribution, fatigue loading, fatigue crack propagation, weld modelling, crack modelling

I. INTRODUCTION

Ship structures are fabricated by welding together large plates. Out of the five basic weld joints, fillet welds are used to join the T-bar longitudinal stiffeners which serve as the main load-bearing part of the ship assembly. The geometry and design of the fillet weld provide a ready-made stress raiser at the weld toe area and make it prone to fatigue cracking. In addition, welding residual stresses in fillet welds are generally distributed in a non-uniform manner and play a significant role in crack initiation and propagation from the small undercut-type irregularities at the weld toes.

Redistribution of the residual stresses occurs under the cyclic loading, which is experienced during service. Furthermore, the combination of the as-welded residual stress, local constraints, and loading can alter the stress field in ways that are extremely difficult to predict. Defect assessment procedures such as BS 7910 offer methods for determining flaw acceptance but there is limited guidance on the assessment of fillet welds and their residual stress redistribution upon mechanical loading. Therefore, this work aims to study a surface-breaking flaw postulated at the weld toe region in a fillet weld under cyclic loads using both numerical modelling and residual stress measurement at pre-defined crack depths.

II. HEAT SOURCE MODELLING

Welding simulation is implemented in this work to model the initial as-welded residual stress distribution on double-sided fillet-welded T-joint specimens. A thermal elastic-plastic analysis is employed using Goldak's double ellipsoid [2] heat source distribution (Figure 1 a) to simulate the welding process of the T-joint specimen. Goldak's heat distribution replicates the torch movement by following the path defined by the coordinate system. In the case of fillet, weld joints transformation of coordinates (Figure 1b) is recommended to emulate the weld torch angle of actual welding.

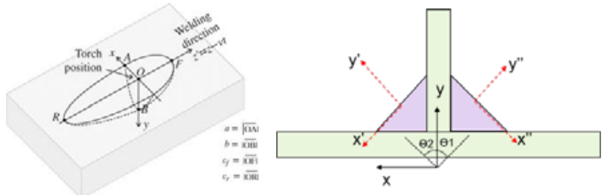

Figure 1: (a) A schematic of Goldak's Double ellipsoid heat source; (b) Coordinate transformation for fillet weld specimen

The crucial part of setting up the weld model is to find the appropriate values of the Goldak heat source parameters, which is determined and validated by the macro cross section of the T-joint specimen. The 2D weld model is compared against the macrograph of the actual sample, thereby determining the optimum heat source parameter for the specimen.

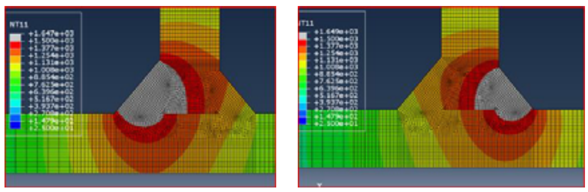

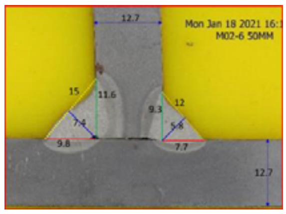

Figure 2: Comparison of 2D model with macrograph of the T-joint specimen

III. CONTOUR MEASUREMENT

The contour method is a destructive residual stress measurement technique and is based on mechanical strain relief. In the contour method, a part is cut into two halves by using a wire electro-discharge machining, and the stress component being measured is normal to the cut surface (Prime, 2001).

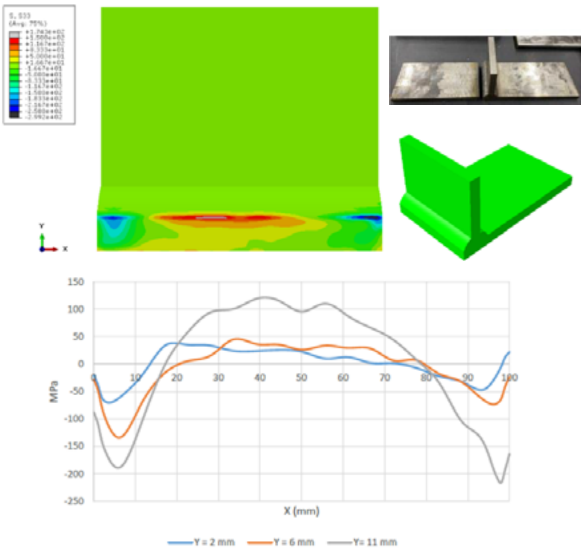

Figure 3: As-welded residual stress profile in the transverse or Z-direction

It is assumed for the cutting stage that the cut surface is flat and no new stresses are incorporated. Followed by the cutting stage, both cut surfaces/halves are measured with a coordinate measuring machine (CMM) to get the displacement profile. Then data analysis is carried out to average, clean and smooth the measured surface displacement data. Finally a 3D FE model of one of the cut surfaces is built and the reverse of the measured contour is applied as the displacement boundary condition. Constraints are applied to the model to avoid rigid body motion. A linear-elastic FE analysis is finally used to calculate the residual stress in the sample.

IV. STRESS INTENSITY FACTOR FOR T-JOINT

The study of fatigue crack growth depends on two main equations, the stress intensity factor (SIF) and the crack growth law. As per BS 7910, the general equation for fracture assessment requires determination of SIF magnification factor M_k . The magnification factor takes care of the stress concentration factor which arises due to the presence of the fillet weld [1]. For the fracture mechanics assessment of cracks at the weld toe, the stress intensity factor (K) solutions are often expressed in terms of the weld toe magnification factor M_k, which is defined as:

$$M_k = \frac{\text{K (in plate with weld attachment)}}{\text{K (in same plate with no attachment)}}$$

The magnification factor M_k in the SIF solution ensures that the crack tip is in a stress field completely defined by the magnified stress field of the fillet weld.

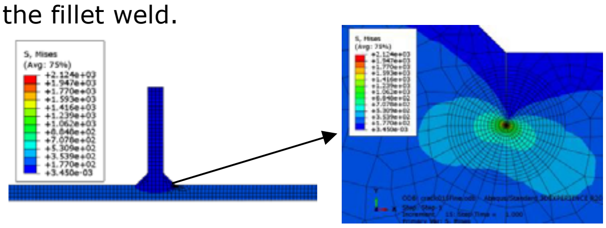

Z(mm)	KI value of plate without attachment (Mpa.mm1/2)	KI value of plate with attachment (T-joint) (Mpa.mm1/2)	Mk
0.15	156.20	270	1.73
1.15	449.2	494	1.10
1.9	627	649.1	1.04
2.65	805.5	824.2	1.02
3.4	1026	1035	1.01
3.75	1139	1158	1.02
4	1366	1237	0.91

Figure 4: FEA model of 2D T-joint specimen with z=0.15mm. The table shows M_k value for different depths along thickness (z)

V. FINDINGS/RESULTS

The Goldak's heat source parameters were determined successfully for the 2D weld geometry. However the same parameters were not sufficient to cover the complete weld bead profile when used in the 3D model. This is due to the presence of different depth and width planes between the 2D and 3D models in the moving heat source analysis. Further work on 3D weld modelling is on-going and the next step would be to calibrate the temperature profile with the temperature data from the weld experiment.

As-welded residual stress was measured experimentally using the contour method. Figure 3 shows the as-welded profile. Tensile residual stresses of magnitude 120 MPa are observed close to the surface at the weld toe and diminish in the thickness direction away from the weld toe.

The initial study on determining the M_k factor for the T-joint specimen showed higher values for the shallow cracks which could be attributed to the notch stress effect, which reduces as the crack depth is increased.

VI. REFERENCES

[1]Bowness, D. and Lee, M. M. K. (2000) 'Prediction of weld toe magnification factors for semi-elliptical cracks in T-butt joints', International Journal of Fatigue, 22(5), pp. 369–387. doi: 10.1016/S0142-1123(00)00012-8.

[2]Goldak, J. A. and Akhlaghi, M. (2005) Computational welding mechanics, Computational Welding Mechanics. doi: 10.1007/b101137

[3]Prime, M. B. (2001) 'Cross-sectional mapping of residual stresses by measuring the surface contour after a cut', Journal of Engineering Materials and Technology, Transactions of the ASME, 123(2), pp. 162–168. doi: 10.1115/1.1345526.

*Lloyd's Register Foundation helps to protect life and property by supporting engineering-related education, public engagement and the application of research.

Hanwei Zhou

Hanwei is an NSIRC PhD student of Brunel University London, based at TWI. She received her Master's degree from Wuhan University of Technology in China in 2019, majoring in Engineering Structures of Ship and Offshores. After graduation, she was sponsored by Lloyd's Register Foundation to study 'Fatigue Propagation from Short Cracks in Thick Welded Steels' at TWI.

Fatigue Propagation from Short Cracks in Thick Welded Steels

Yin Jin Janin[1], Kuveshni Govender[1],Bin Wang[2]
[1]TWI, [2]Brunel University London
3rd Year of PhD

Keywords: SENB, fatigue crack growth, extended finite element, stress intensity factors

I. INTRODUCTION

In this project, fatigue crack growth rate tests were conducted on single edge notch bend (SENB) specimens manufactured using EH47 steel, as shown in Figure 1. Secondly, a numerical model based on the extended finite element method (XFEM) was created using the commercial software ABAQUS, and the relationship between crack length and the number of cycles from both experimental and numerical results was compared.

In the present work, a crack length extraction method and a variable amplitude (VA) loading procedure are presented based on the fatigue crack growth simulations, and the numerical model under different loading methods are validated using test data. The influence of loading methods (CA and VA) on the fatigue crack growth rates（FCGR）are analysed.

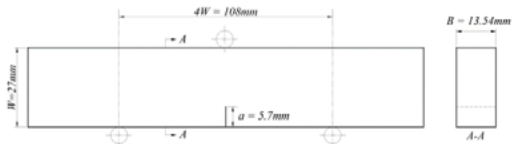

Figure 1 Dimensions of SENB specimens

II. METHODOLOGY

The methodology employed in this work involved the finite element analyses. Based on the numerical model, the secondary development was adopted to achieve fatigue crack growth analysis.

A. Numerical model

In the numerical model, both the stress intensity factor (SIF) and fatigue crack growth rates are obtained using the contour integral approach and extended finite element method respectively. The mesh distribution of the SENB model with full-width surface crack is shown in Figure 2. The continuum 3D 8-node reduced integration (C3D8R) was chosen as the element type.

In the FCGR model, the Paris Law equation is implemented in ABAQUS to define the crack growth rate of a fatigue crack, in which the material constants C and m are obtained from test data.

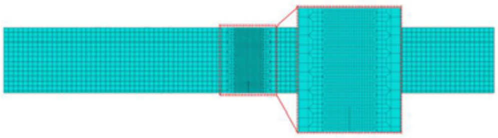

Figure 2 SENB model with full-width surface crack and its element distribution

B. Python scripts for extracting the crack length

Crack length and the number of cycles are two main factors that reflect the fatigue crack propagation phenomenon. However, the crack length is not explicitly set as the field or history output in ABAQUS. In order to quickly extract the crack length, python scripts are developed based on the XFEM method.

Using the python script, the average crack length and the number of cycles can be obtained simultaneously, which makes it possible to extract the crack information directly.IN addition, the python script can also be embedded into other programs, for example, Fortran subroutines, to realise different purposes related to fatigue crack analysis.

C. Variable amplitude (VA) loading procedure

For the VA loading procedure, the loading amplitude should be redefined in order to change the applied force. However, the amplitude for the direct cyclic step cannot be changed directly in ABAQUS, and a UAMP subroutine is required to be implemented into ABAQUS. At the beginning, the initial amplitude was defined for the model, and the python scripts for extracting the crack length will be called by the UAMP subroutine for every increment. A conditional statement will be tested for the crack length, and if the crack length is greater than the initial crack, the amplitude of the applied load will decrease according to the crack length. Eventually, the numerical calculation will end when the specimen is totally ruptured or the predefined number of cycles are met. Using the program, the crack length verses the number of cycles can be obtained. The variable amplitude loading procedure can be seen in Figure 3.

III. EXPERIMENTAL AND NUMERICAL RESULTS ANALYSIS

A. Comparison results under constant amplitude loading

Figure 4 shows the comparison between the crack length and the stress intensity factor range of the experimental tests and the numerical simulations. There is very good correlation between the experimental and the numerical results regarding the stress intensity factor versus the crack length. In general, the comparison of experimental and numerical results proves that the mesh distribution, boundary condition and fatigue criteria in the numerical method is acceptable in the simulation of the fatigue crack growth.

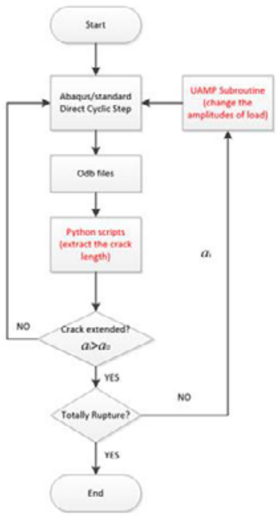

Figure 3 Flowchart of variable amplitude loading procedure

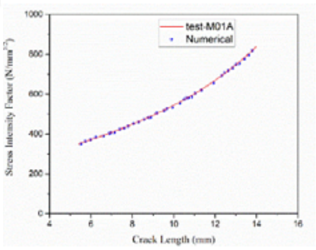

Figure 4 Stress intensity factor range versus the crack length of M01A

B. Comparison results under constant amplitude loading

As can be seen in Figure 5, a deviation between the experiment and numerical data can be observed, however the maximum error between them is less than 10%, and in general, the increasing trend has a good correlation between the experimental data and numerical results. Therefore, it can be concluded that the numerical method to perform variable amplitude loading simulations is reasonably acceptable to some extent, and can be used to simulate realistic cases subjected to variable amplitude loadings.

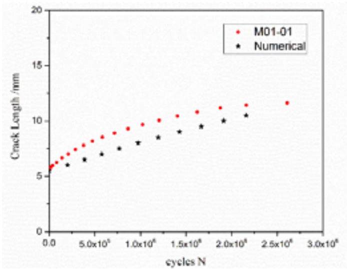

Figure 5 Average crack length of the specimen vs. the number of cycles

Numerical results of three different loading methods are shown in Figure 6. For CL, crack length increases rapidly along the cyclic numbers, and finally the specimen ends up rupturing. While for VAL-1, the fatigue life extends several times to that under constant amplitude loading. The first region, where the crack length slowly rises as a function the number of cycles, can be observed before a sudden accelerating crack growth is apparent. For VAL-2, the crack growth rates are the lowest amongst the three kinds of cases. The crack firstly propagates under fatigue loading; however, the propagation rates gradually decrease, and finally the crack arrests at a certain point and crack length does not change with the cyclic numbers.

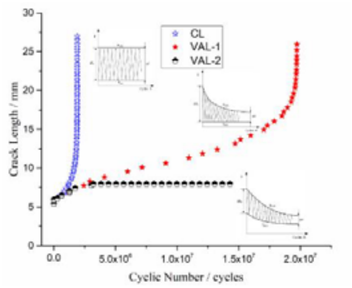

Figure 6 Relationship between crack length and cycles under different loading

IV. FUTURE PLAN/DIRECTION

In the project report, most of the attention has been paid to the analysis of specimens with the full-width surface notches, and the analysis on the specimens with semi-elliptical cracks are currently not adequate. Therefore, in the next stage, a numerical model will be built for specimens with semi-elliptical cracks, and experimental work will be performed in order to validate the numerical results. Furthermore, the numerical analysis will be conducted to investigate both the fatigue crack growth phenomenon as well as the fracture toughness of specimens with semi-elliptical cracks. In addition, comparisons will be made for specimens with full-width surface notches and semi-elliptical cracks.

REFERENCES

[1] Gifford Jr, L.N. and P.D. Hilton, Stress intensity factors by enriched finite elements. Engineering Fracture Mechanics, 1978. 10(3): p. 485-496.

Funke Dacosta-Salu

I studied Mechanical Engineering at Obafemi Awolowo University, Nigeria, and Loughborough University, United Kingdom for my Undergraduate and Master courses respectively. Subsequently, I worked as a Mechanical Engineer in the building services sector for two years, then moved to the oil and gas sector where I worked for about three years as a Senior Subsea and Pipeline Engineer and technology development lead, before starting my PhD with Coventry University as a Lloyd's Register Foundation scholar.

Thermal Fatigue at Mixing Points in Industrial Pipework

Funke Dacosta-Salu[1,2], Micheal E Fitzpatrick[2], Xiang Zhang[2], Tyler London[3], Alessio Basso[3], and James Jewkes[4]

[1]NSIRC, TWI Ltd, [2]Coventry University, [3]TWI, [4]University of Leicester

2nd Year of PhD

Keywords: Temperature fluctuation, fatigue, T-junction, computational fluid dynamics, finite element analysis

I. INTRODUCTION

Thermal fatigue has been affecting operations in many sectors, including nuclear and energy, for many years, despite measures taken to mitigate it. A total of 13 critical failures have been reported in pressurized water reactors in nuclear power plants (NPP) resulting from thermal fatigue . These occurred at different ages of the plants' usage [1]. Thermal fatigue has been considered an aging problem, but damages such as through-wall cracking in Civaux 1, France in 1998, occurred after only 1500h operation of the pressurized water reactor. This episode induced a more focused attention to the phenomenon [2] [3]. A piping section where two or more fluids at different operating temperatures and velocities combine and converge downstream is conventionally named a mixing point or T- junction. These junctions are very common in industrial plants where flow mixing is required, for instance, to locally dissipate heat. The turbulent inhomogeneous mixing of the two fluids at different operating conditions leads to thermal variations that are predominant in the vicinity of the T-junction region. This phenomenon is referred to as thermal striping [4].

During thermal striping, high-magnitude, low-frequency thermal and flow fluctuations propagate from the fluid down to the solid wall, inducing mechanical vibrations and local stress fluctuations in the pipe. If the stress variation is above the fatigue limit of the pipe material, this can lead to crack initiation and propagation over a number of cycles. (The fatigue limit refers to a stress value below which the material, in theory, can undergo an infinite number of load cycles without leading to fatigue failure). The method of utilizing leak before failure as a check to prevent damage has not been effective, as an undetected leak could quickly lead to failure, as was the case of the accident in the gas plant in Pascagoula, Mississippi, in 2016 [5]. A better method of preventing failure could be to ensure proper and adequate checks are carried out at a predetermined frequency. The objective of this research is to understand the combined effect of constraint and temperature fluctuations due to turbulence effects in the vicinity of mixing points, and to develop more effective inspection criteria to investigate T-junctions susceptible to thermal fatigue. This approach makes use of numerical simulation tools such as computational fluid dynamics (CFD) and finite element analysis (FEA).

II. DESIGN/METHODOLOGY/APPROACH

The methodology proposed in this research involves experimental measurements and numerical simulations. The numerical methodology involves sequentially-coupled fluidstructure-interaction (FSI). CFD analysis is used to determine the transient thermal field at the pipe walls which will then be mapped into the FEA solver to determine the subsequent transient thermal stress and strain fields. Ongoing models will provide a better understanding of the phenomena taking place at mixing points, whereas experimental measurements are used to validate the models.

III. FINDINGS/RESULTS

Turbulent mixing of hot and cold fluids at the mixing point can result in thermal fatigue when there is a high magnitude of temperature fluctuation and low frequency. Preliminary results from the CFD simulation carried out have been compared with published papers. The locations with high thermal fluctuation intensities between x/D=2 and x/D=4 at the right and left sides of the pipe have been identified as areas that are susceptible to thermal fatigue under repeated loading of the T-junction. (Where x is the distance along the horizontal axis downstream and D is the diameter of the pipe).

IV. DISCUSSION/CONCLUSIONS

The turbulent flow of two fluids of different temperatures mixing at the T-junction has been investigated and the results compared with other numerical and experimental outcomes. The numerical results of this study are shown to be in good agreement with the experimental and numerical data from other publications in the literature. Locations of high-temperature fluctuations have been identified. The temperature fluctuations result obtained in the fluid will thereafter be used in the subsequent phase of the project

V. FUTURE PLAN/DIRECTION

The next steps of the analysis, summarised below, involve thermal-mechanical coupling, and the assessment of the thermal stress and strain, and subsequent fatigue life:

1. Determine stress fluctuations in the pipe, based on the temperature fluctuations obtained in the previous steps.

2. Carry out thermal fatigue analysis using design codes.

3. Perform an experiment to identify areas of high stress/strain in the pipe.

4. Compare results with existing literature as well as novel experimental data.

The expected outcome will be identification of locations highly vulnerable to thermal fatigue, with changes in parameter such as temperature, location of constraints and momentum ratio. This will help build a database of information to check during the inspection of pipelines pron to thermal fatigue.

AKNOWLEDGEMENTS

This publication was made possible by the sponsorship and support of Lloyd's Register Foundation. The work was enabled through, and undertaken at the National Structural Integrity Research Centre (NSIRC), a postgraduate engineering facility for industry-led research into structural integrity established and managed by twi through a network of both national and international universities. Lloyd’s Register Foundation helps to protect life and property by supporting engineering-related education, public engagement and the application of research. Http://www.lrfoundation.org.uk/

REFERENCES

[1] C .L. Atwood, V. N. Shah, and W. J. Galyean, “Analysis of Pressurized Water Reactor Primary Coolant Leak Events Caused by Thermal Fatigue,” in ESREL ’99 - European Safety and Reliability, 1999.

[2] S. Chapuliot, C. Gourdin, T. Payen, J.P. Magnaud, A. Monavon, “Hydro-thermal-mechanical analysis of thermal fatigue in a mixing tee,” Nuclear Engineering and Design 235, vol. 235, p. 575–596, 2005.

[3] M. Dahlberg, K.-F. Nilsson, N. Taylor, C. Faidy, U. Wilke, S. Chapuliot, D. Kalkhof, I. Bretherton, M. Church, J. Solin, and J. Catalano, “Development of a European Procedure for Assessment of High Cycle Thermal Fatigue in Light Water Reactors: Final Report of the NESC-Thermal Fatigue Project,” Institute for Energy, Petten, 2011.

[4] I. S. JONES, “An Impulse Response Model for the Prediction of Thermal Striping Damage,” Engineering Fracture Mechanics, vol. 55, pp. 795-812, 1996.

[5] B. DuBose. (2020, April 5). Chemical Safety Board: Thermal Fatigue Led to Gas Plant Blast [Online]. Available: https://www.materialsperformance.com/articles/material-selection-design/2019/12/chemical-safety-board-thermal-fatigue-led-to-gas-plant-blast. [Accessed 15 January 2022].

Adam Fisher
I am a second year PhD student based at the University of Warwick. I am part of the HeySys CDT. I graduated from Loughborough University with a Masters in Computer Science and Mathematics

Using Kinetic Activation-Relaxation Technique to Investigate Crystal Growth in NiAl Superalloys

Tyler London[1], Peter Brommer[2], Thomas Hudson[2]
[1]TWI, [2]University of Warwick
2nd Year of PhD

Keywords: Kinetic Monte Carlo (KMC), Nickel Aluminium Superalloy, Kinetic Activation-Relaxation Technique (kART)

I. INTRODUCTION

Superalloys are alloys that can be used at a high percentage of their melting point without losing all their desirable properties[1]. Nickel-based superalloys are used for their resistance to fatigue and creep, coupled with their strength. These types of superalloys are usually chosen because they retain these properties at a higher temperature range than other alloys. Guaranteeing these properties, however, requires control of the alloy structure at the microscopic level. The microstructure of nickel-based superalloys has many different phases, and these phases contribute to the properties that make superalloys so useful.

The γ phase is the matrix comprising most of the alloy structure. This is a face centred cubic lattice (FCC) where there is no order between the species. The γ' phase, an ordered $\mathrm{L1_2}$ structure with atoms sitting on FCC lattice sites, forms precipitates and is one of the main phases that gives these alloys their strength. γ' is usually either formed on $\mathrm{Ni_3Al}$ or $\mathrm{Ni_3Ti}$. It has been shown that the interaction between γ and γ' phases also helps increase superlattice intrinsic stacking fault energies which contributes to the creep resistance of these alloys[2].

On a fundamental scale, the formation of this microstructure is governed by the motion of atoms arranging themselves in the correct fashion. Atomistic models could be used to inform simulations on longer length scales for a bottom-up approach. For example, precipitate growth rates dependent on composition and conditions could be determined. This could allow predictive simulations of microstructure formation.

However, a straightforward simulation of the atomic motion using classical molecular dynamics (MD) cannot access the time scales required: with time steps on the order of femtoseconds, the ageing processes responsible for microstructure evolution are far out of reach. Here, we propose to use kinetic Monte Carlo (KMC) to bridge the gap to longer time scales. By focusing on key events in atomic motion, macroscopic properties such as growth rates can be extracted.

II. DESIGN/METHODOLOGY/APPROACH

Kinetic Monte Carlo (KMC) is a method that studies a system over time as it evolves through a chain of metastable states. KMC uses barrier heights separating these states to calculate the rate at which the system changes state based upon harmonic transition state theory (HTST). In HTST, the rate k^{HTST} with which a system leaves a certain state can be found as

$$k^{HTST} = \mathrm{A}e^{-E_{\mathrm{barrier}}/(k_B T)},$$

where E_{barrier} is the height of the energy barrier separating one state from the next and T is the temperature. A is a prefactor that is ~~an~~ approximated to be $10^{13}\ \mathrm{s}^{-1}$[3]. These rates are assembled for all potential trajectories leaving a state. One of those is then selected, the system is moved to the next state, the clock is advanced based on the total rate, and then the procedure is repeated. Dependent on barrier height and temperature, a single event can propagate the system over a time interval ~~that~~ which would take many thousands (or millions) of MD time steps.

The critical step in KMC simulations is finding the barriers to leaving a certain state. kART [4] is an off-lattice KMC program using the ART nouveau first-order saddle point search to find these barriers in a three-stage process. First, an atom and its neighbours are pushed along a random direction and the eigenvalues of the Hessian matrix are calculated. When one of them is sufficiently negative, the system is deemed to have left the harmonic well. Next, the system is pushed in this direction while energy is minimised in the perpendicular hyperplane, until we find the saddle point. This gives us the barrier energy. The final step is to push the system across the saddle and relax to the new minimum. This process is repeated until all atoms in the system have been sampled for potential events, out of which one is then selected according to KMC rules.

III. FINDINGS/RESULTS

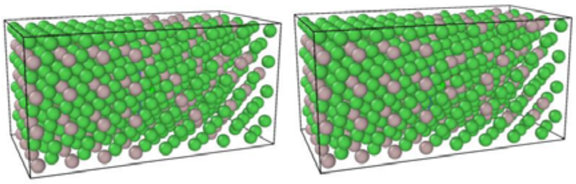

Figure 1:
Simulation cell of 50% $L1_2$ and 50% solid solution of 75% Ni (green) and 25% Al (grey). Initial structure left, final structure right.

To examine the feasibility of using kART to study the growth of $L1_2$, a γ/γ' interface was set up: 256 atoms of $L1_2$ Ni_3Al next to 256 atoms of $Ni_{75}Al_{25}$ random alloy, with one vacancy introduced to facilitate diffusive processes (Fig. 1 left). The system was then evolved over 650 kART steps at 900 K using a published potential[5] for Ni_3Al. At this temperature, $L1_2$ has been shown[6] to form.

Over the 650 KMC steps, the simulation covers more than 450 ns, which would require tens of millions of MD steps. The final structure is shown in Fig. 1 right. Fig. 2 shows the significant decrease of the energy of the system over time.

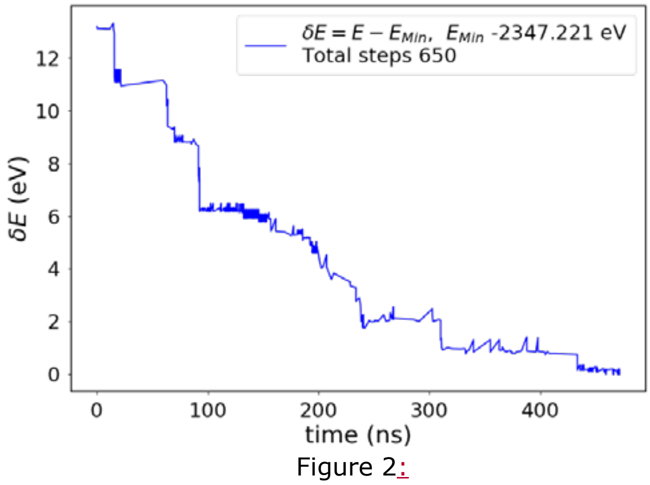

Figure 2:
Energy over simulated time for KMC simulation.

IV. DISCUSSION/CONCLUSIONS

We demonstrate that it is possible to simulate the evolution of a Ni_3Al system using kART over time scales much longer than what is accessible to classical MD. At the simulated temperature, the system progressed towards equilibrium which is shown by the significant drop in energy from start to finish. Visual inspection indicates that in the γ phase, Al atoms move away from each other as a step towards ordering, but this is not restricted to the interface. It would be expected that the $L1_2$ phase would grow from the boundary between the two phases. From the simulations so far, there is no evidence of this, but more simulation time may be required.

Beyond the direct simulation, the catalogue of events that kART collects in a simulation could be used to identify the events and barriers that drive forward the formation of the γ' phase. These events are the ones preceding significant drops in energy in Fig. 2. This information could then be used to infer growth rates.

Figure 2 also highlights one issue of KMC simulations: during some phases (e.g., at 194 ns, it takes 157 steps for 6 ns), the system goes through many KMC steps with little progress. This indicates a rapid back-and-forth flicker across a low-energy barrier, with associated high rates and thus small time increments, taking up computational time without progressing the simulation. Activating a kART feature to average over these flickers could speed up future simulations.

V. FUTURE PLAN/DIRECTION

Here, we want to highlight four areas to take the project forward. In the short term, the NiAl interaction potential[5] used here needs to be validated for this application by comparing barrier energies to calculations based on first-principles methods. This will show whether the potential is adequate or needs further improvement.

With an improved flicker treatment, longer time scales will be accessible, allowing direct study of the growth rate for the $L1_2$ phase at different temperatures. This information could then be used to parametrise a partial differential equation model to simulate the ageing processes in these materials on technologically relevant time and length scales.

Complementary to the direct approach, an identification of rate-limiting KMC events would give deeper insights in the timescales relevant for the growth of the γ' phase.

Finally, all these studies should be extended to varying Al concentration in the γ phase, to examine effects of Al depletion near the growth front. This would then allow a full bottom-up view of the superalloy microstructure formation processes.

REFERENCES

[1] C. T. Sims, Superalloys, vol. 1984, pp. 399-419, 1984.
[2] A. Breidi, J. Allen, and A. Mottura, Acta Materialia, vol. 145, pp. 97-108, 2018.
[3] A. F. Voter, Radiation effects in solids: Springer, 2007, pp. 1-23.
[4] N. Mousseau et al., Journal of Atomic and Molecular Physics, vol. 2012, 2012.
[5] G. Purja Pun and Y. Mishin, Philosophical Magazine, vol. 89, no. 34-36, pp. 3245-3267, 2009.
[6] M. Doi, D. Miki, T. Moritani, and T. Kozakai, Superalloys 2004, pp. 109-114, 2004.

Zeng Chen

Zeng is currently a 3rd year PhD student of the Solid Mechanics Research Group at the University of Bristol. He graduated with his Bachelor's degree and Master's degree in Mechanical Engineering from the Hefei University of Technology in China. With the sponsorships of TWI Ltd and the China Scholarship Council, Zeng started his PhD programme in 2019. His research focuses on developing the approach of assessing the apparent fracture toughness caused by a change in crack-tip constraint, which can assist with making less conservative structural integrity assessments to potentially reduce costly repair and replacement decisions for plant operators.

A Novel Unified Parameter for Characterising Constraint Level of Multi-Axial Bend Specimen

Rob Kulka[1], Mahmoud Mostafavi[2]
[1]TWI, [2]University of Bristol
3rd Year of PhD

Keywords: Constraint, Unified parameter, Plastic strain energy, multi-axiality

I. INTRODUCTION

Crack-tip constraint is defined as the resistance of a structure against crack-tip plastic deformation [1]. A loss of crack-tip constraint can cause an increase in fracture toughness. The factors that can affect the constraint level are often considered to be component thickness, crack and ligament length, geometry, and type of loading. Currently, widely accepted constraint parameters, such as Q and the unified parameter φ, are used to quantify their effect on toughness. The effectiveness of such parameters has been validated using specimens with uniaxial loading such as C(T) and SEN(B). However, a large number of industrial assets experience modes of loading other than uniaxial. Meanwhile, multi-axiality has been considered an important effect in various standards and assessments. It is meaningful to investigate if these characterization parameters are useful in those multi-axial conditions. In this study, parameter φ is applied to the 5 Point Bend (5PB – equivalent-biaxially bent) specimen and the 3 Point Bend (3PB - uniaxially bent) specimen of BS1501-224 28B steel. A novel characterization method based on the plastic strain energy around the crack tip is proposed. The effectiveness of these two methods is compared and discussed.

II. DESIGN/METHODOLOGY/APPROACH

Mostafavi et al. [2] further studied the Anderson–Dodds approach and modified that model, then introduced a unified constraint parameter φ that was defined as the area of the plastic region at fracture normalised by the reference plastic region at fracture for a standard specimen:

- $\varphi = \frac{A_c}{A_{ref}}$ (1)

As the widely accepted definition of constraint states the crack-tip constraint is the resistance of a structure against crack-tip plastic deformation, a method based on the plastic strain energy around the crack tip is proposed. Assume there are N elements around the crack tip reaching to yielding. For element i, the work to cause its total deformation includes elastic and plastic components. The elastic component can be easily calculated from the true stress-strain curve. Then the plastic component of element i is the difference between the total energy and the elastic component. Sum all plastic components in N elements, the total plastic work is:

- $U_p = \sum_{i=1}^{N}\left(\int_0^{\varepsilon_i}\sigma d\varepsilon - \frac{\sigma_i^2}{2E}\right)V_i$ (2)

Due to the complexity of the stress distribution in the crack-tip field, the equivalent stress σ_{eq} and equivalent strain ε_{eq} are applied in the calculation. Then the total plastic strain energy or the total plastic work can be considered as:

- $U_p = \sum_{i=1}^{N}\left(\int_0^{\varepsilon_i}\sigma_{eq} d\varepsilon_{eq} - \frac{\sigma_{eq}^2}{2E}\right)V_i$ (3)

Then, a geometry factor $\frac{1}{Bb}$ is introduced to be multiplied with U_p to form a novel unified characterization parameter.

My colleague, Konstantinos Kouzoumis, did a series of bending tests with a large number of 5 Point Bend biaxial specimens and 3 Point Bend specimens to catch the effect of biaxiality. The material is BS 1501-224 steel and the temperature is around -160℃. One of those 5PB specimens is shown in Figure 1. The "S" shape observed confirms that biaxiality was indeed captured successfully with his experiments. To obtain a more convincing result, a large amount of C(T) and SEN(B) specimens' data obtained previously was collected [3-4].

The numerical modelling was conducted with ABAQUS 6.14. Due to the symmetry, one-quarter models were adopted. 8-noded quadratic elements with reduced integration (C3D8R) were applied. The load roller and a support roller were created as rigid bodies, and the contact condition between them and the specimen was defined as surface-to-surface contact with a finite-sliding formulation. The modelling was conducted by applying a load-line displacement (VLL) to the load roller.

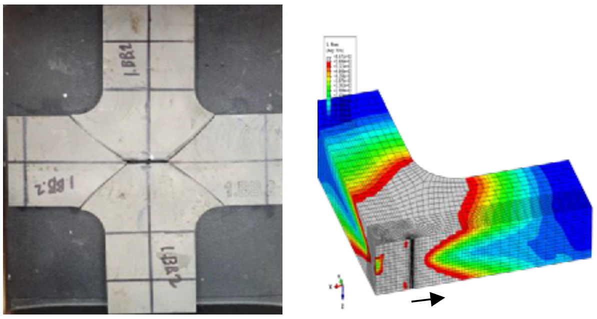

Figure 1. Picture of a cracked 5PB specimen and stress contour diagram of the 5PB model

III. FINDINGS/RESULTS

To validate the accuracy of the biaxial bending and uniaxial bending simulation, the load-displacement curves of the loading punch were drawn to be compared with experimental data, which is shown in Figure 2. It can be seen that the FEA curves agree well with the experimental curves. Their load-line compliances in the elastic region are almost the same. Meanwhile, the stress contour diagram in Figure 1 also shows that the stress concentration area is along the crack propagation line of the tested specimen. Therefore, the numerical model is shown to be accurate. Due to the lack of standard equations for these two specimens, the numerical K_{Jc} are used in the subsequent analysis.

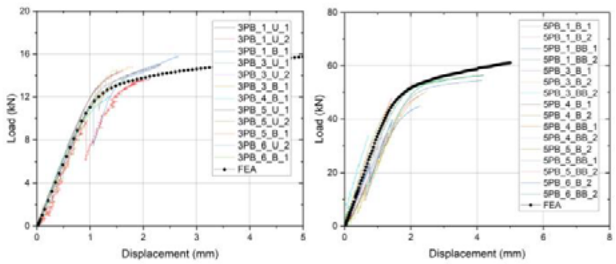

Figure 2. Comparisons between simulated and experimental load-displacement curves

The simulation outputs, J-integral, were extracted at the midplane, at the 10th contour, when the simulated load-line displacement values were equal to the test data at failure. The values of parameter φ and $\frac{U_p}{Bb}$ corresponding to each specimen are shown in Figure 3.

IV. DISCUSSION/CONCLUSIONS

Comparing the two diagrams in Figure 3, it can be found that there is a high order relationship between parameter φ and fracture toughness K_{Jc} when it is applied to C(T) and SEN(B) specimens, but such a relationship does not exist for 5PB specimens and 3PB specimens. On the other hand, the parameter $\frac{U_p}{Bb}$ shows its advantage, for a high order relationship still is found between it and fracture toughness. Such monotonic correlation is preferred to help engineers assess a more accurate fracture toughness estimate for nonstandard components in a complex loading situation.

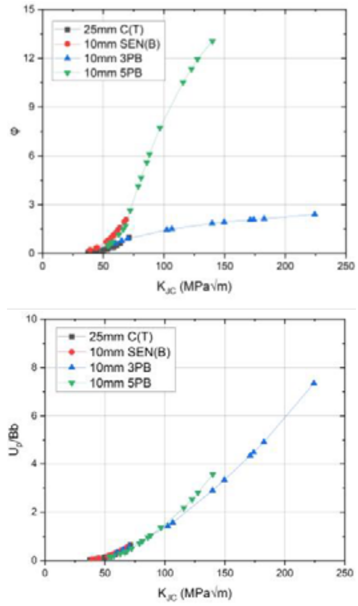

Figure 3. Results of parameter φ and $\frac{U_p}{Bb}$

V. FUTURE PLAN/DIRECTION

1. Complete fracture toughness tests using ASTM A516 Grade 70 steel on SEN(B) and C(T) specimens with different sizes.

2. Once the test is completed, a series of finite element analyses will be conducted to extract simulation results to validate the applicability of the proposed method.

3. Other supplementary experiments with different specimens will be considered to extend the approach's applicability.

REFERENCES

[1] W. Brocks and W. Schmitt, "The Second Parameter in J-R Curves: Constraint or Triaxiality ?." In STP1244-EB Constraint Effects in Fracture Theory and Applications: Second Volume, ed. M. Kirk and A. Bakker, (pp. 209-231). West Conshohocken, PA: ASTM International, 1995.

[2] Mostafavi, M., Smith, D. J. & Pavier, M. J. Reduction of measured toughness due to out-of-plane constraint in ductile fracture of aluminium alloy specimens. Fatigue Fract. Eng. Mater. Struct. 33, 724–739, 2010.

[3] D. G. A. Van Gelderen, Effects of Load History on Low Temperature Fracture of Steels, PhD, University of Bristol, Bristol, 2016.

[4] M. J. Balart and J. F. Knott, Effects of geometry and flow properties on the fracture toughness of a C–Mn reactor pressure vessel steel in the lower shelf region, Int. J. Press. Vessels Pip., vol. 83, no. 3, pp. 205–215, Mar. 2006.

Paul Ukpaayedo Sukpe

Paul joined the NSIRC PhD programme in 2020 after graduating from Brunel University London with an MSc in Structural Integrity (Asset Reliability Management) in 2019 with NSIRC at TWI. He also holds a BSc in Mechanical Engineering from the Kwame Nkrumah University of Science and Technology, Ghana (2008) and an MSc in Mining and Power Engineering from the Wroclaw University of Science and Technology, Poland (2012). Paul's PhD aims to provide enhanced levels of toughness associated with loss of crack-tip constraint that will have major advantages for safety cases involving components with defects. His interests lie in structural integrity and failure of engineering structures, particularly offshore.

Crack Tip Constraint in Typical High Strength Components in Arctic Conditions

Rob Kulka[1], Rade Vignjevic[2], Kevin Hughes[3]
[1]TWI, [2]Brunel University London
3rd Year of PhD

Keywords: crack-tip constraint; low temperature; brittle fracture; through-thickness; integrity assessment

I. INTRODUCTION

Significant efforts have been made in the past decade in fitness-for-service (FFS) and engineering critical assessment (ECA) procedures, that provide a concise framework to relate crack size with applied loading, using failure assessment diagrams (FAD) to evaluate the severity of crack-like flaws. These approaches rely on the use of fracture toughness data measured from deeply notched specimens under bend loading to guarantee high levels of stress triaxiality which drive the fracture process. Several defect assessment methodologies based upon the FAD concept, such as R6 [1] and BS 7910 [2], are now well established, and widely employed to analyse the significance of defects in structural integrity assessment to provide conservative acceptance criteria.

However, most structural defects, such as in offshore pipelines, are very often part-through surface cracks that generally develop low levels of crack-tip constraint associated predominantly with tensile loading. The transferability of experimentally measured fracture toughness data to structural piping components, therefore, remains essential in accurately predicting in-service residual and remaining life [3].

Motivated by these observations, this PhD addresses a two-parameter description of crack-tip fields, in three-point single-edge notched bend (3P SENB), and clamped single-edge notched tension (SENT) specimens, that incorporates the evolution of near-tip stresses with values of the crack driving force, as characterised by the J-integral. This is aimed at presenting more refined defect assessment procedures that include the effects of constraint variation on fracture toughness so that crack-tip constraint in the test specimen closely matches that of the structural component.

II. DESIGN/METHODOLOGY/APPROACH

A substantial test programme, involving low temperature fracture toughness tests of SENB and SENT with different specimen configurations, is underway. The current plan is to use digital image correlation (DIC) to track the change in displacement fields as the SENB and SENT specimens are loaded, and to identify the crack path and crack tip location. Furthermore, combined use of x-ray computed tomography (XCT) and digital volume correlation (DVC) will be utilised to obtain full-field displacements on an aluminium sample, due to the size and capacity limitations of the XCT test rig (5kN). This XCT/DVC technique will enable internal imaging of the aluminium sample under progressive loading, to examine damage and fracture evolution through-the-thickness. The full-field displacement data is then used in a finite element (FE) framework to calculate the through-thickness energy release rate (J-integral) of the sample using the steps shown in Figure 1.

Plane-strain 3D FE computations will be performed for SENB and SENT specimens with varying notch depth (a) to specimen width (W) ratio in the range $0.1 \le a/W \le 0.5$. In addition, 3D FE analyses will be conducted for circumferentially cracked pipeline steel, with a surface flaw of fixed length having different crack depth (a) over pipe wall thickness (t) ratios. The results from the experiment will be used to validate the FE analyses that use different constitutive models. The triaxiality or crack-tip constraint effectwill be quantified based on the two-parameter framework (J-T and/or J-Q). See Figure 2 for constraint effect characterisation by the J-Q theory [4] using a modified FAD approach.

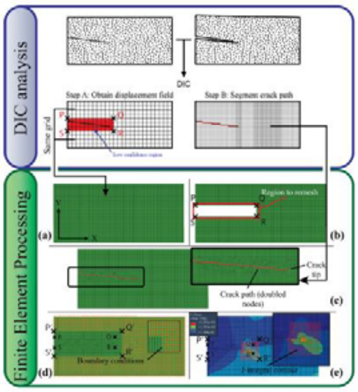

Figure 1. Steps of the J-integral calculation process [3].

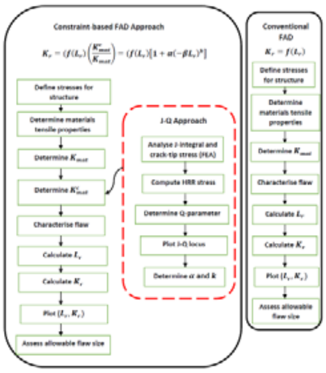

Figure 2. Proposed constraint-based approach compared with conventional BS 7910 procedure for fracture assessment

III. FINDINGS/RESULTS

Much theoretical and numerical work has been done to quantify crack tip constraint effects on fracture toughness in both two- and three-dimensional specimens and structural configurations. However, due to the loss of single-parameter J-dominance, several two-parameter fracture theories have been proposed. The J-T/J-Q approach effectively quantifies crack tip stress fields for low constraint conditions, such as shallow cracked structures or specimens.

Figure 3 illustrates the variation of elastic stress intensity factor (SIF) with crack depth for the 3D SENB specimen, calculated as the weighted average of the through-thickness values, and results based on the relevant stress intensity factor solution from Annex N of BS 7910. It is observed that the FE predicted SIF values agree well with the analytical solution provided in BS 7910, giving confidence in the present FE to be used for the calculation of the T-stress parameter (for elastic analysis) and, subsequently, the Q-parameter (for elastic-plastic analysis).

Similarly, Figure 4 shows the normalised constraint parameter, β_T, variation with crack depth, derived using the reference stress solution for 3-point SENB specimen given in BS 7910. The analyses yield similar results to those used to derived the β_T solution in BS 7910.

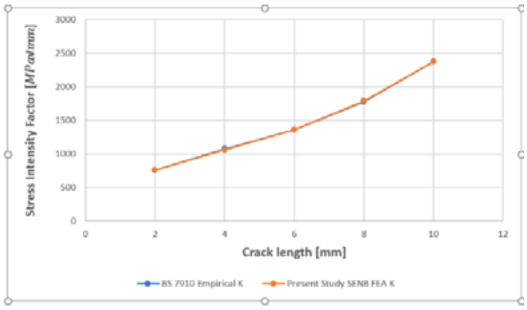

Figure 3. 3D Elastic analysis: stress intensity factor vs crack length, 20000N applied load (comparison with BS 7910 Annex N).

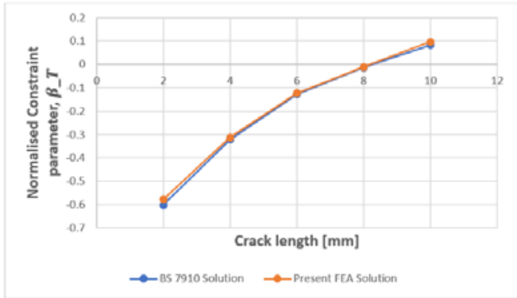

Figure 4: 3D linear elastic analysis- β_T vs crack depths of SENB specimen (comparison of BS 7910:2019 Annex N solution and present FEA evaluated at mid-thickness)

IV. SUMMARY AND FUTURE PLAN

The transferability of fracture toughness data obtained from laboratory specimens to a full-scale cracked structure is key in the integrity assessment of engineering structures. Both in-plane and out-of-plane constraint effects would be considered under different constraint conditions. Under the current plan, we will also be looking closely at the deformations that occur at the crack tip using various SENB and SENT specimen configurations, with DIC techniques planned for measuring the deformations. Parametric FE analyses of cracked pipes subjected to tensile loading and internal pressure will further be performed at varying crack tip constraint conditions.

A novel, modified, constraint-based fracture assessment using the J-Q methodology for specimens with surface flaws at low temperature will be examined, in conjunction with Annex N of BS 7910 to study the influence of constraint level correction on the allowable applied stress.

REFERENCES

[1] British Energy Generation Limited: Assessment of the Integrity of Structures Containing Defects, R6 Revision 4

[2] BS 7910 2019, "BSI Standards Publication Guide to methods for assessing the acceptability of flaws in metallic structures," 2019.

[3] Barhli et al: J-integral calculation by finite element processing of full-field surface displacements,2017

[4] N. P. O'Dowd and C. F. Shih, "Family of crack-tip fields characterized by a triaxiality parameter-II. Fracture applications," 1992

Burak Serhat Sakarya

Burak is a Doctoral Researcher at Brunel University London, based at the National Structural Integrity Research Centre (NSIRC) at TWI. He achieved an MSc in Structural Integrity with distinction from Brunel University London in collaboration with NSIRC in 2017. His master's thesis was titled "Numerical modelling of damage of composite materials for different damage mechanisms". After graduation, he worked as a Mechanical Project Engineer at the General Directorate of State Hydraulic Works as part of his scholarship agreement. Burak's current PhD project is sponsored by Lloyd's Register Foundation. His research interests lie in the areas of composite materials, numerical modelling, failure analysis and composite pressure vessels.

Development of a Quantitative Leak-before-break Design Concept for Composite Pressure Vessels

Dr Nenad Djordjevic[1], Dr Mihalis Kazilas[1,2], Dr Vasiliki Loukodimou[1], Dr Chris Worrall[2]
[1]Brunel University London, [2]TWI Ltd
3rd Year of PhD

Keywords: Control Volume Approach, controlled failure, kinematics of deformation

I. INTRODUCTION

Fibre-reinforced composites play a significant role in the aerospace, automotive, energy, and oil and gas industries due to their high strength-to-weight ratio, corrosion resistance and crashworthiness. Type III, IV and V composite pressure vessels enable lightweight storage solutions of substances such as hydrogen, compressed natural gas, liquid propane gas, and cryogenic fuels such as liquid oxygen, liquid hydrogen helium and nitrogen. To ensure the safety of these structures, cost-effective analytical and numerical simulation tools are developed and used in the design phase. In this research work, this is addressed through the development of the Leak-Before-Break (LBB) capability of the composite pressure vessels. The leakage before burst enables taking preventative action to avoid catastrophic failure during the service life of the vessel. The aim of this project is the development of a design concept to evaluate the strength and leak-before-break capability of Type V composite pressure vessels. To achieve this, three objectives are defined in this project:

- Development of an analytical tool for the rapid investigation of strength of different design patterns.
- Development of an LBB design feature by using finite element analysis (FEA) based on either the controlled composite failure or the structural - kinematics of deformation.
- Proof-of-concept with validation of the best scenario based on both the analytical and numerical approaches.

II. METHODOLOGY

An algorithm for the analytical tool was developed using MATLAB commercial software. Control Volume approach [1] and Lame Equations [2] were introduced to investigate fibre failure stain first-ply-failure for the burst estimation. One thick-walled analysed by Bai et al. [2] and one thin-walled composite pressure vessel developed by Loukodimou [3] were modelled with ABAQUS FEA software. The structural and material responses estimated by the analytical tool were validated with the results from numerical simulations [4].

The LBB design feature is based on the controlled failure by depressurisation of the structure once through-thickness matrix cracking occurs, without any damage within the fibre constituent to form a possible leak path. Burst would be prevented by overcoming the fibre damage progression through depressurisation. This is initiated by an inherited, linear, half-a-thickness deep defect, modelled by significant stiffness degradation, shown in Figure 1 as the green elements. The reference 600mm structure with the wall thickness of 2.4mm consists of $[\pm 55^o]_{2s}$ carbon fibre reinforced epoxy (CFRE) layers. The material response is modelled by using the available damage model with Hashin Failure Criterion damage initiation in ABAQUS.

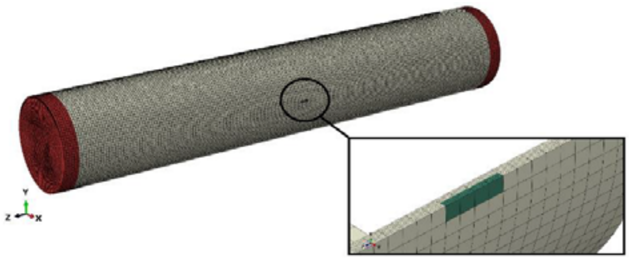

Figure 1. Inherited flaw as the longitudinal crack by artificial damage based on the material degradation

The LBB design feature is based on the kinematics of deformation of dissimilar materials. The best design scenario was investigated by performing simulations with different circular and elliptical plug geometries. Radial extensions on the interior sides of the plugs were bonded to the structure as in Figure 2. $[\pm 55^o]_{2s}$ CFRE layers and 6061-O aluminium alloy plug were modelled with C3D8R elements in ABAQUS.

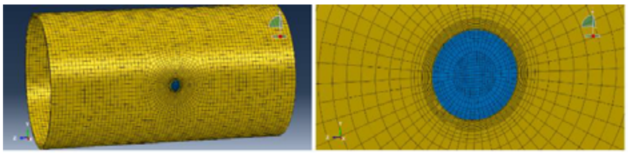

Figure 2. A circular metallic plug for the concept

III. NUMERICAL RESULTS

The developed analytical tool predicted accurate structural and material response for both thin and thick-walled composite pressure vessels. Figure 3 shows the good correlation between the results in the literature and performed FEA-analytical tool estimations for thick-walled structures. Figure 4 also shows that there was a good correlation between FEA and tool results for the thin-walled structure.

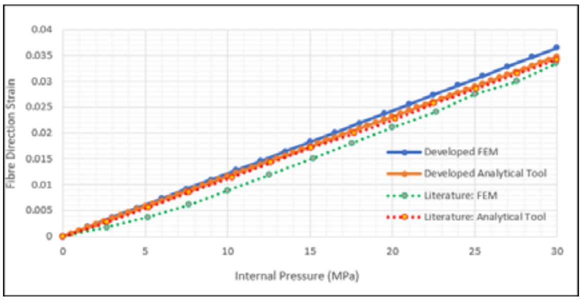

Figure 3. Strain in the fibre direction vs internal pressure within the aramid fibre reinforced layer

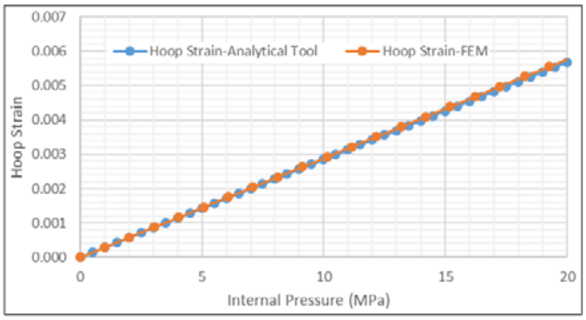

Figure 4. Hoop strain vs internal pressure in Type V composite pressure vessel

The LBB concept based on the controlled failure created the leak path in Figure 5 by through-thickness. The matrix cracked at 18.4MPa. Following with depressurisation of the structure would prevent a significant amount of fibre damage and subsequent burst.

The LBB concept based on the kinematics of deformation predicted the leak at 17.4MPa without any fibre damage around the composite structure in Figure 6.

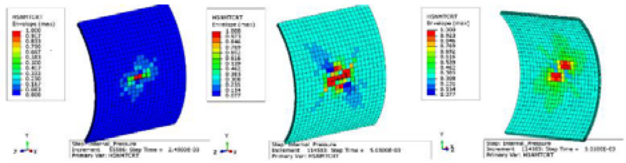

Figure 5. Matrix damage initiation around the inherited flaw at 9MPa and the leak path around 18.4MPa internal pressure

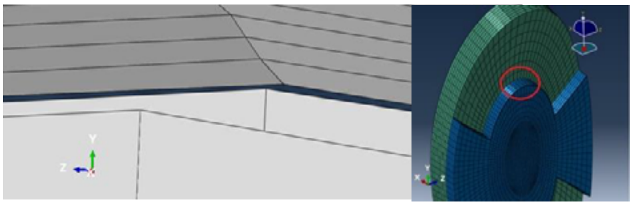

Figure 6. The opening to enable the leak at 17.4MPa

IV. CONCLUSIONS

The analytical tool enables the investigation of various design patterns of thin- or thick-walled composite pressure vessels including the different combinations of winding angles, liner and prepregs, geometry and pressure. It calculates structural and material response of undamaged structure, corresponding to on-axis and off-axis strain and stresses, and burst pressure. The numerical work on both LBB design concepts resulted in through-the-thickness leak paths without fibre damage occurrence within the composite pressure vessel.

V. FUTURE PLAN/DIRECTION

Future work will be on the validation of the developed LBB conceptual design against the experimental work to be done by the end of the project.

VI. ACKNOWLEDGEMENTS

This publication was made possible by the sponsorship and support of Lloyd's Register Foundation*. This research is a continuation of the project performed by Loukodimou [3] from which material properties were utilised for the numerical and analytical study demonstrated here.

REFERENCES

[1] P. C. Chou, J. Carleone, and C. M. Hsu, "Elastic Constants of Layered Media," J. Compos. Mater., vol. 6, no. 1, pp. 80–93, 1972, doi: https://doi.org/10.1177/002199837200600107.

[2] Y. Bai, F. Xu, P. Cheng, M. F. Badaruddin, and M. Ashri, "Burst Capacity of Reinforced Thermoplastic Pipe (RTP) Under Internal Pressure," in OMAE2011-49325, 2011, pp. 281–288, doi: https://doi.org/10.1115/OMAE2011-49325.

[3] V. Loukodimou, "Development of leak-before-break filament wound structures," Cranfield University, 2019.

[4] B. S. Sakarya, "Design of Composite Pressure Vessels with built-in 'Leak- Before-Break' capability," in NSIRC Research and Innovation Conference 2021, 2021, p. 40,41

*A charitable foundation, helping to protect life and property by supporting engineering-related education, public engagement and the application of research. www.lrfoundation.org.uk

Magali Rego

Magali is a 2nd year PhD student studying at The Open University in Milton Keynes and working at TWI in Cambridge. Before moving to the UK, Magali had experience working on industrial research projects developing environmentally-friendly and nanoparticle based coating solutions for textile and wood. The main challenge is the full dissolution and reconstitution of epoxy thermoset resin, a difficult challenge since its discovery in the 1900s. Her PhD project focuses on developing a chemical design approach to allow the regeneration of the precursor materials of epoxy thermoset in a closed-loop recycling cycle, with applicability across high-performance composite related industries.

Developing a Closed-Loop Recycling of Epoxy Thermoset Resins Through a Chemical Design Approach

James Bruce[1], Peter Taylor[1], Alan Taylor[2]
[1]School of Life, Health and Chemical Sciences, The Open University,
[2]TWI
2nd Year of PhD

Keywords: epoxy thermoset, recycling, silica, composites, de-curing trigger

I. INTRODUCTION

Current methods to recycle epoxy thermoset resin (widely used in high performance composites in the aerospace, automobile and renewable energy industries) are immature and still developing. Epoxy thermoset resins, regarded as unrecyclable plastics [1], have a highly crosslinked three-dimensional network, which makes it quite a challenge to cause full degradation, enabling a monomer recovering level. Most methods also cause a downward cycle, which leads to a decrease in the quality and the value of recycled products. Chemical recycling has recently been considered as a promising method because it can produce useful chemicals, and potentially achieve upcycling and a full recycling loop.

Aligning with European Union initiatives for more plastics to be included in a circular economy strategy, the idea of achieving epoxy thermoset closed-loop recycling using silica as a recoverable monomer is one possible solution to the main limitations faced so far. To achieve that, a reversible linking structure must be planned and functionalised onto the surface of the silicas, so it is compatible with the thermoset resin, and sensible to a specific chemical stimulus to incite de-curing.

II. METHODOLOGY

The methodology was stablished by following a structured chemical design plan entailing the following steps: (1) Introduction of labile chemical groups onto silica, (2) Compatibilisation of surface chemical groups with an epoxy system, (3) Functionalised silica incorporation into an epoxy system with a selective decuring trigger. For (1), special attention on studying particle aggregation and chemical surface stabilisation with dynamic light scattering (DLS), nitrogen absorption analysis nd Fourier transform infrared analysis (FTIR), focusing mostly on calculating grafting density with thermal gravimetric analysis (TGA).

III. RESULTS

The results obtained from objective (1)DLS report well distributed and uniform functionalised silica in different solvents such as ethanol, industrial methylated ethanol and butyl acetate. Relating to grafting density determination, thiol and vinyl groups (from different silanes) grafted onto silica surfaces were selected as potential candidates as a labile chemical group. Maximum values of silane grafting density (8.74 μmol/m2 from MPTMS) are close to the ones reported in the literature (6.9 μmol/m2), assuring the functionalisation protocol and calculus to be consensual with previously published work [2]. The washing protocol is a parallel and equally important study on the removal of by-products of the silane grafting reactions. In some cases, 10% of the total weight was removed, with what is believed to be the remaining homocondensates by-products from silane-silane reaction.

IV. CONCLUSIONS

Specific vacuum drying protocols were stablished for each functionalisation, aware that water might be present on the surface of the silica. Grafting density calculation is a key method moving forward towards objective (2), to precisely follow and adjust silica surface functionalisation according to which silane is used. Washing protocol is essential at the level that could influence the particle size, grafting density determination and future chemical reactions on the surface of the functionalised silica. Achieving controlled functionalisation of silica additives and fine tune the resultant surface properties to obtain a versatile recoverable monomer is a complex task but with great value and potential.

V. FUTURE PLAN

Follow through to objective (2) and increase knowledge on vinyl chemistry backed by useful characterisation techniques. Further ahead in the project, the novel materials that are envisaged will need to be assessed and validated against the current state-of-the-art. The next challenge will be to examine and explore this at a larger scale and close the gap that separates these unrecyclable plastics from their full use in a closed life material cycle.

REFERENCES

[1] X. Zhao, X. Liu, K. Feng, W.-L. An, F. Tian, R. Du, S. Xu, L. Chen, G. Wu, Y.-Z. Wang, "Multicycling of Epoxy Thermoset Through a Two-Step Strategy of Alcoholysis and Hydrolysis using a Self-Separating Catalysis System", ChemSusChem 2022, 15, e202101607, doi: 10.1002/cssc.202101607.

[2] A. Spyrogianni, I. K. Herrmann, K. Keevend, S. E. Pratsinis, and K. Wegner, "The silanol content and in vitro cytolytic activity of flame-made silica", J. Colloid Interface Sci., vol. 507, pp. 95–106, 2017, doi: 10.1016/j.jcis.2017.07.096.

Hamad Raheem

Hamad is an NSIRC PhD student at the University of Cambridge. He graduated with honours from Colorado School of Mines, USA with a BSc in Petroleum Engineering. He then obtained an MSc in Petroleum Engineering with distinction from Imperial College, London, after which he worked as an intern at Abu Dhabi National Oil Company (ADNOC), who also funded his PhD. Hamad's PhD focuses on the effect of prolonged fluid permeation at elevated temperature and pressure on polymer ageing, and the feasibility of detecting it through MEMS-based methodologies.

Resonant Coupling of Piezoelectric Micromachined Ultrasound Transducers with Polymer Specimens in Different Media

Dr Bernadette Craster[1], Prof. Ashwin Seshia[2]
[1]TWI, [2]University of Cambridge
3rd Year of PhD

Keywords: Resonant, Coupling, PMUT, Polymer, NDT

I. INTRODUCTION

It is assumed that in instances where physical or chemical alterations occur in polymer morphology due to prolonged exposure to fluids, their elastic properties change accordingly [1]. Hence there is a need for an in-situ, non-destructive testing (NDT) assessment technique for polymeric materials when they are continuously exposed to high temperature and pressure fluids.

The current study is one in a series to evaluate the feasibility of Piezoelectric micromachined ultrasound transducers (PMUTs) to distinguish the material attributions of different specimen. The experiments are conducted through a 3D replica of the actual setup using COMSOL Multiphysics® software. The aim of the study is to characterise the 3-layer model (PMUT-medium-polymer) for the analysis of the effect of input voltage, medium fluid type, and distance on the resonant coupling of PMUT and the polymer specimen. Additionally, a comparison between 1-port and 2-port T/R configurations, with a view towards guiding experimental design, is presented. The validation of the simulation findings is conducted using PMUTs manufactured through PiezoMUMPs fabrication flow [2] and is currently being published.

To be able to acquire the mechanical properties of polymers dynamically, such as density and elastic moduli, is of interest to many industries. However, many available NDT techniques deployed for the extraction of such fundamental properties either involve extensive sample preparation and complex data analysis, or are bounded by sample dimensions below a few millimetres [3]. Acoustic techniques were proven to be the most accurate among various approaches for the extraction of mechanical properties non-destructively [4, 5].

II. DESIGN/METHODOLOGY/APPROACH

The PiezoMUMPs process is a 5-mask level process to manufacture AlN-on-Si microstructures supported by a silicon-on-insulator (SOI) wafer, described in the PiezoMUMPs Design Handbook [2].

A single 1x1 cm^2 chip includes an array of individual PMUT units, and the spacing of these elements with respect to each other is significant for the efficiency of the transducer in terms of eliminating ultrasonic wave interference. It is normal for high frequency PMUT arrays to generate side lobes at specific angles [6]. To minimise grating lobes, element pitch – which is the centre distance from one element to an adjacent element – they must be larger than half a wavelength [7]. Thus, the pitch design in a PMUT array is constrained by the wave velocity and the (λ / 2) pitch rule.

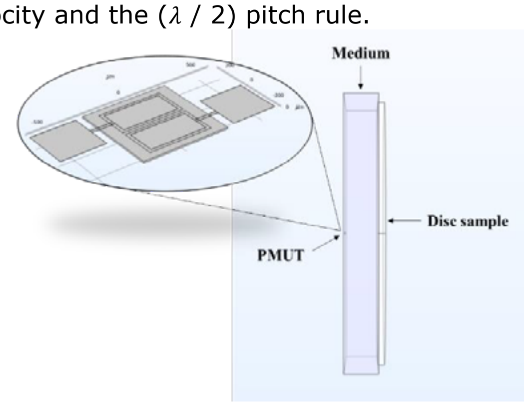

Figure 1. 3D schematic of experimental setup for COMSOL Multiphysics ® software showing the 2-PC PMUT comparison in size to disc sample (white) separated by medium (blue).

A square-plates design was chosen with sides of 500x500µm comprising Al, AlN and SOI layers. The designed eigen-frequency of a single PMUT unit was 0.5MHz, which is a common centre-frequency for commercial transducers for future comparisons. A square isotropic plate model [8] was used to estimate the side lengths of the PMUT membranes, and then optimised by COMSOL Multiphysics ® simulations according to the output eigen-frequency.

Simulation based experiments were achieved through COMSOL Multiphysics® software in 3D setup, where a fluid medium separates a single PMUT unit from a 2mm thickness by an 80mm diameter disc sample. The described setup is illustrated in Fig. 1, which shows that the PMUT is minute in comparison to the sample.

The silicon-on-insulator (SOI) substrate of the PMUT was grounded, whereas the layer on top was electrically actuated with a sinusoidal voltage. The latter caused a flexural response from the sandwiched Piezoelectric layer, AlN, that sent an ultrasonic wave through the medium to the polymer. The edges of the silicon wafer were the only fixed constraints, to allow for full flexural motion.

The matching of resonant peaks between the PMUT and polymer were evaluated by measured sound pressure levels (dB) in the frequency domain. Average percent similarity of resonances, γ, was then calculated from the difference between average sound pressure levels (SPL):

$$\gamma = 1 - \left|\frac{SPL_{Al} - SPL_{polymer}}{SPL_{Al}}\right| \quad (1)$$

III. FINDINGS/RESULTS

The simulation runs were carried out on1-port and 2-port configuration PMUTs in a total of 64 runs, with varying medium types (air, glycerol and water), sample materials (HDPE, PP, PVDF, Al, Cu, Steel), voltages (0.1 to 100V), and at medium thicknesses (0.1 to 100mm).

By keeping voltage and sample material constant, as the air distance increased between the PMUT and sample, γ improved until 0.7mm for 1-PC and until 1mm for 2-PC PMUTs. After which, γ noticeably dropped as the gap spacing between PMUT and sample increased. This trend was less noticeable with glycerol and water as the couplant.

The effect of voltage on γ was not very prominent at values up to 100V.

At constant distance and voltage, γ values for glycerol were consistently the highest, followed by water and then air. Although the PMUTs were originally designed for in-air use, simulation results showed that acoustic waves were less attenuated in denser fluids, as expected.

Different sample material types, when compared while other variables were kept constant, showed there were differences in SPL signatures as material properties changed. Polymers in general (PE-RT, PP and PVDF) showed better matching than metals (Al, Cu, Steel); partly because the PMUT designed was matched for the PE-RT disc resonance. The shift in the output characteristics between polymer and metals, especially, was very noticeable. This fact could be used as an indicator for a specific material property over the course of a specimen's lifetime, for instance.

IV. CONCLUSIONS

Being able to monitor material properties of solid specimens non-destructively is a valuable practice in various industries, especially in operational lines of work where destructive tests can introduce significant operational delays.

Ultrasound methodologies have been proven effective in characterising material types in the described 3-layer setup. The matching signatures of COMSOL simulation indicated that distance and material type greatly affected the SPL match quality between PMUT and sample, and SPL matches were not strongly affected by voltage. Lastly, although the PMUTs were designed for in-air measurement, glycerol and water predictably showed less attenuation.

V. FUTURE PLAN/DIRECTION

An on-going publication aims to validate the simulation results presented here experimentally, by using the fabricated PMUTs in an identical setup. Another follow-up aims to improve the PMUT receiving signal by the use of 2 PMUTs, either side of the sample as a 5-layer model (PMUT-medium-polymer-medium-PMUT).

VI. ACKNOWLEDGEMENT

This publication was made possible by the sponsorship and support of the Non-metallic Innovation Centre (NIC). The work was enabled through, and undertaken at, the National Structural Integrity Research Centre (NSIRC), a postgraduate engineering facility for industry-led research into structural integrity established and managed by TWI through a network of both national and international Universities.

VII. REFERENCES

[1] Merah et al. Plast. Rubber Compos., vol. 35, no. 5, pp. 226–230, 2006, doi: 10.1179/174328906X103178.

[2] A. Cowen, G. Hames, K. Glukh, and B. Hardy, "PiezoMUMPs Design Handbook a MUMPs process, Revision 1.3.," 2014.

[3] M. Agrawal, "Ultrasonic Resonant Cavity Technique for Materials Characterisation," University of Cambridge, 2015.

[4] Agrawal et al. Ultrasonics, vol. 64, pp. 186–195, 2016, doi: 10.1016/j.ultras.2015.09.001.

[5] E. Moritzer, M. Hüttner, B. Henning, and M. Webersen, AIP Conference Proceedings 1914, 090003, 2017;

[6] A. Ben Amar, H. Cao, and A. B. Kouki. Microsyst. Technol., vol. 23, no. 10, pp. 4659–4669, 2017, doi: 10.1007/s00542-016-3205-8.

[7] K. K. Shung and M. Zippuro. IEEE Eng. Med. Biol. Mag., vol. 15, no. 6, pp. 20–30, 1996, doi: 10.1109/51.544509.

[8] Wong et al. Sensors Actuators, A Phys., vol. 247, pp. 430–439, 2016, doi:10.1016/j.sna.2016.06.029.

Maciej Gierulski

Maciej graduated with an MEng Aerospace Engineering from the University of Sheffield in 2019. His research experience includes a year's internship at the Nuclear Advanced Manufacturing Research Centre in Rotherham, and an extensive MEng project, building a high pressure combustion testing rig for measuring emissions from various aviation fuels. Maciej is currently pursuing a PhD, in electrofusion welding of thermoplastic composite pipes, at the University of Sheffield, funded by the Non-metallic Innovation Centre (NIC) and based at TWI.

Electrofusion Welding of Thermoplastic Composite Pipes

Mike Troughton[1], Rachel Tomlinson[2], Anthony Ryan[2], Matt Smith[3]
[1]TWI, [2]University of Sheffield, [3]AMRC
3rd Year of PhD

Keywords: electrofusion welding, thermoplastic composite pipes, polyethylene composites

I. INTRODUCTION

Oil and gas producers have been struggling with the maintenance of their steel pipelines as crude oil greatly promotes corrosion. In addition, the bolted joints between individual pipes are relatively complex and vulnerable to environmental conditions. Thermoplastic pipes connected with electrofusion (EF) joints are an attractive solution as they do not suffer from corrosion and are flexible, which, in combination with excellent end-load resistance of joints, can guarantee a maintenance-free service life of 50 years or more. Thermoplastic pipelines can even endure earthquakes.

Therefore, to reduce maintenance costs and risk to the environment, oil and gas operators are looking to change some of their pipelines to fully non-metallic. Recently, thermoplastic composite pipes (TCPs) have been developed, which consist of a polyethylene (PE) liner which is glass wrapped reinforced PE tapes and then a PE cover is extruded over the top, and have been developed to have pressure capacities comparable to those of metallic solutions. However, they still are joined using steel connectors. The aim of this project is to design a thermoplastic connector for polyethylene (PE) TCPs that utilises EF welding technology.

II. DESIGN/METHODOLOGY/APPROACH

The objective of the project is to design a bespoke EF coupler specifically for joining TCPs. In order to do this, a finite element (FE) model of a joint between a conventional EF coupler and TCPs was developed using Abaqus software. Whole joint mechanical testing (hydrostatic pressure and axial tension tests) were then carried out, with strain gauges attached to both the EF coupler and the TCPs in order to validate the model, which will then be used to optimise the geometry and structure of the EF coupler.

One issue with TCPs is that, due to the way they are stored and transported, they are not perfectly straight or round. To prevent this from having an adverse effect on the results of the whole joint mechanical tests, a straightening/re-rounding jig was made, and the pipes were straightened and re-rounded before welding.

III. FINDINGS/RESULTS

The typical long-term failure mode for EF joints between conventional unreinforced PE pipes under pressure, is by slow crack growth through the coupler wall, from the stress concentration area at the inner cold zone notch. In axial tension, they usually fail through the pipe wall, starting at the outer cold zone notch (see Figure 1).

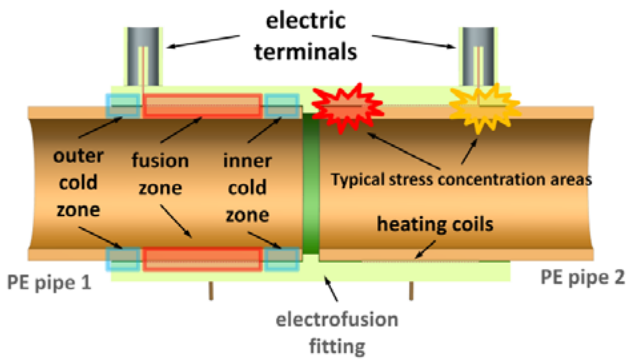

Figure 1. A cut through of an EF joint in conventional unreinforced PE pipes with two typical stress concentration areas indicated.

One question investigated while modelling, was whether the stress concentrations change their positions if the conventional PE pipes are replaced by TCPs. The simulation results suggested that the areas of highest stress concentration were similar in both tests, see Figure 2. It was also apparent that for the same loading conditions, the stresses in the joint were significantly reduced in the TCP case.

The model predicted failure in the tensile test to start in the joint at the inner cold zone notch, and that strains should be similar on the pipe and coupler.

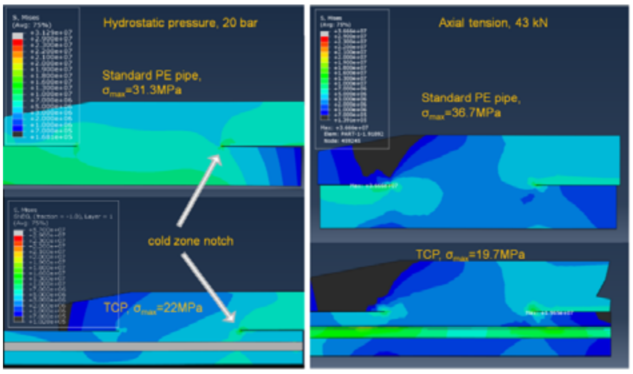

Figure 2. Simulated stress concentrations in a PE and TCP electrofusion joint for a) hydrostatic pressure and b) axial tension test.

However, when the whole joint tensile test was performed, the strains in the coupler were only half those in the pipe in the proximity of the joint, and the sample failed at a load of 48kN at the outer cold zone, through the outer cover of the pipe (see Figure 3). The reason for this was found to be that the EF weld was stronger than the weld between the reinforcement layer and the outer cover, because rather than having a fully welded structure as initially assumed, the TCP samples actually had cracks and/or weak interfaces between the three layers. As a result the load was mainly acting on the outside PE layer, so it was sheared off the TCP without substantially affecting the other two layers.

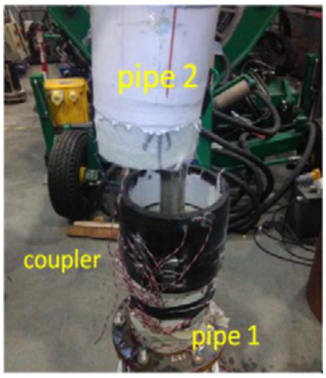

Figure 3. Photograph of the failed whole joint tensile test sample.

In the hydrostatic pressure test, at low pressure, the highest strains were recorded on the coupler, as expected from the simulations, but the sample actually failed in the pipe (see Figure 4) at a pressure of 14bar. The probable explanation for the failure is that the pressurised water entered between the reinforcement layer and outer cover, travelled up the pipe, past the end of the coupler and then burst the outer cover.

Figure 4. Photograph of the failed hydrostatic pressure test sample. A debonded strain gauge is visible on top.

IV. DISCUSSION/CONCLUSIONS

The purpose of the mechanical tests on EF joints in TCPs was to verify the FE model of these joints under identical conditions. However due to the unexpected failure modes produced, it was not possible to verify the model when assuming the pipe layers were fully welded together. Nonetheless, the two tests can still be modelled using a low weld strength between the three TCP layers. This will require information about the normal and shear strength of these interlaminar interfaces, which can be obtained from the following lap shear and flatwise tensile tests:

- ASTM C297 to find interlaminar strength
- BS 6464 (B.6) to establish the shear bonding strength between the pipe layers

It is planned to do this work in the near future. Currently, the design recommendations include adding an inner sleeve to the coupler that would weld to the liner in order to protect the reinforcement layer from transported liquids, and extending the fusion zones so they can transfer loads to the reinforced layer rather than them affecting only the outer jacket.

V. FUTURE PLAN/DIRECTION

Once the required mechanical properties of the liner, reinforced layer and cover of the TCP have been determined from the specimen tests, the models will be verified against strain measurements collected from the whole pipe tests. It should then be possible to design an EF coupler that will successfully weld the pipes provided for the project.

ACKNOWLEDGEMENTS

This work was made possible by the sponsorship and support of the NIC. The work was enabled through, and undertaken at, the National Structural Integrity Research Centre (NSIRC), a postgraduate engineering facility for industry-led research into structural integrity, established and managed by TWI through a network of both national and international universities.

Mohammad Alghfeli

Mohammad achieved a BEng in Chemical and Process Engineering from Arizona State University, USA in 2018. He later pursued an MSc in Chemical Engineering at ASU, graduating with distinction, with research focused on gas separation analysis of thermoplastics using He, CO2 and N2. Mohammad then did a 3-month internship at Abu Dhabi National Oil Company (ADNOC) in the Research & Development department, focused on repellent polymer coatings and the ongoing industrial problem of pipeline corrosion. The primary objective of his PhD project is to establish the feasibility of building on the know-how in surface modification within TWI, with the analytical expertise of Cambridge University, in developing new, surface functionalised nanostructured fillers into HDPE for industrial use as pipe liners.

An Approach to Enhanced HDPE Nanocomposites

Dr. Alan Taylor[1], Prof. Mick Mantle[2]
[1]TWI-NIC, University of Cambridge[2]
3rd Year of PhD

Keywords: Compatibility, interfacial chemistry

I. INTRODUCTION

Pipeline corrosion is an industrial problem that leads to high maintenance costs. Globally, approximately 2% of oil and gas revenue is spent on pipeline corrosion [1]. There are a number of approaches to mitigate corrosion in production with the aim of reducing maintenance and replacement costs, and lengthening operational lifetimes. One such approach is the use of polymer liners. Augmentation of the properties of polymers with the addition of additives and fillers has long been carried out [2]. Such additives/fillers fundamentally change the composition of the polymer, impacting the structure at a range of length scales, and can also introduce additional regions of anisotropy. Identification of the most appropriate and beneficial additives is, therefore, a key step in the development of enhanced particle, reinforced polymer composites.

High density polyethylene (HDPE) thermoplastic pipe resins are widely used due to their relatively low cost, high chemical resistance and well balanced mechanical properties when compared to other polymeric solutions. HDPE has proved its robustness for its target applications such as water service, and low GOR and BTEX content at certain temperatures. However, when aiming to use it in more demanding applications outside its normal limits, key properties require ehnacement. These include thermal stability, stiffness, weathering and creep resistance. The incorporation of small amounts of inorganic nanoparticles has been shown to significantly enhance the creep, thermal, tensile and mechanical properties [3-5]. The emerging consensus is that improved compatibility between the inorganic filler and the polymer matrix leads to enhanced material properties [6].

The key, overarching criteria relating to the development of such nanocomposites are compatibility between the additive the HDPE, processability and functional performance.

This PhD project will focus on developing a deeper understanding of the interfacial characteristics between inorganic fillers, specifically silica based additives and HDPE with a view to establishing new, high performance nanocomposite systems. The primary output of the programme will be the establishment of design rules and guidelines enabling optimisation of the interfacial chemistry. A secondary output will be provisional data relating to the mechanical, thermal and chemical properties of selected candidate HDPE-silica nanocomposites.

II. METHODOLOGY

Commercial nanoscale silicas with different surface functional groups have been evaluated using spectroscopic, nitrogen sorption and thermogravimetric techniques to provide detailed insight into their surface chemistries.

To determine the different structures of the silicas, solid-state ^{1}H, ^{13}C and ^{29}Si nuclear magnetic resonance (NMR) tehcniques were used. Rheological behavior of these silicas in model non-polar, aprotic liquids at multiple loading levels (1,3,5,7,10 & 12%) has been undertaken, to provide a phenomenological assessment of the influence of surface chemistry, on the room temperature viscosity of the mixtures over a range of shear rates.

III. RESULTS AND DISCUSSION

Solid state NMR methods ^{1}H and ^{29}Si have been extensively used in literature to study the surface chemistry of silica. Different chemical species can be identified by their characteristics' positions (chemical shift) on NMR spectra. Typical ligands that appear on the surface of silica substrates are shown in Figure 1.

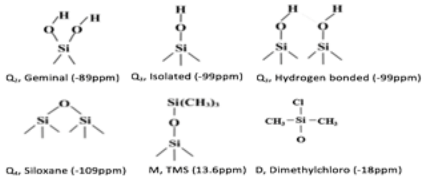

Figure 1: Different species that can be identified on the surface of silica

The ^{1}H MAS NMR of commercial pyrogenic silicas A200, R812s, R8200 & R9200 is given in Figure 2. The spectra clearly shows the difference between the pure silica sample (A200) and the functionalised. Since the R series silicas are functionalised with methyl groups, the proton (^{1}H) NMR is not capable of differentiating between them. However, the 13C and 29Si NMR probes are able to do so.

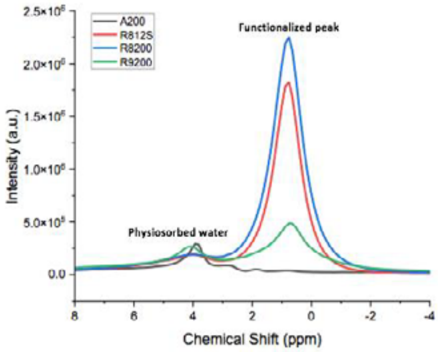

Figure 2: ^{1}H MAS spectra of commercially functionalised fumed silicas

The ^{29}Si Cross Polarisation (CP)-MAS spectra is show in Figure 3 below. The spectrum clearly displays the different species on the surface. The R812S & R8200 both have an M peak obtained by the functionalisation of hexamethyldisilazane.

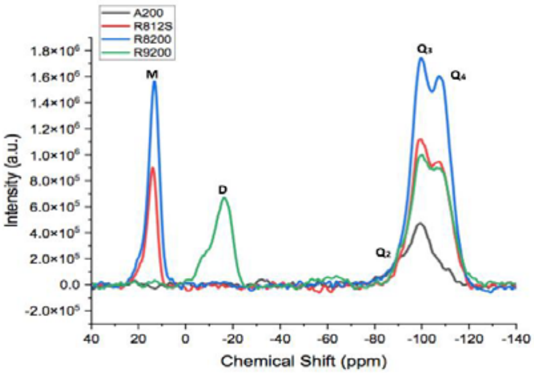

Figure 3: 29Si MAS spectra of commercially functionalised fumed silicas

The R9200 however, has a D peak from the functinalising agent dichloromethylsilane. The ^{29}Si CP MAS technique is semi-quantitative and gives a good resolution of the Q sites. Quantification can be done using HPDEC ^{29}Si MASNMR. Recent developments in the quantification will be employed later in this project.

The initial rheological assessment when the fumed silicas where dispersed in the hydrocarbon solvents D40 & xylene indicates that the R8200 is the most functionalised silica. Figure 4 displays the viscosity as a function of silica loading percentage, with a clear trend that shows the incorporation of the silica types investigated; R8200 leads to the lowest increase in viscosity with increase in loading. The results are further demonstrated by the solution in Figure 5 where the non functionalised A200 fully gelled at 10% loading, whereas the R8200 was highly compatible with the xylene matrix.

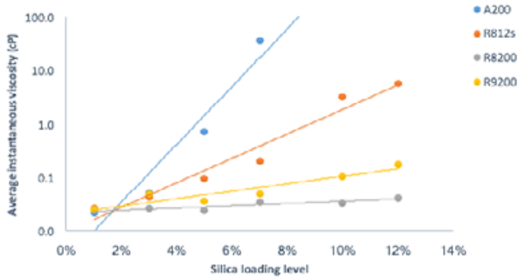

Figure 4: Viscosity of silica in xylene at shear rate of 100/s at different loadings

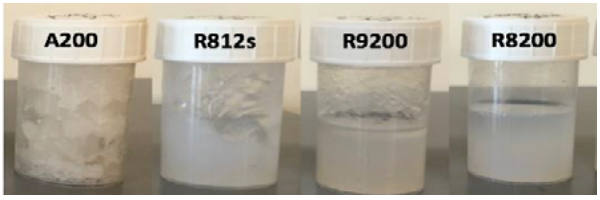

Figure 5: 10% fumed silica samples in xylene

IV. FUTURE PLAN

Provisional conclusions will be presented relating to the chemistry of the silica surfaces' compatibility in the model solvents. The candidate fillers will be incorporated into HDPE by melt compounding techniques, then the silica-HDPE composites prepared will undergo evaluation to determine rheological properties, permeability examinaiton via NMR methods, micsoscopial imaging, thermal analysis and mechanical testing. The silica-HDPE composites will be compared to the parent HDPE to assess the optimisation after filler addition and the affect on processability.

REFERENCES

[1]A.Al-Khowaiter,Sep.(2019).“FutureofPlasticand Composite Pipeline Technologies”, NIC, TWI UK.

[2] Harito C, Bavykin D V, Yuliarto B. Dipojono H K and Walsh F C, 2019: ‘Polymernanocomposites having a high filler content: synthesis, structures, properties and applications.’ Nanoscale, 11 4653.

[3] Dorigato, A.; D’Amato, M.; Pegoretti, A. Thermo-Mechanical Properties of High Density Polyethylene – Fumed Silica Nanocomposites: Effect of Filler Surface Area and Treatment. *Journal of Polymer Research* 2012, *19* (6).

[4] Pegoretti A, Dorigato A, Penati A. Tensile mechanical response of polyethylene – clay nanocomposites. Expr Pol Lett 1 (3):123–131. (2007)

[5] Cui Y, Kumar S, Rao Kona B, Van Houcke, D. Gas barrier properties of polymer/clay nanocomposites: *RSC Advances, (2015), 63669-63690, 5(78).*

[6] Luna, M. S. D.; Galizia, M.; Wojnarowicz, J.; Rosa, R.; Lojkowski, W.; Leonelli, C.; Acierno, D.; Filippone, G. Dispersing Hydrophilic Nanoparticles in Hydrophobic Polymers: HDPE/ZnO Nanocomposites by a Novel Template-Based Approach. *Express Polymer Letters* 2014, *8* (5), 362–372.

Thamasha Samarasinghe

Thamasha is a NSIRC PhD student of Brunel University, based at TWI. She graduated from University of Moratuwa, Sri Lanka with a BSc. (Hons) degree in Mechanical Engineering in 2016 and completed her MPhil degree in Engineering from University of Liverpool, UK in 2019. Thamasha is currently pursuing a PhD on the "Design and development of composite panels with variable thermal conductivity for Li-ion battery module, funded by Lloyd's Register Foundation.

Design and Development of Composite Panels with Variable Thermal Conductivity for Li-ion Battery Module

Stuart Lewis[1], Mihalis Kazilas[2]
[1]TWI, [2]Brunel University
3rd Year of PhD

Keywords: Heat transfer, Temperature distribution, Li-ion battery module

I. INTRODUCTION

The global concerns of reducing the dependence on fossil fuels and ultimately producing less harmful emissions are aiding the focus on Electric Vehicles (EVs) and Hybrid Electric Vehicles (HEVs). The performance of EVs and HEVs depends on batteries and Lithium -ion (Li-ion) battery is considered as the first-choice candidate for a power source for EVs and HEVs due to its low -self discharge rate. However, thermal performance of Li-ion batteries limits long term stability and safety characteristics since the optimum operating temperature is between 30-40 ℃ [1]. In addition, thermal runaway may occur in a cell when heat is not properly controlled. Uneven temperature distribution can also cause an electrically unbalanced module and shorten battery life. Therefore, it is necessary to operate battery modules at uniform temperature.

Thermal management can be achieved by active or passive built in sources that provide cooling. Air, liquid and phase changing materials or a combination of these three methods are used in existing thermal management systems. Current solutions with active cooling are adding weight and complexity to EV and HEV batteries.

An innovative idea for a composite casing for car batteries is considered in this project. The composite casing will have variable thermal conductivity, defined by the local volume fraction of carbon fibres and other conductive elements (including copper pins) within the composite. The selective high thermal conductivity in areas of the casing will create "thermal avenues" close to the hot areas of the battery in order to provide passive heat dissipation in the areas needed the most. The composite casing will provide a low weight, simple thermal management solution that requires minimum maintenance.

II. DESIGN/METHODOLOGY/APPROACH

A 3D model of a Li-ion battery single cell was developed and used to evaluate several geometries of a battery module currently being used by battery manufacturers. Heat transfer simulations are currently being validated by experimental results from a custom jig that emulates the battery module arrangement. Heating elements of similar size and power/heat output to individual cells have been used for the experiments.

Batteries mainly generate heat during charge and discharge.The energy balance equation for a cylindrical Li-ion battery cell is developed by considering the energy conservation laws and the volumetric heat generation of the battery cell. Lumped capacitance model was applied to simplify the Li-ion battery cell heat transfer and the simplified equation can be presented as follows.

$$\rho C_p \frac{\partial T}{\partial t} = hA(T - T_{amb}) + \dot{Q} \quad (1)$$

where, ρ is the density of active battery material ($\mathrm{kg/m^3}$) and C_p is the specific heat capacity (J/kgK). T and T_{amb} denote the absolute temperature(K) and absolute temperature in ambient (K) respectively. h denotes the heat transfer coefficient ($\mathrm{W/m^2}K$) and A represents the cross sectional area of the cell ($\mathrm{m^2}$). Furthermore, $\dot{Q}$ denotes the volumetric heat generation rate for the battery(W).

The 3D simulation model for the single cell was developed as a CFD model using COMSOL multiphyiscs commercial software and the single cell model was then extended for a battery module heat transfer modelling. A bespoke test rig was designed and built in order to validate the simulation results. In order to replicate the cylindrical battery cells, cylindrical heating elements with similar dimensions were used. In order to emulate the operation of a battery module, nineteen (19) heating elements were used, each one connected to a single heating element. The rig consists of a bench power supply, a ceramic material base for insulation and K-type thermocouples for temperature measurements at various locations.

The charge-discharge behaviour of battery cells was simulated by having the power switched on and off every 600s. The experimentswere run for three geometry scenarios by changing the gap between the heating elements and also for with and without airflow scenarios. The airflow supply was provided by using PC fans.

The composite casing will be manufactured using three main methods including hand lay up, resin infusion and with a caul plate. With the metallic pin arrangement, the suitable casing will be selected and validate with the bespoke test rig for the thermal conductivity.

III. FINDINGS/RESULTS

3D simulations for both single cell and module were run. The initial temperature for the simulation is taken as 25℃ and the convection heat transfer coefficient was taken as 10 W/m^{2}K by considering forced convection. The airflow velocity is 2 m⁄s for the simulation and a square wave function is used to represent the alternating charge and discharge current at a 7.5 C rate with a cycle time of 600s including a relaxing period after 1500s. The cell is set to an initial State of Charge (SoC) of 10%. Initial results (Figure 1) indicate that the maximum temperature occurs at the centre core (the active battery material) of the single cell.

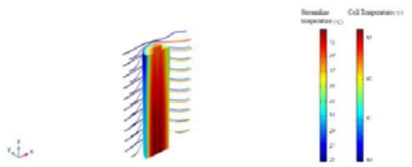

Figure 1. Temperature distribution results of a single cell with the airflow

Simulations were also run on single cell without any airflow. The results indicate that the maximum temperature without any airflow is 92℃. This is about 30°C higher compared to the results obtained with airflow of 2 m/s.

The temperature distribution in battery modules depends on cells spatial arrangement and the inter -cell distance. To investigate that , four cell arrangements were considered: 1×24, 3×8, 4×6 rectangular arrays and 19 cells in a hexagonal arrangement.

REFERENCES

[1]A A Pesaran, "Battery thermal management in EVs and HEVs: Issues and solutions," in Advanced automotive battery conference, Las Vegas, 2001

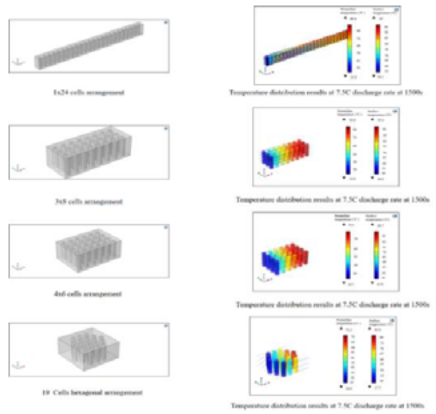

Figure 2. Temperature distribution in terms of different cell arrangement

Although the results confirm that the 4×6 cubic structure is better in terms of cooling capacity ,since the 19 cells hexagonal arrangement shows good cooling capacity and has optimal space utilisation, this arrangement will be used for further investigation.

Experimental results and their comparison with the simulation are presented in Figure 3 for hexagonal arrangement.Centred cell was chosen because it was the element which has the highest temperature in both simulation and experiments.

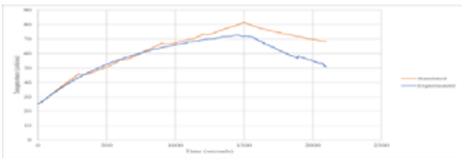

Figure 3. Experimental and simulation results for a centred cell of a battery module

IV. DISCUSSION/CONCLUSIONS

Although there is good agreement between simulations and experimental results,minor deviations are attributed to fixing issues of heating elements.

V. FUTURE PLAN/DIRECTION

A prototype composite case with variable thermal conductivity will be validated with the bespoke test rig. The required thermal conductivity of the composite case will be confirmed through the heat dissipation requirements.

ACKNOWLEDGEMENT

This publication was made possible by the sponsorship and support of Lloyd's Register Foundation. The work was enabled through, and undertaken at, the National Structural Integrity Research Centre (NSIRC), a postgraduate engineering facility for industry-led research into structural integrity established and managed by TWI through a network of both national and international Universities.

Nokhaiz Sabir

I am a second year Ph.D. student at the National Structural Integrity Research Centre (NSIRC) at Cambridge, UK. I am registered with the Department of Engineering at University of Warwick, and currently on a funded PhD studentship in partnership with Lloyd's Register Foundation, TWI Ltd and University of Warwick. I also work as a Graduate Teaching Assistant at University of Warwick and support the academics with teaching Engineering Undergraduate students. Prior to starting my PhD, I completed an MSc in Oil and Gas Engineering at Brunel University which was also in partnership with TWI Ltd. I was a recipient of the NSIRC Scholarship as well as the Postgraduate Academic Excellence Scholarship in recognition of my academic achievements. My first degree is BSc in Chemical Engineering from University of Lancaster which I completed with First Class Honours.

Characterization and Early Detection of Hydrogen Embrittlement in Offshore Bolts using Acoustic Emission

Dr Stephen Grigg[1], Dr Duncan Billson[2] Dr David Hutchins[2]
[1]TWI, [2]University of Warwick
2nd Year of PhD

Keywords: Hydrogen Embrittlement, Acoustic Emission, Corrosion, Cracking, Fastener.

I. BACKGROUND AND SCOPE OF THE PROJECT

In the offshore oil and gas sector the most commonly used material for the construction of critical fasteners are high-strength steels, which provide substantial saving as compared to the low strength steels as they are stronger, light weight and provide longer durability. They are however prone to hydrogen absorption, which leads to corrosion and cracking, increasing the likelihood of premature failures [1][2].

Acoustic Emission (AE) is the spontaneous release of strain energy which is emitted during a damage event (such as corrosion or cracking) [3]. AE sensors placed on a structure can be used to detect, locate, and characterize damage [4]. This can be used to determine the useful remaining life of critical bolts, fastenings, and connections. Therefore, this research will use the AE technology to explore the relationship between hydrogen embrittlement and AE for the monitoring of critical bolts, fastenings, and connections.

II. LITERATURE REVIEW

A. HYDROGEN EMBRITTLEMENT

In metals and alloys, hydrogen embrittlement (HE) occurs when hydrogen, combined with stress, either externally or internally, leads to a permanent loss of ductility [5]. Figure 1 shows the factors that contribute to hydrogen embrittlement within steel structures. When high-strength steel is tensile stressed, such as when tightening a high-strength fastener, the tension forces atomic hydrogen within the steel to diffuse (migrate) to the point of maximum stress (e.g., at the first engaged thread or at the fillet radius under the head of a bolt).

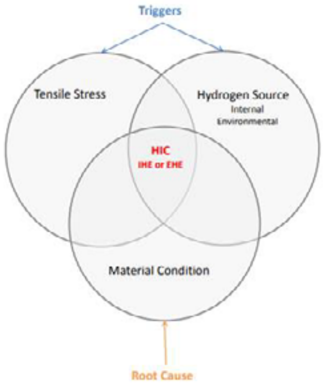

Figure 1. Conditions contributing to the failure due to hydrogen embrittlement [1]

Steel that is ordinarily ductile gradually turns brittle when larger and higher quantities of hydrogen collect at this region. A hydrogen produced (brittle) microcrack eventually results from a concentration of tension and hydrogen in one place. As hydrogen flows to follow the tip of the developing fracture, the brittle microcrack continues to grow until the fastener is overloaded and ruptures. This hydrogen degradation mechanism can cause the fastener to fail at stresses far lower than the fastener's fundamental strength as evaluated by a typical tensile test.

B. ACOUSTIC EMISSION

The AE technique has previously been suggested for detecting and monitoring hydrogen embrittlement and cracking and will be investigated in this study in bolts. AE is a non-destructive evaluation (NDE) approach for identifying active growing in the materials [3]. There is an energy release when a fracture propagates (i.e. grows larger). Elastic waves propagate through the material as a result of the linked events, resulting in measurable AE signals, as shown in figure 2.

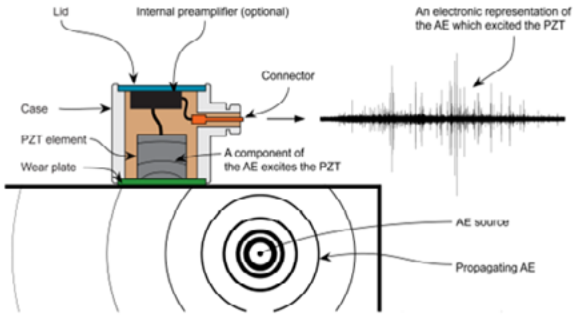

Figure 2. An illustration of how an AE is converted into an electric representation [3]

Determining AE sources is a challenge, as many people consider corrosion as mainly a manifestation of erosion and damage, where the acoustic source is not the corrosion itself, but its consequences, including bubble evolution, crack propagation, growth, and evolution of corrosion product deposits. As a matter of fact, there are good correlations between specific AE parameters and corrosion damage in various cases [6].

III. INITIAL TESTING PLAN

The initial testing setup will be axial fatigue testing to be conducted on the property class 10.9 M20 bolt chosen following ISO 3800 standard [7]. Figure 3 below shows the rig designed for the fatigue testing of the bolts. The aim of this axial fatigue testing would be to test the bolt at varying loads and generate an S-N curve with the fatigue data obtained.

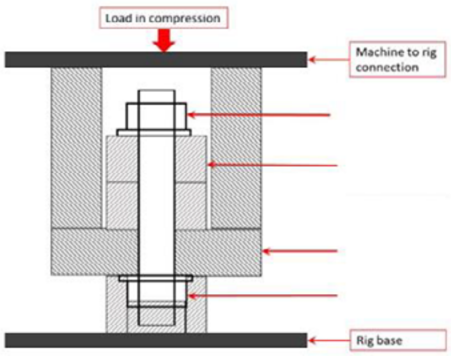

Figure 3. Schematic of the Rig Design for Fatigue testing of M20 bolts

The key feature will be to test several bolt grades to see which one will be most suitable for final testing bolt grades like AISI 4340 and property class 10.9 are the two options based on ISO 898 – 1 standard [8]. Along with axial fatigue testing, sensors will be located at appropriate parts of equipment to capture the AE signals which will then be co-related to the SN curves obtained.

For various values of mean stress in the range $0<\sigma m<Sy$, where Sy is the material's yield strength, a series of S-N curves will be formed. The ISO 3800 standard shall be followed to obtain the S-N curve. Figure 4 depicts a typical S-N curve that can be built using the provided data.

Figure 4. Example of basic pattern of S-N curve generated using ISO 3800 standard[7]

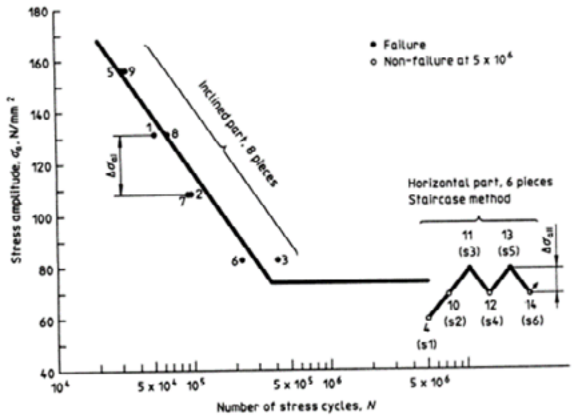

IV. CONCLUSIONS

For the forthcoming year, the most important task planned will be to conduct initial fatigue testing on the bolts. This testing will be essential for the project as it will check and justify the bolts material and size that have been chosen for the project as well as relate the S-N curves to the AE data gathered during testing. By the end of this year, it is hoped that initial testing will be finished, specimens introduce to hydrogen blistering and subsequent tests conducted to them.

V. REFERENCES

[1] S. Brahimi, "Fundamentals of hydrogen embrittlement in steel fasteners," IBECA Technology Corp, 2014.

[2] Y. Chung and L. Fulton, "Environmental hydrogen embrittlement of G41400 and G43400 steel bolting in atmospheric versus immersion services," Journal of Failure Analysis and Prevention, vol. 17, no. 2, pp. 330-339, 2017.

[3] R. Unnþórsson, "Hit Detection and Determination in AE Bursts. Acoustic Emission-Research and Applications. Ed. by W. Sikorski," ed: InTech, 2013.

[4] A. Bhattacharya, N. Parida, and P. Gope, "Monitoring hydrogen embrittlement cracking using acoustic emission technique," Journal of materials science, vol. 27, no. 6, pp. 1421-1427, 1992.

[5] J. Billingham, J. Sharp, and J. Spurrier, "Review of the performance of high strength steels used offshore," 2003.

[6] V. Smanio, J. Kittel, M. Fregonese, T. Cassagne, B. Normand, and F. Ropital, "Acoustic emission monitoring of wet H2S cracking of linepipe steels: Application to hydrogen-induced cracking and stress-oriented hydrogen-induced cracking," Corrosion, vol. 67, no. 6, pp. 065002-1-065002-12, 2011.

[7] B. S. I. Staff, Threaded Fasteners. Axial Load Fatigue Testing. Test Methods and Evaluation of Results. B S I Standards, 1994.

[8] E. ISO, "898-1 Mechanical properties of fasteners made of carbon steel and alloy steel–Part 1: Bolts, screws and studs with specified property classes–Coarse tread and fine pitch thread," Belgium: CEN, 2009.

Kranthi Maniam

Dr Kranthi currently work as a Senior Project Leader-Technology at the Surface Corrosion and Interface (SCI) Engineering, joined after working for a few years in different industries after his PhD in Chemical Engineering from the Indian Institute of Technology Madras, India. His primary research and engineering activities revolve around electrodeposition of metal and metal alloys, ionic liquids, coatings, corrosion, fuel cells and surface finishing. He is a recipient of the Marie-Sklodowska Curie Actions Individual Fellowship, Indian National Academy of Engineering (INAE)-Students Innovative Project Award at Doctoral Level and Gandhian Young Technological Innovation Award, and has presented his work in various international conferences and is currently as a member of Institute of Science and Technology (IST), Institution of Engineering and technology (IET), Royal Society of Chemistry (RSC) and the Institute of Materials Finishing (IMF).

REACH Compliant Aluminium Pre-treatments (Cr(VI) Replacement (33541)

Coatings Technologies

Download

Available to TWI Industrial Members

Project Outline

This project seeks to address the current need for chromium-free aluminium alloy conversion coatings for improved corrosion resistance. There are a variety of chromium-free conversion coatings commercially available, however, there is little impartial information comparing their corrosion performance. The majority of testing that has been carried out has been performed in either an academic environment, not using commercial products, or comparing coating performance solely with Cr(VI) analogues, either chromating or anodising.

This project seeks to provide a clear understanding of the performance of alternative chromium-free conversion coatings with regards to both their corrosion resistance and self-healing capability. Technologies are expected to include phosphating, plasma electrolytic oxidation, zirconium/titanium conversion coatings, cerium conversion coatings, and chromium-free anodising. Results will be used to develop a decision support tool to guide industry in replacing chromium-based technologies.

Benefits to Industry

The project will provide industry with a clear direction as to the most promising chromium-free conversion coating methods, in order to avoid the increasingly restrictive and costly Cr(VI) based approaches.

A decision support tool will be available online to recommend the most appropriate coating technologies as replacements for chromating and chromic acid anodising in different use cases.

Key Findings

- Mechanical tests and microstructural analysis show that pierced composite coupons have superior tensile properties but inferior compressive properties, compared with drilled composite coupons.
- These findings will determine those applications that can benefit from the TAP perforation process in the future and those for which the process is not suited.
- Microstructural analysis of pierced coupons showed that the reinforcing fibres create a path around the holes that results in the tensile strength increase, but also the formation of local kink bands that cause the reduction in compressive strength.
- Numerical modelling of the process is challenging, and a validated model has not yet been achieved. A suitable model does not need to include the flow of a molten matrix and the displacement of every individual fibre; assumptions can be made to simplify the computation while still generating volume fraction and orientation distributions for the perforated composite.

Abbasi Gandhi

Dr Abbasi Gandhi is a Principal Project Leader in the Thermal Processing Technologies (TPT) section at TWI. Abbasi is material scientist (PhD) with engineering background (BEng and MEng) and over 15 years of R&D experience in highly regulated industries, such as medical device, automotive, pharmaceutical, aerospace, novel testing instruments, data storage, power generation and materials safety.

As well as having written 35 peer-reviewed journal papers, 3 granted patents and 3 book chapters, Abbasi has presented his work in 53 national/international conferences. Abbasi is a reviewer for material science related international journals.

Addressing the Challenges of Electrification and Recycling (33559)

Joining Technologies

Download

Available to TWI Industrial Members

Project Outline

The overall project concept is two-fold. One priority will be to focus on research related to battery pack joining and joint performance using techniques suitable to connect cells and other features to bus bars. The second focus will be around developing new capability in terms of design, testing, recycling and other knowledge relevant to electrification.

Limited data exist in the public domain related to mechanical and electrical performance as a function of the different joining techniques, which makes the design of battery modules a more empirical process. Recent literature typically provides a top level review rather than process specific data. A suitable design for a cell to bus bar assembly will be developed in order to standardise a test methodology. This design will address the challenge of the variety of joint geometries created by the different joining processes.

Design concepts and opportunities for disassembly and recycling will be investigated. Opportunities based on the concept of design for disassembly will be developed that may facilitate better reuse/recycling of battery packs. A key aspect of this activity will be engagement with industry to identify future trends in pack design.

The final activity will focus on identifying gaps in current standards and identifying areas where the application of a standard could be beneficial. This could range from control and qualification of a joining procedure and associated inspection through to minimum levels of mechanical or electrical performance. TWI will work with other R&D organisations as well as industry, industry bodies and other stakeholders e.g. HSE, to identify and contribute to new standards as required.

Benefits to Industry

- Ability to reliably manufacture battery packs with reduced failure rates.
- Mechanical and electrical joint properties to allow for optimised designs.
- Understanding of requirements related to design for disassembly and second use/recycling.
- Validated mechanical testing methodology for QA.
- Non-destructive testing protocols for QA.

Cui Er Seow

Dr Cui Er Seow joined TWI in March 2020 as a welding engineer in the Arc processes and Welding Engineering (AWE) section. Prior to working for TWI, she completed her PhD research with NSIRC on arc-based additive manufacturing of nickel-based superalloys, investigating the effects of heat treatments on its microstructure and mechanical properties.

During her time at TWI she has been involved with a variety of projects, including projects part of the Core Research Programme such as arc-based additive manufacturing, European funded projects such as WeldGalaxy, and industrial member funded projects involving welding engineering support for repair of structures, as well as TWI's software product development.

Investigation of Integrated Additive Manufacturing from Feedstock to Part Quality (33631)

Additive Manufacturing

Download

Available to TWI Industrial Members

Project Outline

The aim for any additive manufacturing (AM) route is for it to be a digital process with (semi-) automated design, modelling and simulation, and manufacturing procedure generation all taking place to define an optimised process.

Operation of the AM process should result in a part with known properties, and in-process monitoring should then ensure the physical part meets that expectation, without the need for further inspection.

This multidisciplinary project will support this for WAAM and move AM for large structures closer to the vision of high quality design, simulation and right first time every time digital manufacturing.

TWI's expertise in processing, metallurgy, numerical simulation and inspection will be combined to develop the deposition process in order to:

- Make thermal history more regular.
- Understand microstructure as a function of feedstock composition and thermal history.
- Enable the build of complex parts with more consistent geometry and mechanical properties than is currently possible.
- Include on-line non-destructive evaluation to further understand and quantify the process and correlate this with the microstructures generated.

Benefits to Industry

The project will provide industry with a clear direction as to the most promising chromium-free conversion coating methods, in order to avoid the increasingly restrictive and costly Cr(VI) based approaches.

A decision support tool will be available online to recommend the most appropriate coating technologies as replacements for chromating and chromic acid anodising in different use cases.

Kyriakos Flentzeris

Kyriakos is a Reliability Project Leader working within the NDE group since May 2021. He has a working experience of 7 years within the quality control of the welding industry in the fields of infrastructure, offshore and oil and gas.

His academic background consists of an MEng on advanced materials and engineering mechanics from the National Technical University of Athens and a Master's degree on advanced metallurgy from the University of Sheffield. He is an International Welding Engineer and he is certified in several NDE techniques at a level 2.

Characterisation of Discontinuities with Advanced UT (33578)

Inspection and Monitoring

Download | **Available to TWI Industrial Members**

Project Outline

The project will assess the current sizing capabilities of AUT applications with reference to ISO 16827:2012 ("Non-destructive testing — Ultrasonic testing — Characterization and sizing of discontinuities") and investigate best practice for a variety of AUT techniques for sizing in butt-welded joints. The current methods for sizing with AUT are taken from manual ultrasonic testing (MUT) standards. During this project, these techniques adopted from ISO 16827:2012 will be reviewed and assessed to see how applicable they are for AUT techniques and whether different characterisation and sizing techniques may be more appropriate.

Probe manipulation for AUT is more rigid than for MUT. Standard AUT inspections involve the probe having a constant index offset from the weld; the probe moves along the length of the weld at a set rate. Flaw analysis in AUT is typically completed after inspection. The data collected during the inspection are recorded, allowing the operator to characterise and size indications later. The physical methods of collecting and analysing data for MUT and AUT, are different, but they currently still adopt the same techniques for characterising and sizing defects. An investigation into the characterisation and sizing capabilities and methods for AUT will develop new knowledge and expertise in the field for on-site sizing of defects in newly manufactured structures and ageing assets.

Trialling the variety of sizing methods (maximum amplitude, 6dB drop, 12dB drop, 20dB drop, etc) will provide a greater understanding to how these methods perform in different applications and inspections. Testing these methods on a range of sample thicknesses and defect types and sizes will build a far greater understanding of their capabilities and limitations.

Benefits to Industry

The The assessment of the characterisation and sizing capabilities of AUT methods adopting the techniques from ISO 16827:2012 will allow a greater level of confidence in sizing defects for lab and site purposes.

The work on defect critical sizing with PAUT and FMC will increase the level of confidence in sizing for new and ageing assets, and reduce the conservatism for defects for engineering critical assessment (ECA).

New expertise and knowledge in the field of FMC will assist with development of upcoming standards on the method.

Miles Weston

Dr Miles Weston is a technology consultant at TWI, responsible for development of novel non-destructive testing and evaluation technologies from concept through to commercialisation. With over 12 years of industry experience he has managed teams delivering inspection solutions in sectors including military, aerospace, oil and gas and power generation.

In 2012 Miles gained his Engineering Doctorate in Advanced Ultrasonic Digital Imaging and Signal Processing for Applications in the Field of Non-Destructive Testing.

Within TWI Miles has also held roles including Inspection Suite Manager, supporting the delivery of core internal research activities across the NDT group, as well as being former chair of the BINDT Full Matrix Capture working group, seeking standardisation of the technology.

Development of Novel Ultrasonic Inspection Capability for Sizing of Rough Cracks (33596)

Inspection and Monitoring

Download

Available to TWI Industrial Members

Project Outline

FMC ultrasonic inspection offers a number of benefits over existing ultrasonic inspection techniques, to support fitness for service assessments, including amongst others: detection and sizing of near-vertical and off-specular planar flaws; fully focussed inspection through complex-geometry; and ability to interrogate the inspection volume using a range of wave modes from a single scan.

This project will develop a number of novel techniques and apply these to TWI's FMC inspection software package, Crystal, in order to demonstrate sizing accuracy of FMC for rough cracks (Ra = 50µm or greater) in austenitic or ferritic steel.

Novel FMC features/techniques to be developed within this proposed scope of work include:

- Development of a novel technique to differentiate corner trap signals when masked by geometric reflections. The intended approach will use differences in ultrasonic interaction between a corner trap signal and that from a geometric reflection to enable corner trap signals to be detected and used along with the tip response for flaw sizing.
- Development of an innovative crack tip enhancement feature to increase sensitivity to crack tip response from the major face of a rough crack. Tip and facet responses from a rough crack are typically an order of magnitude (or more) weaker than those of the corner trap, geometric reflection, or specular response from the major face of the flaw. This algorithm will exploit differences in the ultrasonic interaction between a tip/facet and that from material grain structure, corner trap or geometric reflections to enhance the signal to noise ratio of a crack tip/facet.

Benefits to Industry

The project outcomes will improve confidence in flaw detection and sizing accuracy, and provide documented evidence of capability for use by industry during inspection procedure qualification to reduce the time and cost for qualification using advanced ultrasonic testing.

Emre Akgun

Emre joined TWI as an affiliate within the NSIRC PhD programme in May 2018 and is currently working as a Senior Project Leader in Fatigue and Fracture Integrity Management (FIM) section.

He is experienced in finite element analysis for the purpose of structural integrity calculations and mechanical testing with a specialisation in growth of fatigue cracks from material defects.

Emre has more than 10 years of experience in the field of structural integrity, which extends to metal additive manufacturing industry during PhD research and hydropower industry as a structural analysis engineer for hydro turbines and steel structures.

Investigation of Corrosion Fatigue of Offshore Wind Substructures (33593)

Structural Integrity

Download

Available to TWI Industrial Members

Project Outline

There is a global push towards the use of renewable energy, and the offshore wind industry is growing rapidly. Offshore structures are subject to environmental loading. For example, offshore wind substructures (OWSs) are subjected to severe cyclic loads caused by wind, waves and dynamic structural response. Although most of these structures are protected by coating and/or cathodic protection against corrosion, some parts of the structures may be subject to free corrosion in seawater. The current fatigue design of offshore structures are based on data principally from welds in tubular steel jacket structures for the oil and gas sector. This project will investigate the pit to crack transition in steels for OWSs and mooring chains and the results can be used for other offshore structures.

The project will be composed of three parts: experimental testing, numerical modelling to determine the stress/strain concentration surrounding corrosion pits, and constitutional modelling of the corrosion pit to crack transition. Two types of steels will be investigated: structural steels commonly used in OWSs and high strength steels commonly used for mooring chains. For each type of steel, corrosion pits of various sizes will be introduced artificially. Fatigue testing of pitted plate or strip specimens, some containing a girth weld, will be carried out in both air and free corrosion seawater to establish the critical pit size and pit aspect ratio corresponding to the transition. The test specimens will be sufficiently large to be as closely as possible representative of the actual components. Linear elastic finite element analysis (FEA) will be performed to determine the local stress and stress concentration factor (SCF) for various pit aspect ratio or shapes.

Corrosion pit transition to crack can be influenced by many factors. This project will mainly investigate the following three key factors: (1) effect of corrosion pit geometries on crack initiation; (2) weld profile; (3) effect of small stresses.

For (1), specimens with different pit geometries will be tested to determine the threshold stress range for crack initiation.

For (2), specimens with different weld profiles, representing that typically seen in OWS, will be tested to determine the conditions at which the fatigue strength of the weld is comparable with that of pitted specimen.

For (3), the study will focus on the effect of small stresses on crack initiation from corrosion pits.:

Benefits to Industry

The new data and fatigue design guidance generated from the project will allow offshore wind energy companies to design OWSs more efficiently and safely.

The results are expected to be included in future revisions of BS 7608 "Guide to Fatigue Design and Assessment of Steel Products".

Yin Jin Janin

Employed by TWI since July 2012, Dr Yin Jin Janin is a highly experienced structural integrity engineer with a thorough knowledge and experience in defect assessment, mechanical testing and other fracture mechanics-related topics.

She is a member of BS 7910 Main Committee and various Panels of both BS 7910 and R6. Along with other UK colleagues, she also sits in the fracture toughness committees of both BSI on ISO.

Yin Jin is also an UK delegate for IIW Commission X and theme lead for Codes and Standards of UK FESI. She has an Engineering Doctorate in Nuclear Engineering

Integrating Diverse Approaches to Reliability of Engineering Structures (32878)

Structural Integrity

Download

Available to TWI Industrial Members

Project Outline

The project will develop TWI's capabilities in assessing the reliability of safety-critical welded structures, and integrate two different approaches: Method 1 (risk-based, or 'top-down') and Method 2 (fracture-mechanics-based, or 'bottom-up'). The benefits for industry are expected to be substantial, including: (i) integration of two disparate methods of quantitative reliability assessment, which are currently typically undertaken by different teams; and (ii) an understanding of the probability of failure associated with Engineering Critical Assessment (ECA) carried out using currently-accepted deterministic methods.

The project will focus initially on a single failure mode (brittle fracture under monotonic loading), both because of its practical importance and because of its amenability to modelling using fracture mechanics techniques, both deterministic and probabilistic. Different types of welded structure will be considered, with particular attention paid to:

- Structural redundancy: for example, fixed offshore structures exhibit a high degree of structural redundancy, so that failure of one member will not lead to failure of the overall structure, whereas non-redundant structures such as pressure vessels may fail catastrophically because of breach of the shell only. Nevertheless, it is standard practice to manage structural integrity of both types of structure using a range of techniques including: ensuring certain levels of materials toughness and strength, post-weld heat-treatment of thick sections, pre-service/in-service inspection and control of stresses/stress concentrations.
- The role of residual stress in welded steel joints. Residual stresses associated with both the as-welded (AW) and post-weld heat-treated (PWHT) condition will be considered, along with the implications of rules and standards that mandate application of post-weld heat-treatment for steels above a certain thickness.

Where possible, fatigue crack growth will also be modelled probabilistically, with a view to linking current risk-based research addressing fatigue with a probabilistic fracture mechanics-based fatigue approach. This is expected to be a more challenging, but equally important, endeavour compared with consideration of brittle fracture, since the uncertainties associated with fatigue crack growth parameters and initial flaw size can lead to even greater uncertainties in fatigue life.

Benefits to Industry

The outcomes of the project will be fully documented, transparent and traceable; consequently, it will be possible for industry to apply the methods developed during this project to their own structures.

This will increase the accuracy of assessments of the reliability of structures, improving safety, and potentially reducing both fabrication and operating costs.

Mike Troughton

Dr Mike Troughton has been carrying out research for the plastics industry for almost 40 years. He is the Technology Fellow for plastics joining at TWI, where his main areas of expertise include the welding, mechanical testing and inspection of PE pipes, on which he has written over 30 technical papers.

He is also the editor of the Handbook of Plastics Joining – A Practical Guide. He has managed over 150 research projects for clients all over the world and is the UK representative on various ISO, CEN, BS, ASTM, IIW, AWS and ASME committees on the welding of plastics and plastics pipes.

Effect of Insufficient Homogenisation of Pigmented Resin During the Extrusion of Polyethylene Pipes on the Mechanical Performance of Butt Fusion Joints (30554)

Composites and Polymers

Download

Available to TWI Industrial Members

Project Outline

The concept of this project is to undertake a detailed investigation into whether poor homogenisation of pigmented resin in PE pipes, which results in windows does reduce the integrity of the subsequent butt fusion welds, and if there is a clear link, to create a cost effective test to determine an unacceptable amount of inhomogeneity in the pipe.

A number of PE pipes containing varying amounts of windows will be obtained and analysed using optical microscopy, scanning electron microscopy (SEM), X-ray microscopy, Fourier transform infrared spectroscopy (FTIR), local reheating and nanoindentation to map the distribution of windows, the concentrations of carbon black and areas of incomplete fusion of the parent material at the ends of the pipe. The pipes will then be butt fusion welded using standard welding procedures, and the welded joints will be mechanically tested using both short-term (tensile, bend) and long-term (whole pipe tensile creep rupture) tests, as well as analysed using X-ray microscopy. The fracture surfaces will be examined using optical microscopy, SEM and FTIR to determine and analyse the positions of failure initiation.

A number of pipes, made from the same grade of PE, that do not exhibit windows will also be analysed, butt fusion welded and mechanically tested using the above methods. The results will be compared to determine whether there is an acceptable amount of windows that does not affect the mechanical performance of the joint, what happens to the windows and concentrations of carbon black that are at the joint interface during the welding process, and whether it is areas of high concentrations of carbon black or areas of incompletely fused PE that causes a reduction in joint integrity.

Benefits to Industry

The new mandatory Appendix to Section III of the ASME code for HDPE Class 3 piping states that all PE pipes must undergo fusibility testing in all combinations of suppliers, diameters and thicknesses before being fused in production. This is a very onerous and expensive task, but must be carried out to ensure that the PE pipes are of sufficient quality to produce acceptable butt fusion welded joints. Variable homogenisation of pigmented resin is considered the primary quality issue when joining PE pipes.

Insufficient homogenisation of pigmented resin during the extrusion of polyethylene (PE) pipes may result in features called “windows”. These are mainly seen in black pigmented pipes that have been produced using a process where the natural PE resin pellets are dry-mixed with carbon black masterbatch pellets before going into the pipe extruder rather than being pre-compounded. The windows are areas where there is a lack of carbon black pigmentation and normally occur in thicker-walled pipes, towards the mid-wall thickness. They can be seen in the shavings from the end of the pipes, which are produced during the trimming stage of the butt fusion welding process.

A number of published reports, as well as some internal work at TWI, show that insufficient homogenisation of pigmented PE resin, resulting in windows in the pipe has a detrimental effect on the performance of both the pipe and its welded joints However, no research has been published that determines the exact reason for the reduction in performance or to define an acceptable amount of windows for welding.

TWI Innovation Network

ANNUAL CONVENTION

22 JULY 2022, 09.00 – 15.00 BST

AGENDA

Friday 22 July, 09:00 – 15:00 BST
TWI Cambridge, Meeting Room G3

09:00	Registration and Refreshments
09:30	Welcome and Introduction – **Cem Selcuk**, Head of Business Development, TWIIN (Chair)
09:45	Keynote Presentation – **Prof Hasan Mandal**, President of TÜBİTAK
10:15	TWIIN Updates – **Cem Selcuk** (Chair)
	TWIIN Training Courses:
10:45	Outline of Programme – **James Foden**, Section Manager, Technology Innovation Management, TWI
	Knowledge Development – **Heidi Dyson**, Group Manager - Public Funding Management, TWI
11:15	*Break*
11:35	International Successes with TWIIN in European Projects (TWI–Floteks–TÜBİTAK) – **Omer Beysel**, Assistant General Manager, Floteks Automotive
11:55	Singapore Opportunities – **Abbas Mohimi**, Head of Public Funding and Regional Engagement, TWI
12:15	Partner Matching and Brokerage Introduction - **Sally Shi**, Collaborative Proposals Programme Manager, TWI
12:25	Round Up of Morning Session and Afternoon Expectations – **Cem Selcuk (Chair)**
12:30	*Lunch, networking and exhibition stands*
	Partner Matching and Brokerage**:**
13:30	Horizon Europe September – November 2022 Funding Opportunities – **Sally Shi,** Collaborative Proposals Programme Manager, TWI
13:50	Project Concept Pitches for Partner Matching - **Innovation Centres** (TWI-Universities Partnerships) and **TWIIN Subscriber Organisations**
15:00	Closing Words – **Cem Selcuk** (Chair)
	Networking and exhibition stands

TWIIN SUBSCRIPTION PROGRAMME

Our TWIIN Subscription Programme options are designed for companies and organisations looking to build on their technology development ambitions to bring more products, systems or services to market, and would benefit from joining forces with TWI's international networks, Innovation Centres and Industrial Membership base.

A TWIIN subscription facilitates mutual collaborations to help subscribing partners enable engineering advances in specialist areas, across a wide range of industry sectors, relevant to their business, in response to commercial needs. This includes tailored support to maximise capabilities in advancing new concepts through the Technology Readiness Levels (TRLs) to market delivery, as well as 1-2-1 innovation management consultations, partner matching and brokerage workshops, and opportunities to join R&D projects. The TWIIN Subscription Programme offers a flexible approach to technology innovation management:

- Original TWIIN Subscription – for start-ups through to SMEs who also become Premium Technology Acceleration Programme Members (TAPs)
- Collaborative Innovation Partnership (CIP) Subscription – for larger companies with national and/or overseas operations
- European-based Organisations Subscription – for RTOs and universities outside the UK with industrial interests

If you are interested in exploring a TWIIN Subscription, simply email to **info@twi-innovation-network.com.**

INNOVATION CONSULTANCY SERVICES

The Innovation Consultancy Services (ICS) helps to create opportunities for technology acceleration, promote products and services, and identify new markets through research and networking activities.

It offers one-to-one support to companies and organisations that includes evaluating their technologies and services, clarifying goals and outlining viable, cost effective outcomes, and creating company plans to accelerate innovation processes. ICS also focuses on new product and service development to help maximise potential for exploiting new markets..

Unlocking opportunities

- Dissemination and marketing
- Events management
- Innovation consultancy
- Key partner matching
- Selection of business-specific funding opportunities
- Workshops and webinars

Technology focus

- CPD courses
- Foresight review
- Industrial targets
- Marketplace strategies
- Product innovation
- Technology development
- Trending subjects
- Value chain analysis

Road mapping

- Future development focus
- Ideas generation
- Key Performance Indicators
- Roadmap canvas
- SWOT analysis
- Technology mapping
- Trends analysis

TRAINING COURSES

Introduced this year in response to market demand, the new training courses from TWIIN are designed to upskill recipients in key aspects of bidding for collaborative funding and managing resultant projects together with their consortium partners.

Research Proposal Concept Development for Horizon Europe (HE) Thematic Calls

- Aimed at new and experienced proposal writers from the private sector, higher education institutions, RTOs and other research-performing organisations.
- Course focuses on HE thematic calls under Pillar 2: Global Challenges and European Industrial Competitiveness, and includes an introduction to HE, guidance on reading thematic calls in the context of concept development and alignment of research, knowledge exchange on expert evaluator expectations, an exploration of considerations for key partners, user cases and more.
- Takeaway – participants will be able to make informed decisions on progressing a concept further and investing in writing an application for submission.

Writing for Success for Horizon Europe Calls

- Aimed at new and experienced proposal writers from the private sector, higher education institutions, RTOs and other research-performing organisations.
- Course provides hands-on training with practical tools and techniques attendees can use to plan and write collaborative proposals for public funding. It includes mapping your proposal idea, objective setting, demonstrating impact, project implementation, partner selection and consortium building, resourcing, project finances and more as well as practical exercises.
- Takeaway – skills gained on this course are transferable to any public funding stream and will be useful in guiding proposal writing teams.

Preparing Your Organisation for Public Funded Project Audit

- Aimed at new and experienced Contracts and Finance teams from the private sector, higher education institutions, RTOs and other research-performing organisations.
- Course includes what attendees need to do to prepare their company or organisation for audit and who should be involved, in-depth detail on the contractual and financial documents required to deliver public funded projects, common problems experienced when meeting audit requirements, monitoring costs and grant management, identifying financial and non-financial audit requirements, effective record keeping and more.
- Takeaway – participants will gain an in-depth understanding of the actions they can take to successfully navigate public funded project audits.

Introduced this year, our courses are available in-person, online and as in-house training.

If you are interested in exploring training options, simply email to **info@twi-innovation-network.com.**

2012...

2022...

nsirc 10th ANNIVERSARY

ENQUIRIES@NSIRC.CO.UK
+44 (0) 1223 899 000
NSIRC.CO.UK/CONFERENCE2022

00.10.09.21.00